UNIVERSIDADE D
COIMBRA

Rodrigo Ferreira Martins

CELL-TYPE SPECIFIC NEURONAL MANIPULATION OF CORTEX AND STRIATUM DURING ACTION SELECTION

Dissertação no âmbito do Mestrado em Biologia Celular e Molecular – especialização em Neurobiologia orientada pelo Doutor Andreas Klaus e pela Professora Doutora Ana Luísa Carvalho e apresentada ao Departamento de Ciências da Vida da Universidade de Coimbra

Janeiro de 2021

Faculdade de Ciências e Tecnologia
da Universidade de Coimbra

Cell-Type Specific Neuronal Manipulation of Cortex and Striatum during Action Selection

Rodrigo Ferreira Martins

Dissertação no âmbito do Mestrado em Biologia Celular e Molecular – especialização em Neurobiologia orientada pelo Doutor Andreas Klaus e pela Professora Doutora Ana Luísa Monteiro de Carvalho e apresentada ao Departamento de Ciências da Vida da Universidade de Coimbra.

Janeiro de 2021

UNIVERSIDADE D
COIMBRA

Acknowledgements

After two and a half years, that started with my admission in this Master's program and culminated with the delivery of this Master's thesis, there is a group of people that deserve my words of gratitude and appreciation for their contribution to my personal and professional development.

To Rui, thank you for the amazing opportunity of developing my master thesis' project in your lab, and for being the standard of professionalism and passion for neuroscience, which is easily transmitted to everyone working under your wing.

To Andreas, a "thank you" is not enough for everything you did for me this last year. I will forever remember your lessons and support, and for always pushing me to achieve the best version of myself. In addition, thank you for your contribution to this thesis by performing the surgeries and providing me the code to run the behavior analysis.

To Ana, your kindness throughout the entire year, willing to help me in my project and the concernment for my well-being during the experiments, deserves my deepest appreciation. Your participation on this project, by providing me great help with the behavioral experiments, was admirable. You truly are a special person.

To the entire Costa Lab, thank you for providing me such an amazing environment, for your willingness to help me, and for the jaw-dropping moments when I observed you at work. You made me realize what it takes to be successful in this field, and your passion at work will always stick with me.

To all my professors in Coimbra, a huge word of appreciation for your teaching, and for leading me to such a profound passion for neuroscience.

I am really fortunate to have such an amazing group of friends. To the special ones (they know I am talking to them), thank you for your daily presence in my life, for always giving me a state of comfort, tranquility and well-being.

To my family, words are not sufficient to explain what you mean to me. Thank you for helping me in the worst situations, and for cherishing my best moments, always. You will forever have my deepest love.

To Bea, thank you for being my best friend. You are the most kind, generous and bright person I have ever met. Thank you for everything. These years would not be the same without you by my side.

Abstract

Actions get us closer to accomplishing the goals we set, given any context that is presented to us. Choosing the most appropriate one, based on the context we encounter, is important for improving the odds of attaining our goals, while its proper execution is crucial to efficiently handle the requirements we face. Thus, purposive behavior depends not only on the ability to select the most suitable action, but also on its proper initiation and execution.

The neuronal circuits underlying these processes are still not fully understood [1]. The primary motor cortex (M1) and the basal ganglia (BG) are neuronal areas thought to be involved in the generation of movement, with the M1 being the main driver for activity in the largest BG input nucleus, the striatum. Specifically, M1 is mainly linked to functions involving the control, planning and commandment of the action to be exerted [2–5], while the striatum is known to be majorly involved in the proper initiation and execution of actions [6,7]. Additionally, the striatum has been suggested to exert a role in what concerns the selection of the actions to be executed [8–10], since most of its anatomical features properly match the requirements for the performance of the action selection process at a neuronal level. Furthermore, the M1 may play an important role in this process as well, as suggested in models that propose that the close interaction between this cortical region and the striatum is essential to correctly perform the selection of actions. In detail, the M1 is suggested to provide motor plans to the striatum, from which the latter selects the more appropriate one after evaluation, while also integrating BG feedback, which may update the same motor plans previously submitted. However, studies simultaneously describing the effect that M1 and striatum, together, may have on this process and for the initiation and execution of actions, are still lacking. This scarcity prevents the comprehension of which stages are assigned to which region.

To shed light on this topic, the project developed for my Master thesis aimed at characterizing the role that M1 and dorsolateral striatum (DLS) possess in the control of action initiation, execution and selection. To assess it, we performed optogenetic inhibition experiments, using a last generation inhibitory opsin, by manipulating M1 and DLS on mice performing a probabilistic three-alternative-choice task. Behavioral analysis assigned a delay on action initiation after DLS or M1 inhibition, while also revealing the involvement of M1 in the proper execution of the action. Finally, DLS inhibition prior to action initiation led to significant changes in the actions selected by mice in the subsequent trials, an effect not observed after M1 manipulation.

Overall, this study presents a solid case for the involvement of DLS on both

action initiation and selection, while the appropriate timing to initiate and execute an action seems to be linked to M1 activity.

Keywords: action selection; striatum; primary motor cortex; action initiation; action execution; optogenetics.

Resumo

As acções deixam-nos mais próximos de alcançar os objectivos que definimos, face a qualquer contexto que nos é apresentado. Escolher a mais apropriada, com base no contexto com que nos deparamos, é importante para melhorar as probabilidades de alcançarmos os nossos objetivos, enquanto a sua execução adequada é crucial para lidarmos eficientemente com as exigências que encontramos. Consequentemente, comportamento deliberado depende não só da habilidade de selecionar a ação mais indicada, mas também da sua adequada iniciação e execução.

Os circuitos neuronais subjacentes a estes processos ainda não são totalmente compreendidos [1]. O córtex motor primário (M1) e os gânglios basais (BG) são áreas neuronais que se pensa estarem envolvidas na geração de movimento, sendo o M1 o principal responsável pela atividade no maior núcleo da BG, o estriado. Especificamente, o M1 está principalmente ligado a funções que envolvem o controlo, planeamento e comando das ações a serem tomadas [2–5], enquanto o estriado é conhecido por estar essencialmente envolvido na iniciação e execução apropriadas de uma ação [6,7]. Adicionalmente, é possível que o estriado exerça um papel no que diz respeito à seleção da ação a ser executada [8–10], dada a extensão das suas características anatómicas que coincidem com grande parte dos requisitos para a performance do processo de seleção de uma ação a um nível neuronal. Além disto, o M1 pode igualmente desempenhar um papel importante neste processo, como sugerido em modelos que propõem que a interação próxima entre esta região cortical e o estriado é essencial para realizar correctamente a selecção de acções. Em detalhe, é sugerido que o M1 providencie planos motores para o estriado (dos quais este selecciona o mais apropriado após avaliação), sendo que também integra BG *feedback*, o qual pode actualizar os planos motores previamente submetidos. No entanto, estudos que descrevam simultaneamente o efeito que a atividade do M1 e do estriado, em conjunto, possam ter neste processo e para a iniciação e execução de ações, ainda são escassos. Esta escassez impede a compreensão de quais estágios são resultado de que região.

Para clarificar este tópico, o projecto desenvolvido para a minha tese de Mestrado ambiciona caracterizar o papel que o M1 e o estriado dorsolateral (DLS) possuem no controlo da iniciação, execução e selecção de uma acção. Para avaliar estes efeitos, realizámos experiências optogenéticas inibitórias, usando uma opsina inibitória de última geração, ao manipularmos o M1 e o DLS de ratinhos que realizaram uma tarefa probabilística de três escolhas alternativas. Análise comportamental revelou um atraso

na iniciação de uma ação após inibição do DLS ou M1, ainda revelando o envolvimento do M1 na execução apropriada da ação. Por fim, a inibição do DLS antes da iniciação da ação levou a mudanças significativas nas ações selecionadas por ratinhos nas tentativas subsequentes, um efeito não observado após manipulação do M1.

Globalmente, este estudo apresenta um caso sólido para o envolvimento do DLS na iniciação e seleção de uma ação, enquanto o *timing* apropriado para a execução de uma ação aparenta estar relacionada com atividade do M1.

Palavras-chave: Seleção de uma ação; estriado; córtex motor primário; iniciação de uma ação; execução de uma ação; optogenética.

Table of contents

List of Figures

List of tables

Abbreviations

ADHD	Attention deficit hyperactivity disorder
ACRs	Anion-conducting channelrhodopsins
ALM	Anterior lateral motor cortex
BG	Basal ganglia
BF	Brightfield
CT	Corticothalamic
DAPI	4,6-diamidino-2-phenylindole
DLS	Dorsolateral striatum
DMS	Dorsomedial striatum
gc	Genomic copies
GPe	External segment of the globus pallidus
GPi	Internal segment of the globus pallidus
HD	Huntington's disease
IT	Intratelencephalic
ITI	Inter-trial interval
M1	Primary motor cortex
OCD	Obsessive-compulsive disorder
PBS	Phosphate Buffer Saline
PD	Parkinson's disease
PDF	Probability density function
PETH	Peri-event time histogram
PFA	Paraformaldehyde
PPN	Pedunculopontine nucleus
PT	Pyramidal tract
RPE	Reward prediction error
SC	Superior colliculus
SNc	Substantia nigra pars compacta
SNr	Substantia nigra pars reticulata
SPNs	Spiny projection neurons
StGtACR2	Soma-targeted Guillardia theta anion-conducting channelrhodopsin 2
STN	Subthalamic nucleus
VLS	Ventrolateral striatum
VS	Ventral striatum

VTA	Ventral tegmental area

1. Introduction

1.1 Action and movement

An action can be described as any sort of intentional and conscious activity exerted by an agent to achieve a particular goal. A cornerstone for its completion is movement, which we regularly use on a daily basis. To increase the odds of achieving these goals, proper movement performance is essential, with goal and execution being intimately related to fulfill our needs.

For example, when we feel thirsty, our immediate need is to be satiated and therefore we will get a cup of water. To reach for it, the execution of the motion to get the cup of water has to be adequate, so that the cup does not fall or tilt in a way that causes the water to spill. However, preceding the act of attaining what we intend, the planning and selection of the action we subsequently want to execute is equally important. Having in mind the last scenario, past events assure us that the best way to grab the cup of water is with our dominant hand, in a precise manner, since previous experiences have provided us the information to know the most efficient way to grab it. On a broader scale, to cleanly perform these processes of planning and selection we evaluate, comprehend and interact with our surroundings, obtaining contextual information that ultimately helps us to select the most appropriate action to execute.

Nevertheless, since the environment surrounding us is constantly changing, to select and execute an action is a feat persistently put to the test, since the plans on how to act to meet our goals are continuously switching. If after the event previously described a sound surges behind us, we could possibly turn around to locate the source of the noise. In a short time-interval, two extremely distinct movement activities are performed to match two completely different goals. The action selection process is crucial, since it allows us to behave quickly and efficiently in face of the diversity of changes and problems that consistently arise, which requires high decision-making performance.

Although motor output is a concept present in our every-day lives, understanding the full picture of the chain of processes that enables it is still challenging [1]. In what we can call the final stages of the neuronal circuitry of action, it is assumed that movement is elicited by spinal cord interneurons' activity, which output information to motor neurons [11–13]. These spinal circuits are viewed as the executive modules that drive the body to produce the commands formed in the brain, requiring upstream directives for the generation of motor patterns. Positioned in a rostral position to the spinal cord, the

brainstem forms direct pathways with its downstream structure, and its neuronal populations are viewed as effectors for the commands assimilated in spinal cord circuits [14].

The brainstem was first thought to be a mere relay center to convey the motor plans formed in higher brain areas to the spinal cord. However, a myriad of basic motor functions assigned specifically to its neuronal populations have been discovered, such as locomotion, breathing and posture, among others [15]. However, despite its involvement in a vast array of behaviors, its functions seem to be restricted to rhythmic, strictly executional, outputs. It seems that, at this level, the processes underlying motor behavior only concern its executional aspect, but do not participate in higher-level processing necessary to correctly plan what action should be exerted, and when it must be performed.

Brain areas in charge of these processes must be located upstream to the brainstem, presenting descendent pathways to this region in order to communicate these high-order commands. M1 and the BG fit this description in anatomical terms [16–18], while also sharing connectivity principles at different levels (M1 sends inputs to the BG, while the latter sends feedback projections to M1, among other cortical regions, via thalamus), suggesting that the completion of higher-order functions related to action may be the result of this crossed interaction.

Much of what is known concerning their roles in action and movement match those required to properly initiate the action process. The M1, although its functions are still not totally clear, is thought to be involved mainly in motor control, planning, learning and commanding [3,19–21], while the activity of the main nucleus of the BG, the striatum, is responsible for proper initiation and execution of actions [6,7,22], movement dynamics [23], and to determine the vigor of the movements exerted and the commitment to perform them [24–26]. Additionally, the ties linking the striatum to movement are particularly evident when observing the plethora of movement disorders related with striatal dysfunction, ranging from hypokinetic disorders, such as Parkinson's disease (PD), to hyperkinetic disorders, as the case of Huntington's disease (HD) [27]. More so, corticostriatal dysfunction seems to be a central piece in the development of obsessive-compulsive disorder (OCD), which is characterized by difficulties in controlling when and what to act and to disengage from the action under performance [28,29]. It is important to highlight the absence of the assignment of an action selection role to either M1 or striatum in these last sentences. The identification of which region is responsible for this process (or if it is a combinatory role between these two areas), and the mechanisms that underlie it are still poorly understood.

Considering the requirements for proper action selection mechanisms in light of the

environment's complexity that animals face, the brain region in charge of such functions must fulfill a list of requirements. First, it must be in a position to which is provided a massive amount of inputs encoding different sets of information, due to the necessity of evaluating relevant information for the execution of actions that are appropriate in a particular context. Also, it must present an architecture that not only exerts an effect in brain areas known to play a role in motor functions, but that also hints at the ability to switch actions in a way that matches the requirements the environment presents, for the selection of the most effective and correct behavior in each context.

Since it fills the aforementioned requisites, the striatum evolved from promising to primary candidate to what concerns a role in the action selection process [8–10,30,31]. Receiving motor plans from M1, striatal activity would be required to select the most appropriate plan and commit to execute it, disinhibiting downstream brainstem motor centers. Moreover, the feedback projections from the BG to M1 suggest that the striatum can influence the selection of future actions, through modulation of cortical activity [32,33]. Nonetheless, despite this hypothesis, the lack of experimental evidence connecting striatal activity and an effect on action selection continues to stall the concept that the striatum is indeed involved in this process.

Moving from theory to practice, manipulating striatal neuronal activity on animals performing an action selection task may constitute a step towards a more comprehensive understanding concerning this topic. Furthermore, in the event that the striatum is responsible for the process of action selection, it is also important to evaluate M1 activity under the same challenge, since M1: 1) is thought to convey information concerning motor plans to the striatum, with this input being crucial to initiate striatal activity, and 2) its activity is modulated by BG feedback and is likely to update its action-related content and consequently project it back to the striatum and downstream motor centers. Simultaneously studying the activity of M1 and striatum, upon conditions that trigger the action selection processes at neuronal level, may give insight about the functionality of the connectivity between these two areas respective to this process. Furthermore, assessing the importance of M1 and striatum in the same parameters is necessary to consolidate and clarify at what level both areas participate in action generation. Functions in initiation and execution of actions have been attributed to both areas, and both seem intrinsically related to an action selection role. However, studies describing their effect on these functions under the same parameters are scarce.

Therefore, in this project we evaluated the roles of M1 and striatum on action initiation and execution by analyzing the importance of their activity on the timing to

initiate and execute actions, while also evaluating their participation on action selection, by assessing their contribution to behavioral switching. To study the possible effects of M1 and striatum on these functions, we developed an action selection task that allows the analysis on the contribution of both areas on each of these action processes, under the same behavioral conditions.

1.2 Striatum

The striatum is a neuronal area included in a wider region of subcortical nuclei known as the BG. The largest input nucleus of the BG, the striatum projects downstream to other BG nuclei, such as the internal and external segment of the globus pallidus (GPi and GPe, respectively) and the substantia nigra pars reticulata (SNr) [34–36] (Figure 1).

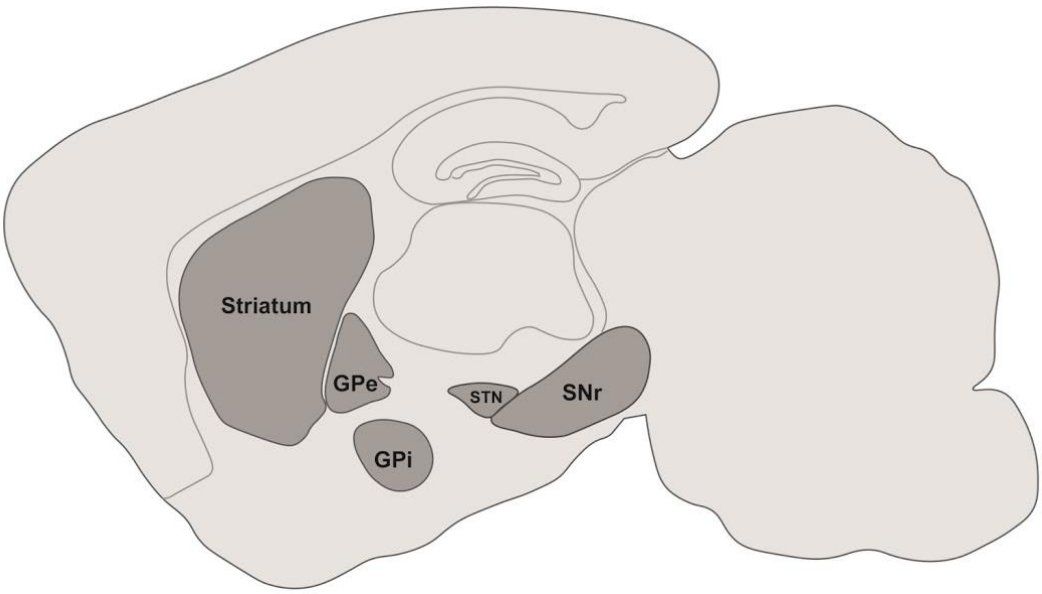

Figure 1 – **Basal ganglia position within the mouse brain.**

The basal ganglia comprise a wide number of subcortical nuclei, including the striatum, the GPe and GPi, the subthalamic nucleus (STN) and the SNr. Adapted [22].

Subjects with neurological disorders related to disturbances and malfunctioning of the BG present abnormal behavioral outputs in terms of movement [27], with the striatum being at the epicentre of such problems. Imbalanced striatal activity is strikingly

implicated in disorders characterized by inappropriate movement kinetics, ranging from hypokinetic to hyperkinetic disorders such as PD and HD [37–42], respectively, while disturbances in its activity have also been linked to disorders in the neuropsychiatric field like OCD or attention deficit hyperactivity disorder (ADHD) [29,43–49]. Given the behavioral outputs observed in these disorders, it is intuitive to consider the striatum as an essential structure in the performance of motor functions.

However, it is interesting that such a distinct variety of motor behaviors, arising from these disorders, have as their common source the malfunction of the same neuronal area. This observation puts in question how the striatum has an effect on such a broad and distinct repertoire of movement's aspects, participating both in action performance-related functions and cognitive aspects of action generation.

To comprehend what underlies this versatile impact, a description of the main characteristics of the striatum will be provided throughout these next set of subchapters, clarifying the ties between striatal activity and its effect on action processes, while contextualizing the idea that an action selection role may be attributed to striatal activity.

1.2.1 Anatomy and circuitry

Anatomically, the striatum is composed by the caudate nucleus and the putamen in its dorsal regions, as well as the nucleus accumbens and olfactory tubercle in the most ventral area. Among its neuronal populations, the striatum contains a small percentage of different subtypes of GABAergic interneurons (5-10%) [50–52], while 90-95% of its composition can be attributed to two classes of inhibitory spiny projection neurons (SPNs) (90-95%) [53–56].

The distinction between these two types of SPNs is evident from their differences in gene expression, namely dopamine receptors' expression (D1-SPNs express D1-type dopamine receptors, while D2-SPNs express D2-type dopamine receptors) and their downstream connectivity [57]. D1- and D2-SPNs projections reveal a differential efferent connectivity with downstream BG nuclei. These differences led to the classification of these neuronal populations as the striatonigral and the striatopallidal pathways, respectively (also known as the direct and indirect pathways) [58]. D1-SPNs inhibit basal ganglia output nuclei directly (direct pathway), whereas D2-SPNs' activity affects them indirectly, first inhibiting the GPe, whose neurons inhibit the STN's excitatory neurons that project to the GPi (indirect pathway) [34,35,55,59].

Beyond this subcortical network of connectivity, the BG projects to other brain areas, inhibiting them tonically [60,61], modulating their activity. In detail, BG output nuclei target various thalamic nuclei, which in turn projects to cortical areas (including motor-related ones) [33,59,62,63]. Additionally, brainstem motor centers are also targeted directly via SNr projections [16–18,64]. Among those, well characterized projections include the ones to the peduncolopontine nucleus (PPN) [18,65] (Figure 2). Other targets of the BG projections include the cerebellum, via STN [66,67], and the superior colliculus (SC) [33,68,69].

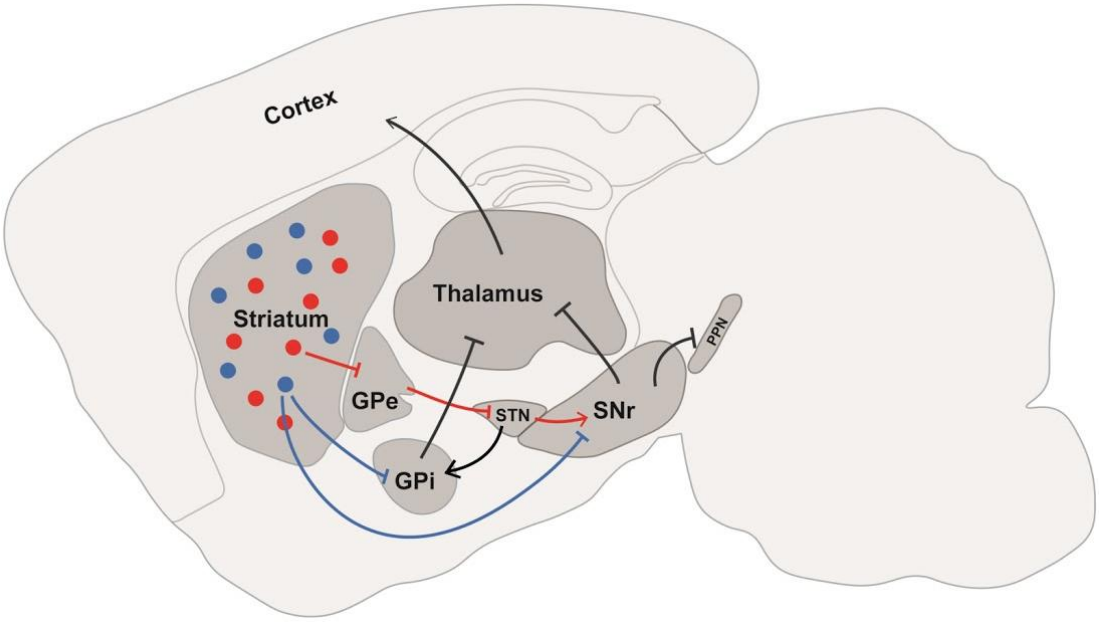

Figure 2 – **Basal ganglia intra-circuitry and downstream targets.**

Image depicting the downstream projections from D1- (blue circles) and D2-SPNs (red circles) to BG' nuclei, and the BG' output targets. Adapted [22].

Overall, the BG output influences brain areas involved in motor functions, either directly (brainstem motor centers and cerebellum) or indirectly (cortical motor areas, through modulation of thalamic activity). Given the effect its SPNs populations exert on the BG output nuclei, the striatum positions itself at the top of the influence on the tonic inhibitory control upon these motor-related brain regions, consequently modulating their activity and allowing their functions to be exerted. Therefore, to evaluate the importance of the striatum on an action process such as action selection, the ability to manipulate its activity in appropriate contexts for the study of the process under consideration, may provide the evidence necessary to attribute functions to the striatum that have been theorized to take place within the BG.

1.2.1.1 Models of striatal function

But how do both D1- and D2-SPNs populations interact in order to correctly modulate the BG outputs to downstream targets? Is their different efferent connectivity to downstream circuits suggesting that both pathways exert different roles on the performance of BG functions? Different models have been proposed to explain what each pathway's activity represents and how they complement each other in order to, in concert, influence BG outputs.

The differences in their downstream projection' targets led to the formulation of the rate model, which is based on the opposing effects of both pathways [27,70]. This model attributes pro- versus anti-kinetic effects to the direct and indirect pathways, which in simplified terms refers to low D1-SPNs activity during immobility and higher activity during movement, while the opposite is applicable to D2-SPNs [23]. Nonetheless, this model attributes a very simplistic, kinetic-related, importance to these pathways' activity.

Cell type–specific experiments in the last decade challenged this classical view on how each striatal pathway contributes to the correct functioning of the BG, a contribution that appears more complex and dynamic than what was previously thought. These studies presented results showing that both striatal populations are more active during movement than during immobility, as well as having minimal activity during immobility, which contradicts the rate model [6,71–73]. Models based on these results, such as the support/suppress model, postulate that there is simultaneous activity of D1- and D2-SPNs during action performance, with D1-SPNs triggering the initiation of a specific action, whereas D2-SPNs activity plays the role of a general suppressor of alternative actions [9,61]. In this model, the two pathways work in concert to facilitate the performance of desired movements while simultaneously suppressing competing actions.

Other models suggest that both pathways can be simultaneously active but that their timing of activity influences basal ganglia output nuclei activity [74,75], that is, direct pathway activity would inhibit the SNr prior to the arrival of the indirect pathway activity at this same nucleus, which would result in a de-inhibition window of basal ganglia output targets. If the opposite happens and indirect activity precedes direct pathway activity, this window does not exist. In this model (race model), the timing of the activity in both pathways represents a variable that strongly determines their effect on basal ganglia outputs.

Even if these models present valid aspects about the roles of each pathway, recent studies have added new elements regarding both pathways' activity. Approaches taking into account SPNs activity from a spatiotemporal point of view, revealed that both SPNs populations are action-specific, as the execution of specific motor programs relate to the activation of specific SPNs ensembles [72,76,77]. Furthermore, this action-specific representation in the striatum suggests that, more than a general suppressor of all competing actions, D2-SPNs populations may guide the correct exertion of movement by suppressing specific motor-related aspects that could impair correct action performance.

What function each pathway has in the completion of the striatal functions, and how their combined pattern of activity contributes to a striatal common goal are questions that need further addressing on studies focusing on the striatum. Nonetheless, to evaluate the striatal impact on the action processes of our interest for this project, we decided, as a first approach, to perturb striatal outputs irrespective of specific manipulation on D1- and D2-SPNs activity. The addressment of the potential dichotomy between both SPNs striatal populations, regarding their contribution for these processes, is not present in this thesis (see Conclusions and Future Directions).

1.2.2 Inputs

Although striatal activity is responsible for the modulation of the BG signalling to other motor areas, ultimately resulting in the generation of movement, understanding the nature of the information it receives, from a functional and conceptual perspective, is crucial to comprehend how the striatal SPNs populations generate their activity and in which functions it may intervene.

Following this rationale, and although the striatum integrates a vast set of information from a wide number of brain regions, I will primarily focus on describing the more relevant inputs to the striatum that modulate and drive SPN activity (e.g., dopaminergic, thalamic and cortical inputs) (Figure 3).

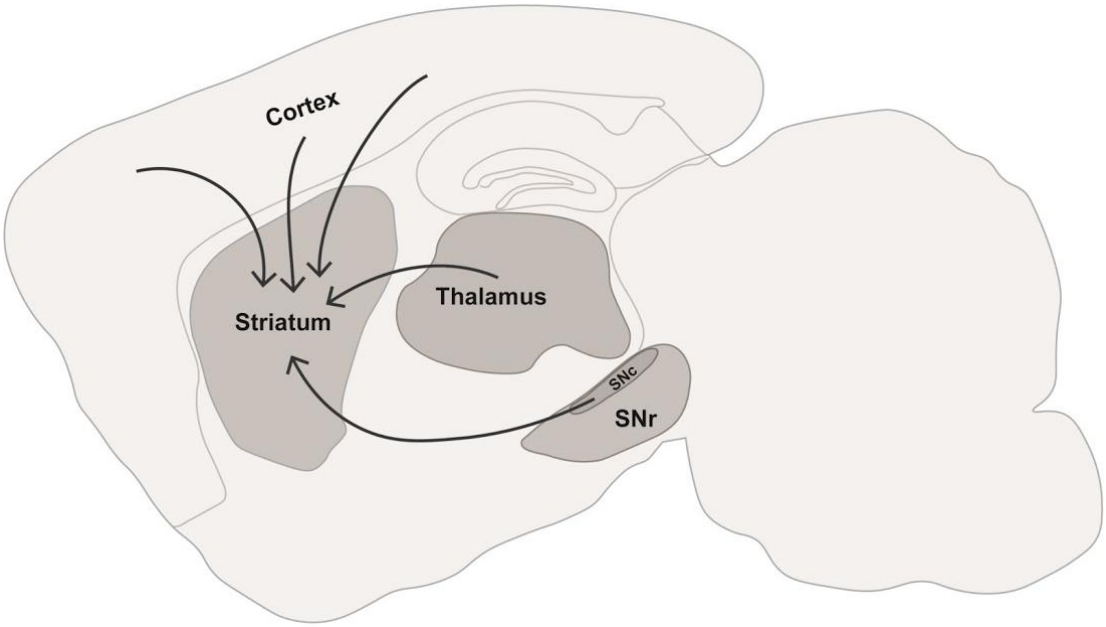

Figure 3 – **Striatal inputs.**

Image depicting the thalamic (from thalamus), cortical (form cortex) and dopaminergic inputs (from SNc) to the striatum. Adapted [22].

First, the dopaminergic afferents from SNc to the striatum have been immensely studied, since their degeneration is thought to be at the origin for the development of PD. The importance of these neurons' activity to the striatum has been studied for a long time [78,79]. Initially, it was thought that the phasic activity observed in the neurons forming this nigrostriatal pathway resembled that of a reward prediction error (RPE) signal, suggesting that a learning component was sent to the striatum through these neurons [80–84]. However, during the last decade, transient fluctuations of neuronal activity have been revisited in a different context, one that supports the idea that dopaminergic activity arising from the SNc to the striatum encodes information that encourages movement initiation and defines the vigor of upcoming movements [85–89]. Thus, the nigrostriatal pathway signals the striatum to modulate its activity based on the outcome from prior actions (RPE signalling) and to inform when movement should be implemented, by preceding striatal activity that would then result in movement initiation [22,90].

A large set of glutamatergic inputs to the striatum arises from various thalamic nuclei, in particular from the intralaminar thalamic nuclei [91–97]. Despite extensive work on the anatomical field, studies concerning the functionality underlying this connectivity are scarce and, altogether, lack the conceptualization of a global role for the

thalamostriatal pathways. Experimental work on specific neurons directly targeting the striatum has revealed the interference of thalamic populations on motor-related behavioral switching [98], appropriate timing for action initiation and participation on action performance [99]. Furthermore, thalamic nuclei containing populations projecting to the striatum have been described to be involved in motor functions such as movement preparation [100], or movement inhibition [101].

It is interesting that a preferential target for BG outputs, the thalamus, also consists of one of its main input sources. This connectivity architecture is not unique to the thalamus, as other target regions of BG output nuclei also project back to the striatum, either in direct and indirect fashion, such as the cerebellum [102,103] and the PPN [97,104,105], or strictly through indirect interaction such as the SC [69,106]. It is curious to theorize about this dense interconnection between the BG (emphasis on the striatum) and other subcortical regions. Although not explored in this thesis' project, it is important to understand if these feedback projections are important to implement in the striatum features that resembles the computations necessary for the generation of other subcortical nuclei's functions, or to simply provide information about their current state of activity. This would enable the comprehension of the nature and importance of these communications.

The limbic system also participates in the huge set of inputs to the striatum, as known by the projections coming from the basolateral amygdala and prefrontal cortex [92,95,97,107–109]. In line with the functions it regulates, amygdalostriatal connectivity has shown to contribute in motivational and reward-related learning and performance [110,111].

Within the BG, it is also important to refer that the circuitry does not follow a strict downstream path, as both GPe [112,113] and STN [114,115] have been proven to project back to the striatum. Studies exploring the functionality of such connections are still nonexistent in the case of the subthalamicstriatal pathway, while the GPe-striatum network has been proven to be critical for the suppression of actions originating from striatal activity [116].

Finally, the main driver for activity in the striatum comes from cortical input. Virtually all the cortex projects to the striatum [94,95,97,117,118] in a topographical manner [62,109,119]. This signalling stream seems to provide a large set of sensory, motor and cognitive information [120–124], helping the striatum to exert its functions based on the context and situations in which the animal is present. Functional and connectivity properties of the corticostriatal pathways will be further explored in the context of the M1-striatum connectivity, since this interface constitutes a focal point for the development of this thesis' project.

To conclude, it is important to mention that this innervation of the striatum from multiple brain areas is not homogeneous. This is, different clusters of inputs preferentially target different cell-type specific populations within the striatum, underlying the patterns of depolarization of striatal interneurons and SPNs. Furthermore, the input organization within the striatum appears to be spatially segregated. This led to the division of the striatum in dorsomedial striatum (DMS), DLS and ventral striatum (VS) [125,126]. In detail: the VS receives inputs from the basolateral amygdala, SNc, VTA, prefrontal cortex, hippocampus and anterior cingulate cortex (mainly regions associated with the limbic system) [127–130]; the DMS serves as the region that integrates the widest set of cortical inputs (although there is a bias for the prefrontal cortical areas to innervate this striatal region) [95,117]; and finally, the majority of inputs received by the DLS arise from the sensorimotor cortical regions (M1, secondary motor cortex, and the somatosensory cortices) [95,117] (Figure 4).

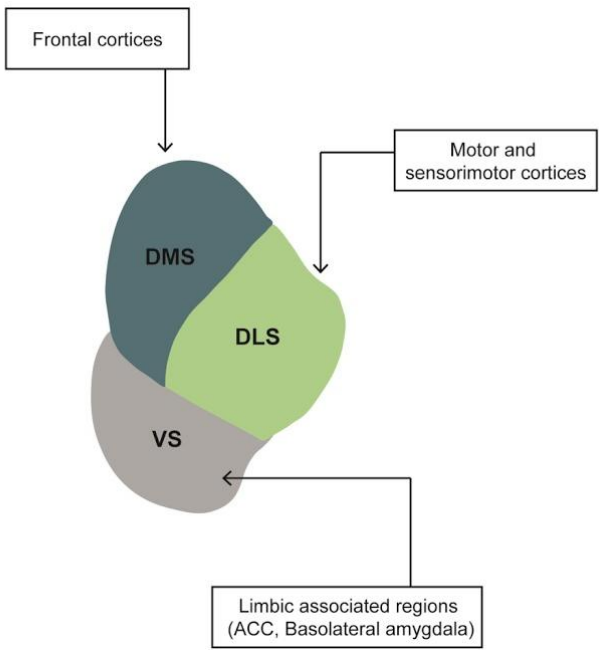

Figure 4 – **Striatum' input organization and functional division.**

Adapted from [126].

1.2.2.1 Primary motor cortex (M1)

The M1 is a cortical area divided into 6 layers, with its neuronal populations being composed of pyramidal cells and a large group of interneurons [131,132]. The pyramidal cells may be further divided into three different categories: pyramidal tract (PT), intratelencephalic (IT) and corticothalamic (CT) neurons. PT neurons send ipsilateral afferents to the striatum, brainstem, STN, SC and spinal cord, IT neuronal projections are confined to ipsilateral and contralateral connectivity with the striatum, as well as projecting contralaterally to cortical regions, and CT neurons connect with thalamic nuclei [14,132–134].

Concerning the efferents that target the M1, similarly to what is seen in the striatum, the set is large and diverse. M1 receives information from somatosensory cortices, thalamus, cerebellum, dopaminergic areas such as the ventral tegmental area (VTA), and GPe and GPi [132,135–137]. Furthermore, it has been shown that M1 activity is also modulated by BG activity, via thalamus [32,138,139].

Some of the implications resulting from this connectivity have been thoroughly investigated, providing interesting insights to how they participate in M1 functions. In particular, both the somatosensory [140–142] and dopaminergic activity [143,144] have been linked to a participative role in action learning at motor cortical level. This particular process has been extensively studied in this region [2,145–147]. Patterns of M1 neuronal activity are reorganized through learning of a motor skill [148], and although its inhibition impairs the performance of an acquired skill [149] it appears that this action component is stored in subcortical nuclei, as lesions in M1 in well-trained mice do not impair the performance of the learned skills [150].

These findings support that, although responsible for the learning properties, M1 activity transmits the motor skills' functions, during the learning phase, to subcortical nuclei such as the BG, which are able to implement those functions even in the possibility of M1 damage. This suggests that the M1 link to subcortical nuclei may underlie the foundation upon which specific motor processes are functionally exerted outside M1.

Somatotopically organized, the M1 is responsible for conveying command signals downstream to generate voluntary movements in the forelimbs, hindlimbs, head and face [2,19,151,152], with its activity preceding muscle activity [137,153]. Nonetheless, to be able to exert these execution functions with a high degree of efficiency, the M1 has to either have access or perform functions related to action representation and motor control. Representations of movements at motor cortical level have been described [21,154], but do not prove that M1 activity is able to control movement at such tuned precision. More

recent studies have provided answers to this topic, with the observation that M1 signals the timing for the initiation of movement [4,155], prevents the generation of movement previously to when it should be exerted [156] and that its disruption leads to delays in movement initiation and execution [157]. Thus, M1 activity demonstrates the precision to temporally control the initiation and execution of actions.

Finally, given the role that M1 has in action performance and control, it seems appropriate that its activity also encodes for the planning of such actions, since this function is crucial to establish a bridge between decision-making functions and action generation. Preparatory activity is a good indicator of planning functions, which has been observed in M1 prior to muscle activity [3,20]. M1 is able to prepare this planning function without translation to action generation [158], and modulate in a flexible way this preparatory activity to movement-related activity within the same neuronal populations [159].

However, despite this ability to generate action plans and translate them to activity related with the onset of movement, it is not clear if M1 contains the role of deliberating which action plan should be exerted. Although it has been revealed that competing alternative plans arise in M1 and that its activity leads to the commitment of a singular plan [5], the evaluative process characterizing the choosing of the action plan to be committed is suggested to not be performed at M1 level [157]. Whether it is performed in other cortical areas or in subcortical nuclei (such as the BG), is still a matter of debate. If it is the latter, is important to understand the significance of the circuitry between M1 and striatum, in particular what are the specific features conveyed by M1 that assists the striatum in performing action selection.

Overall, the M1 constitutes an essential node for action-related functions. In the scope of our project, M1 activity is suggested to be crucial for action initiation and execution, through influence on these processes' timing, while a role in action selection appears to be performed upstream to the M1 circuitry. Regardless, in our study we assessed the importance of M1 for all these action functions by observing the effects that disturbance of its normal activity may have on the timing to initiate and execute action, and the probability to behavioral switching.

1.2.2.1.1 Corticostriatal connectivity

As previously explained, the main source of glutamatergic inputs into the striatum comes from almost the entire cortex [92,95,117], which provides motor, sensory and

cognitive information [121–123,129,160]. The cortex projects to the striatum in a topographical manner, forming parallel circuits [62,109,119].

Also, different cortical regions have a preference for distinct cell-targets in the striatum, e.g., although corticostriatal afferents mainly project to SPNs, the M1 preferentially innervates D2-SPNs populations, while somatosensory and limbic cortices mainly projects to D1-SPNs [97]. Furthermore, different types of cortical neurons have preferential SPNs targets, as IT neurons mainly connect with D2-SPNs, while PT neurons target a higher number of D1-SPNs [161–163].

Additionally, given the relative size of the striatum compared to the size of the cortex, it is intuitive to conclude that there is a convergence of cortical inputs at striatal level. This relation has been observed with multiple cortical projections from single or different cortical regions converging into single neurons in the striatum [119,160,162]. Since SPNs have shown action-specific activity, forming neuronal ensembles to elicit specific actions [72,76,77], each cluster of neurons, whose combined activity results in a given action, may have access to the same set of inputs. Taking this into consideration, to what extent does this information flow contribute to the correct activation pattern of SPNs populations, resulting in the efficient performance of striatal functions?

Evidence that corticostriatal activity might be important for the correct exertion of striatal functions, comes from studies stating that several disorders associated with impaired striatal activity are related to corticostriatal dysfunctions [49,120,164]. Moreover, various experiments have shown that the activity of multiple cortical areas act upon striatal neuronal populations to influence a wide range of behavioral aspects. In detail, interventions on prefrontal corticostriatal projecting neurons revealed an effect on behavioral control and decision-making functions, from a learning [165,166] and motivational [124,167,168] point of view, while manipulations in the orbitofrontal cortex influence the striatum to exert goal-directed action strategies [121], presumably by providing contextual information about the environment [169]. Regarding the M1-striatum interaction, it has been shown that its corticostriatal circuit supports behavioral responding in a sensory-guided task [122], while a different set of experiments revealed that both areas work in concert to promote behavioral flexibility within an action sequence [170].

Nonetheless, regardless of its contributions to motor control (whether it contributes the functions described above or others), it is important to understand what is the nature of the information conveyed from M1 to striatum. Since both preparatory activity and depolarization at movement onset were found in M1 corticostriatal neurons [171], it is theorized that the striatum receives motor plans and commands from M1. The functional implications of the integration of this information within the striatum still

requires additional studies, raising the question about what the purpose of this signal is, given the direct connection that M1 has with the spinal cord in order to readily generate movements it planned. Furthermore, knowing that the signal transmission within M1 corticostriatal neurons differs from the one projected to the spinal cord and brainstem [171], and that SPNs responsiveness to cortical activity may be selective [123], suggests that the M1-striatum link may be required for alternative, more refined, action-related functions. Additionally, a different suggestion would be that the corticostriatal inputs are necessary to modulate the tonic inhibitory control that the BG exerts on the same downstream motor centers that M1 projects to. In this model, the generation of activity on downstream' brain motor centers would require both the excitatory inputs from M1, and the absence of the BG inhibitory signaling.

Overall, the massive set of inputs that the striatum receives enables it to have access to a wide set of information. But what is the meaning of this integration in the context of motor control? May this allow the striatum to act as an evaluative hub in the brain, in charge of selecting what actions must be exerted at any given time, by influencing BG outputs to downstream motor centers? If it is the case, there are two possibilities to the contribution of the motor plans arising from the M1 inputs: either contributing to the completion of an evaluation process or be the subject upon which evaluation is exerted.

1.2.3 An action selection role?

Experimental evidence have shown the relationship between striatal activity and a wide repertoire of motor control features such as movement generation [23,73,172], initiation and execution of actions [6,7,173,174], which is crucial for the construction of action sequences [71,86,175–178], as well as learning and acquisition of motor skills [179–183]. Furthermore, regarding movement kinetics, previous studies have shown that the striatum encodes kinetics' properties derived from motor execution and is able to implement them in future motor outputs [26,184,185].

Overall, incorporating all the information described above, the striatum would serve as a station whose activity is intimately linked to action performance, influencing motor control and being actively involved in the execution of motor skills, a function performed with fine precision given its involvement in translating specific movement properties (such as speed) into the generation of movement.

However, it has long been proposed that the overall function of the BG/striatum is related to the evaluative process of action selection [8–10,31], mainly given its anatomical features. A brain region in charge of such function would have to intimately communicate with distinct brain motor centers whose activity is directly related to the generation of movement. Fitting this requirement, as already stated, the BG tonically inhibits brainstem motor centers and motor cortical areas via thalamus. Consequently, the striatum can modulate the activity in these areas through inhibition and disinhibition of the BG output nuclei [60]. Furthermore, the fact that the BG' output circuitry is inhibitory suggests that it suppresses spurious activities of its downstream motor targets to prevent undesired movements, while the modulation of its signal would support downstream motor centers to only exert what the BG would consider as desired motor output [61]. But if this is the case, how would the striatum be able to detect what is a desired action at any given context? How would it be able to distinguish between competing motor plans and evaluate which one is appropriate?

This capacity seems to be derived from the diverse set of inputs that the striatum integrates. Among those, the ones that transmit motor commands and plans, sensory and contextual information and RPE signals constitute pillars for the performance of evaluating the value of these plans and decide which one constitutes the best action option for the achievement of the animals' goals [82,84,117,160]. To decide the optimal action course within a set of various action alternatives, it is crucial to be able to associate motor activity and the value of its outcome. In turn, this allows a continuous update on action value and provides the tools to select the best action plan for any given context. Consistently, striatal SPNs respond to the outcomes of motor output by encoding the value of the actions exerted [186–190]. Furthermore, in a switching two-alternative choice probabilistic task, Tai and colleagues [191] elegantly demonstrated that the selective stimulation of both SPNs populations (which resembles additive changes in action value), prior to the initiation of movement towards a specific choice, influenced the choice selection depending on previous reward outcomes. These results showcase that the encoding of action value from previous actions allows the striatum to mediate action selection.

How both striatal SPNs populations would contribute to such a function has been an intense topic of discussion. Early on, it was postulated that D1 and D2-SPNs would contribute in striking opposing manner to the process of selecting the most appropriate action. D1-SPNs activity would be responsible for the support of the chosen action, while D2-SPNs activity encoded the suppression of all other competing actions [9]. However, recent studies have shown that both SPNs populations are highly action specific [72,76,77], which is starting to give rise to a new order of thinking that states that

instead of a general suppression of multiple action plans, D2-SPNs activity actually relates to the inhibition of specific movement features that allow the proper performance of the movement intended. Think of the extension/flexion of the arm as an example, for which the combination of excitation and inhibition of certain muscles is needed to achieve optimal performance. The same studies also demonstrate that the relationship between striatal activity and the exertion of specific actions derives from specific striatal neuronal ensembles, which in turn suggests that the striatal pattern of depolarization represents a single action plan. Therefore, instead of signalling a combination of the chosen and discarded actions, the striatum would only signal the action it considers the most appropriate.

Overall, the striatum appears, from a macro to a microscopic scale, to constitute a suitable neuronal stage to evaluate and select the ideal action plan within a number of different ones. As a model, the striatum would integrate various action plans from M1, evaluate which action plan should be exerted at any given context and consequently project the result of this process to downstream motor centers, in order to elicit the generation of the action it considered appropriate. Since the information containing the action plans is conveyed by M1 and integrated in DLS [117,119], we decided to study both areas in the same behavioral paradigm to not only give further insight on the role the striatum contains in action selection, but to also elucidate about the importance of this M1-DLS corticostriatal link to the performance of this process at striatal level. Furthermore, besides evaluating the M1 and DLS contribution to the process of action selection, we also assessed the role of both regions for proper initiation and execution' timing of actions, functions that have been linked to both M1 and striatum activity [6,7,153,155]. Studying both areas upon identical conditions may clarify the importance of both regions in these processes.

1.3 Methodology

1.3.1 Probabilistic three-alternative-choice task

In order to evaluate and characterize the role of the M1-DLS corticostriatal circuit for action selection, a behavioral task that allows such study must follow a number of requirements.

First, the task presented to the animals must require an evaluative process by the animal, that is, to select one action from a set of alternative choices. Taking into account the requirements for the exertion of such a process, the task must provide a framework in which animals learn to associate their action choices with the outcomes that result from it (while integrating the value of such outcomes with their internal state), and consequently use that information to properly choose the next action course.

In this project, a probabilistic three-alternative-choice task was designed to match these requirements, in which water-restricted mice received a water reward depending on the probabilities of water delivery respective to each choice (one of the choices had a higher probability of delivering water). During task performance the choice with the higher reward probability shifts in a block-wise manner, thus requiring the animal to adjust their behavior accordingly.

Furthermore, the implementation of a probabilistic approach on our task was to encourage the exploration of all choices by the mice (i.e., mice did not simply exploit the option with the highest reward probability). Finally, the addition of a third choice is crucial to guarantee that the mice are evaluating the task and selecting actions that are appropriate for the task correct resolution. With a two-alternative choice task, one cannot assess if the animal is indeed choosing one option, since in this case selecting one option is equivalent to suppressing the alternative one. By adding a third choice these limitations are easily circumvented.

Overall, this task was thought to match the aforementioned requirements to provide a suitable stage to assess the importance that striatal and motor cortical neurons may have in action selection. Furthermore, the design of the task allows the dissociation of the processes concerning the initiation and execution of actions, within the task ‘performance. This provides a platform to assess the importance of M1 and DLS activity for the timing on each of these processes. More details of this three-alternative-choice task will be further described in the “Materials and Methods” section.

1.3.2 Optogenetics

To evaluate the participation of the M1 and DLS on action selection, the use of a method that allows the disturbance of both these regions’ neuronal populations while mice perform the three-alternative-choice task would provide us a greater comprehension regarding the importance of these neuronal circuits for the exertion of such function.

In order to correctly complete the three-alternative-choice task, mice need to comply with some requisites that need to be fulfilled. These requisites allow to dissociate various phases of the task in a way that action initiation, execution and selection functions may be separately studied. Therefore, to investigate the contribution of M1 and DLS for each of these functions the technique employed must allow a precise temporal manipulation of these regions' neuronal activity.

In 1979, Francis Crick mentioned that the ability to manipulate individual components of the brain would be extremely valuable for the proper study of the brain function, stating "a method by which all neurons of just one type could be inactivated, leaving the others more or less unaltered" [192]. Nowadays, Crick's hopes and dreams have come to fruition, with the development of tools that allow such type of manipulation, with a high degree of specificity. In detail, both optogenetic and chemogenetic strategies fit Crick's description [193,194], although only the use of optogenetics allows neuronal manipulation at very precise temporal windows, leading us to opt by this method for our experiments.

Optogenetics allowed neuroscience to take a step forward in how to control neuronal activity, providing a set of tools to either excite or inhibit specific neuronal populations [195,196]. Defining what kind of manipulation (inhibitory or excitatory) must be implemented depends on the requirements of the experiment itself. In this project, we wanted to assess the necessity of M1 and DLS neuronal populations in different action aspects and therefore opted for an inhibition strategy. Optogenetic inhibition has the also the advantage that it is inherently more specific. While optogenetic excitation activates all opsin-expressing neurons within a given brain volume, inhibition only directly perturbs the neurons that would be activated under the normal task conditions. Thus, a general excitation approach would fall short on mimicking the natural neuronal depolarization elicited to respond to the situations presented in the task.

However, optogenetically inhibiting neurons is generally more difficult to implement than excitation methods, since the usage of inhibitory opsins poses a wide set of constraints [197]. The more commonly used inhibitory opsins (light-driven ion pumps) require continuous illumination to achieve prolonged hyperpolarization given their poor ion-photon stoichiometry, which in turn is highly problematic due to risks of tissue heating (which can alter neuronal physiology, such as increased neuronal firing rates) [198,199] and phototoxicity [200]. Furthermore, it has been shown that vast periods of illumination result in photocurrent amplitude decreases of 50-90%, leading to reduced silencing efficacy over time [201,202]. Additionally, following the offset of light illumination the targeted-neuronal populations may increase in firing rate (also referred to as rebound activity) [203].

Altogether, there are a series of caveats with the use of inhibitory approaches within optogenetic experiments. However, recent developments on this topic have revealed new promising optogenetic tools that present answers to the constraints described above. Within this new class of inhibitory opsins, one of the more recently described ones display optimal properties for the use of optogenetic inhibitory approaches, which led us to opt for its use in our experiments [204]. This opsin, soma-targeted *Guillardia theta* anion-conduction channelrhodopsin (stGtACR2), will be described in the next section of the introduction.

1.3.2.1 stGtACR2

The discovery of a class of anion-conducting channelrhodopsins (ACRs) provided a promising alternative in relation to the oldest set of inhibitory opsins, since their properties present the capacity to surpass most of the caveats previously identified in the use of light-driven ion pumps. Named GtACR1 and GtACR2 (in reference to the algae from where they were discovered, *Guillardia theta*), this class of ACRs distinguish themselves from the light-driven ion pumps due to their restricted anion selectivity, high single-channel conductance, which leads to the generation of powerful photocurrents in response to light, and increased ion-photon stoichiometry [205]. These properties enable the design of inhibitory experiments in which light exposure may be of lower power when compared with the most widely used inhibitory opsins, preventing the tissue heating and phototoxicity problems that arise from longer, higher power, light pulses into the animal's brain.

However, ACRs response to light may induce neuronal depolarization, instead of inhibition, when intracellular chloride concentration is high. Spatially, this may happen in the synaptic and axonal compartments of neurons, which contain high chloride levels. Consistent with this hypothesis, activation of GtACRs has been shown to induce antidromic spikes [206] and presynaptic release [201]. Furthermore, as it frequently happens in various types of opsins, ACRs also display poor membrane targeting in mammalian cells [204].

In order to circumvent these limitations, Mahn and colleagues [204] developed stGtACR2, which displayed very interesting characteristics for its use in inhibitory experiments. In detail, the addition of membrane- and soma-targeting sequences restricted the localization of the opsin to the somatodendritic compartment and improved its membrane targeting. This improvement led to generation of more powerful

photocurrents, higher light sensitivity and lower frequency of antidromic spikes when compared with GtACR2, in both electrophysiological and *in vivo* conditions. Furthermore, inhibition of the basolateral amygdala, through stGtACR2 expression, of mice performing a behavioral task intended to study a known functional link (basolateral amygdala and formation of extinction memory) led to similar results to those previously published, showcasing that stGtACR2 efficiently silences targeted neuronal populations *in vivo*.

This set of results compelled us to utilize this opsin in our inhibitory experiments.

1.4 Aims and hypothesis

Both M1 and striatal activity seem to be thoroughly involved in multiple aspects of action, sitting atop the chain of events that ultimately lead to movement generation. Considering their impact on the timing for action initiation and execution[4,6,7,155–157,173,174], and the hypothesis that action selection is performed at striatal level[8–10,191], while the M1 contributes to this role by providing the action plans upon the selection process is performed, we developed a probabilistic three-alternative-choice task to provide results that may enable the comprehension of the importance of these areas for each of these functions.

Given the published results that support the participation of M1 and striatum on these action processes, leads us to hypothesize that: 1) both M1 and DLS participate in action initiation, 2) M1 and DLS neuronal activity is important for action execution and 3) DLS participates in action selection.

To test these hypotheses, we aim to:

1. validate the use of stgtACR2 in M1 and DLS, through histology assays;
2. optogenetically inhibit M1 and DLS at different timepoints in a probabilistic three-alternative-choice task to assess their role in the timing for action initiation and execution, and in the action selection component of the animals' motor behavior.

2. Materials and Methods

2.1 Animals

All animal procedures were reviewed by and performed in accordance with the Champalimaud Center for the Unknown ethics committee guidelines and approved by the Portuguese Veterinary General Board (Direcção Geral de Alimentação e Veterinária; DGAV).

Experiments were carried out using adult (≥ 3 months) male C57BL6 wildtype mice, housed on a 12 hour light/dark cycle with ad libitum access to food and water. After fiber implantation (see below), mice were single housed. Mice used in behavioral experiments were submitted to a water restriction regime 1 day prior to the start of the training period until the end of the experiments.

In total, 33 mice were used for experiments in this project. 9 mice were used for histological evaluation during the optimization of opsin expression' experiments (annex; Table S1), while 24 mice were used for behavioral experiments (annex; Table S2).

2.2 Stereotaxic virus injections and fiber placement

Animals were submitted to surgeries performed under sterile conditions and isoflurane anesthesia (0.5%–4%, plus oxygen at 0.8-1.5 l/min) on a stereotaxic frame (Kopf instruments).

Mice heads were shaved, cleaned with 70% ethanol and iodine, and a small incision on the head skin was made (from posterior to anterior). Following the skull alignment and craniotomies procedures for the virus injections, animals were bilaterally injected either with pAAV1-CKIIa-stGtACR2-FusionRed (Addgene plasmid # 105669; titre = 1.5*10^13 genomic copies (gc)/ml) for opsin expression (stGtACR2 experimental group), or pAAV1.CamKII(1.3).eYFP.WPRE.hGH (Addgene plasmid # 105622; titre: 1.9*10^13 gc/ml) for eYFP expression in mice belonging to the control experimental group. After virus injection, 400 µm diameter optic fibers (Doric Lenses) were implanted, bilaterally, 100 µm above the injection site, either in M1 (AP: 1 mm, ML: 1.4 mm, DV: 0.3 mm) or DLS (AP: 0.5 mm, ML: 2.5 mm, DV: 2.0 mm). Fibers efficiencies were measured before implantation. Once in place, the optic fibers were secured to the skull using a combination of Superbond (Sun Medical/Parkell, C&B) and black Ortho-Jet powder and liquid acrylic resin (Lang Dental, USA), forming a dental-cement-based

cap. Stainless-steel screws (1 per mouse) were attached to the skull to provide a scaffold to build the cap.

In order to optimize the volume, titer and number of viral injections to achieve optimal opsin expression in M1 and DLS, we tested different strategies in a cohort of mice prior to the behavioral experiments. In the first section of the results, the rationale and findings that led to our final strategy will be described in detail. Therefore, if not stated otherwise, for both eYFP and stGtACR2 experimental groups, the virus quantity delivered and injection coordinates were: 990 nl for expression in M1 (AP: 1 mm, ML: ± 1.4 mm, DV: -0.4 to -0.9 mm) or 1000 nl for expression in DLS (AP: 0.5 mm, ML: ± 2.5 mm, DV: -2.1 to -2.5 mm). In both M1 and DLS injection procedures, the viral cargo was diluted in order to reach a final titer of 1.5*10^12 gc/ml (1:10 dilution for stGtACR2 injections; 1:12.5 dilution for eYFP injections). To achieve a broader area of expression in the targeted regions, horizontally, 2 injections were made on each hemisphere in DLS (500 nl of virus delivered per injection), while M1 was targeted, in both hemispheres, in 3 different locations (330 nl per injection). These injections were administered 100 and 120 µm apart from the coordinates for fiber implantation in DLS and M1, respectively (Figure 5). To reach the same goal vertically, for each injection the pipette was retracted 100 µm, approximately, every 2 minutes, in a total of 9 minutes for DLS targeting (DV: 2.5 - 2.1 mm) and retracted 100 µm every minute, in a total of 6 minutes in the case of M1 targeting (DV: 0.9 - 0.4 mm).

Injection procedures were performed using glass pipettes coupled to a Nanoject II Injector (Drummond Scientific, USA) at a rate of 4.6 nl per pulse every 5 s. The injection pipette was left in place for 8-10 minutes, post-virus delivery. The virus aliquots were stored at −80 °C, thawed before surgery and kept on ice until the injection procedure. After the injection/implantation procedures, the head scalp was sealed with Vetbond tissue adhesive (3M, USA) or sutured with braided stitches (Ethicon, USA). Animals were allowed to recover for at least 7 days before the behavioral experiments were initiated.

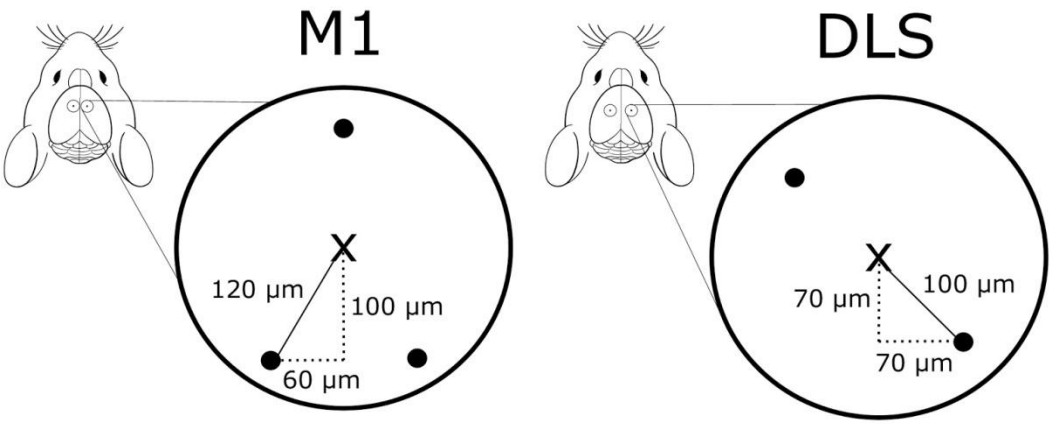

Figure 5 - **Strategy for injection positions in DLS and M1.**

Graphical depiction of the strategy to achieve a wider opsin expression in both M1 and DLS, by performance of multiple injections per hemisphere. Inside each circle, black dots correspond to the injections position in relation to the coordinates for the center of the fiber implant (represented in the figure as X). Dotted lines correspond to representative traces of the mathematical operations performed in order to achieve the same distance for each injection.

2.3 Behavioral training and probabilistic three-alternative-choice task

Behavioral experiments were conducted by using water-restricted mice performing a probabilistic three-alternative-choice task. Due to fiber misplacement (observed after histological evaluation; > 500 µm displacement relatively to the intended AP coordinates), loss of fibers during the behavioral experiments and poor performance of the behavioral task (see Data analysis section of the Material and Methods, below), 6 out of 24 mice were excluded from the behavior analysis.

We used custom-made behavior boxes (inside sound-attenuating mouse operant chambers) with 3 side pokes and a central initiation poke hole using the pyControl framework [207] (Figure 6A)). The task can be divided in three different events: mice nose poking a central hole, to initiate a trial (Center In); mice reporting a choice by nose poking one of three side holes (left, right and high in relation to the central one) (Side In), with only one supplying water with a higher probability; and outcome (400 ms delay after Side In) according to the assigned probabilities (p=0.25 and 0.75, respectively). Furthermore, the next trial initiation was only completed if the next center poke (Next Center In) occurred after an inter-trial interval (ITI) of 1-1.5 seconds. Therefore, the

mice's attempt to initiate the next trial may, or may not, lead to the initiation of the next trial, depending on the timing of execution of this attempt.

Lights, at each side hole, turned on when mice nose poked the center hole, and off after they nose poked one of the side options, signalling trial initiation and successful report of their choice, respectively (Figure 6B)). Holes had appropriate dimensions so that mice had easiness in nose poking them, and nose entries on the holes were recorded using an infrared beam. Water was supplied through a metal tube inside each side hole. Mice run one session per day.

Behavioral sessions lasted for 45 minutes and mice obtained 4 µl of water for each rewarded trial. Mice had to choose between the three side options, with only one of those rewarding water with a higher probability (0.75, compared to 0.25 on the other options). The option with a higher water reward probability changed, randomly, after a set number of trials (average of 40 trials), dividing the session in a block-wise manner.

In order to perform the task while being submitted to light stimuli with high behavioral performance (3 weeks of light manipulations in the behavioral experiments), the mice had to be trained in simpler versions of the task at an initial stage. Mice initially performed a probabilistically-free version of the task, obtaining 10 µl water rewards from all side pokes in a 90 minute session. Maximum number of rewards per poke was 30 in the first session, with the mice typically exploring all three pokes. Next, animals began training in fixed probabilistic task' versions, where the probability for water delivery gradually changed from 0.95/0.05 to the final values of 0.75/0.25, and the session length trended to the final value of 45 minutes (Figure 7). Training took an average of 3 to 4 weeks until mice achieved high behavioral performance.

We developed a custom-made system, with coupling of the mice' fibers to optic fibers hooked to a rotatory device sitting atop the mouse operant chamber (Figure 8), in order for mice to habituate to performing the task with patchcords connected to its optic fibers (for optogenetic experiments). This strategy was implemented starting from the second week of training until the end of the training period.

Water was restricted throughout the period of behavioral experiments and mice were controlled throughout all training phases and experiments to be above 85% of their original body weight. When dropping below that value, mice were supplemented with a volume of water typically between 0.5 and 1 ml, in order to increase their body weight. In situations where mice were getting close to 85% of their original body weight, or a combination of poor behavioral performance and a body weight percentage between 85-90%, the goal was to maintain the mice body weight so it didn't drop below the set value of 85%. In these cases, the water volume supplemented was determined accordingly with the water amount the mice ingested in the session, so that they drank

a total of 0.5/0.6 ml of water a day (water obtained from the experimental sessions plus the water supplied) [208].

In addition to the poking behavior, animal behavior was recorded using a lickometer, a head-mounted, wireless 9-axis accelerometer (200 Hz sampling) and a video camera (60 frames/s, PointGrey) mounted at the top of the operant chamber. Timestamps of nose entries, licks, accelerometer and video data were recorded using a HARP base-station and synchronizer developed by the Champalimaud Hardware Platform. For behavior analysis in this thesis, only the nose pokes and lick datasets were used.

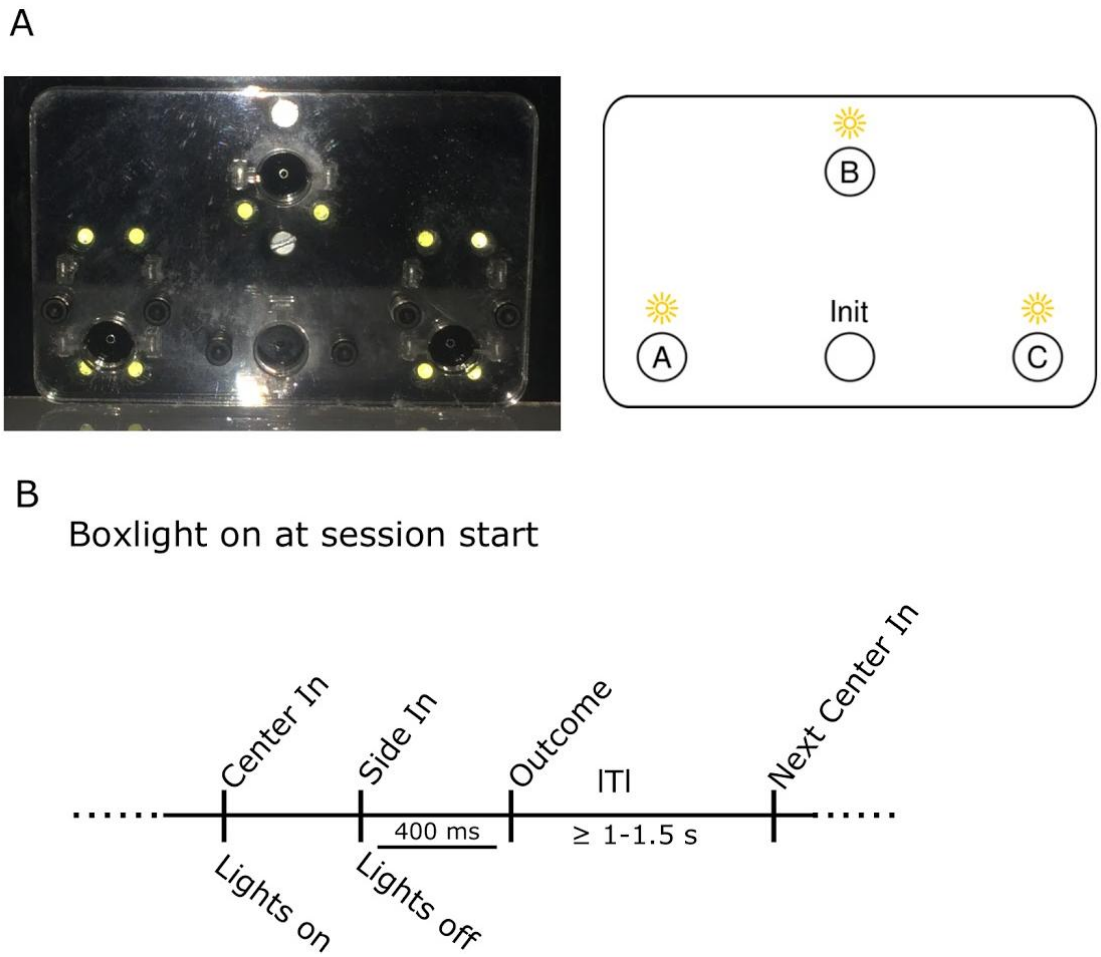

Figure 6 - **Structure and layout of the behavioral task.**

(A) Left image showcases an example of one of the acrylic boards where mice executed the task. Right image displays the schematics of the board, representing the event after mice initiate the trial, as observed by the light atop each side hole. “A”, “B” and “C” represent the left, high and right holes, respectively. “Init” refers to the central hole, which, if nose poked, leads to trial initiation.

(B) Task design for trial execution. “Lights on” correspond to the turning of the lights in the side pokes, after Center In (i.e., trial initiation), while “Lights off” refers to

the turning off of the lights at Side In (i.e., signalling report of choice). Note that Next Center In only corresponds to next trial initiation if the mice's next center poke occurs after the ITI.

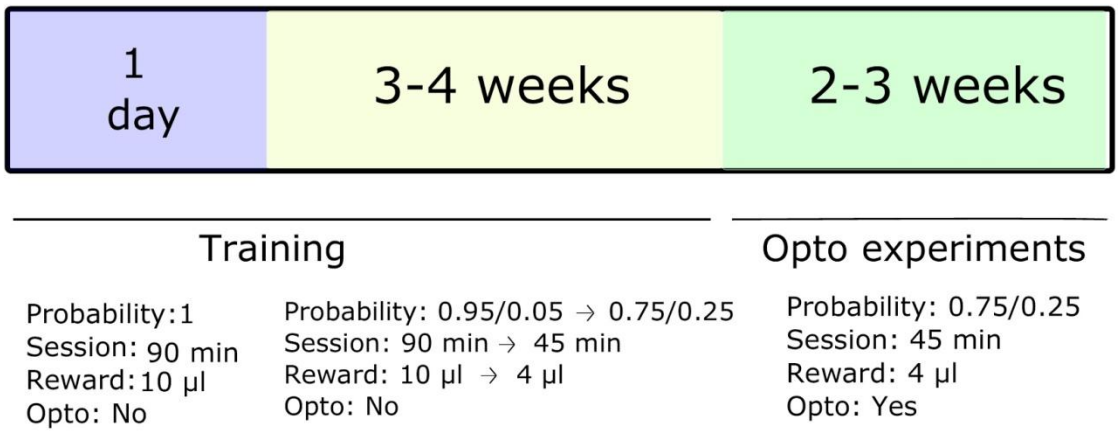

Figure 7 - **Task parameters across different training' phases and behavioral experiments.**

Structure of the average time period for the training phases and behavioral experiments, along with the parameters used in each of those phases. "Opto" stands for optogenetics.

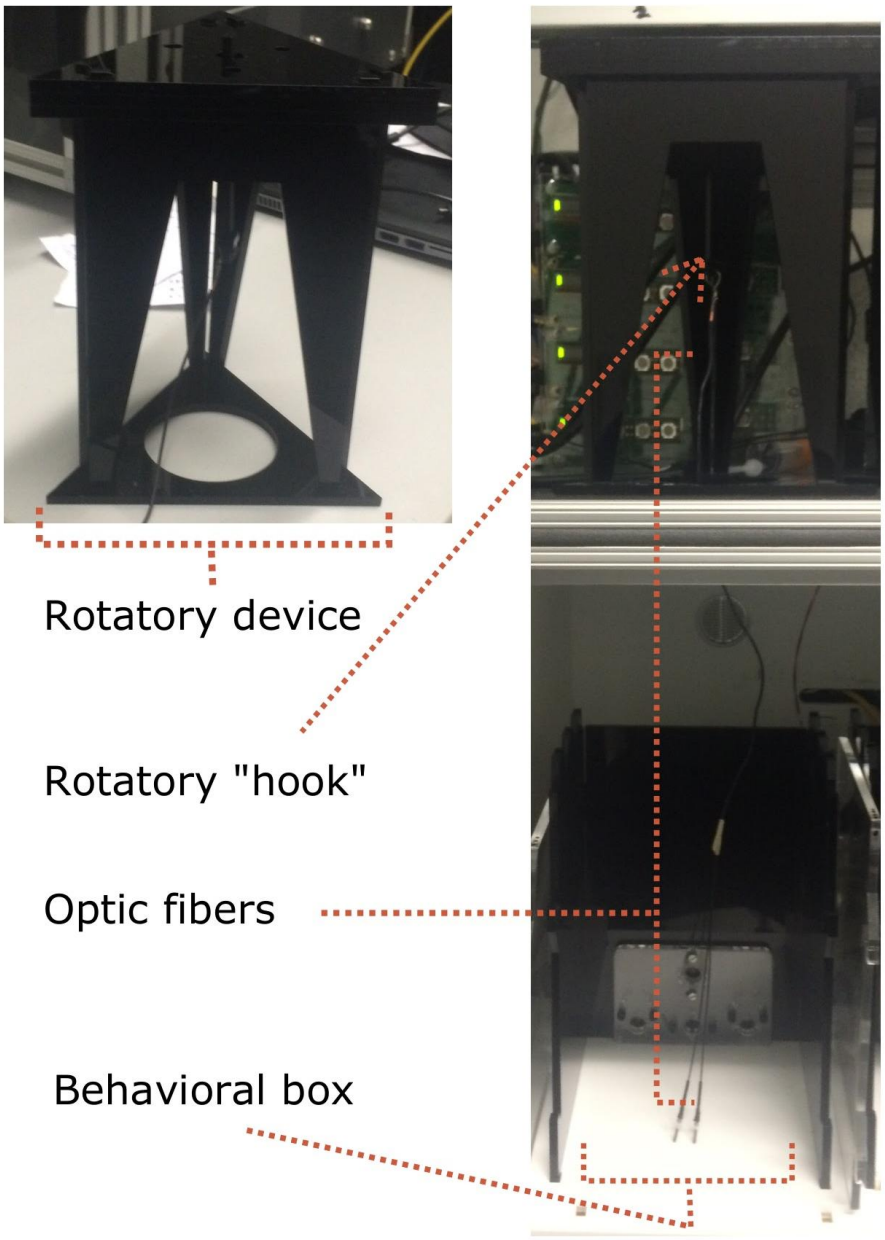

Figure 8 - **Custom-made rotatory device used during the training phase to improve mice behavior during behavioral experiments.**

To acclimate mice to the placement of optic fibers during the performance of behavioral experiments, during the training phase the custom-made rotatory device depicted above was used. “Practice” optic fibers would be placed to the optic fibers implanted in the animal and consequently locked to the rotatory “hook”.

2.4 Light manipulations in vivo

Inhibition of neurons expressing stGtACR2 after optical stimuli, in mice performing the behavioral task, was achieved through 400 µm diameter optic fibers (Doric Lenses) coupled to 400 µm diameter patchcords (0.48 numerical aperture) connected to a single 470 nm-blue LED. A fiber optic rotary joint (Doric Lenses) was used in order to ease the movement of the mice without entanglement of the patchcords. Light delivery was controlled via external analog modulation, through a LED driver (LEDRVP_2CH_1000).

Light delivery in optogenetic sessions had either light powers of 8 mW (8 mW sessions) or 0mW (0mW sessions), at the fibers' tips. Two consecutive no-light sessions (no coupling of optic fibers to the fibers implanted in the mice's head) were carried out after five 8 mW sessions, for a period of 2 weeks. The final week consisted of 0 mW sessions intertwined with 8 mW sessions in which light delivery was executed for 10 consecutive trials (8mW_10stim sessions) (Table 1). To avoid the surge of firing rates superior to the baseline neuronal activity (rebound activity), a caveat observed in light-based inhibition experiments, offset of the light pulses contained a 50 ms ramp down section, a strategy implemented in optogenetic experiments that has successfully prevent rebound spiking activity [201,203,209].

To set up the protocol for light-stimulation durations we had to take into account the different events that the task comprises, as well as the average time that mice took to complete each event. The time values were based on previous imaging data from mice performing the same behavioral task (data not shown), and the current data (0 mW) is consistent with those values: after choice report (Side In), the median time for mice to attempt to initiate the next trial (Next Center In) depends whether they were rewarded (4.89 ± 1.85 s) or not (1.76 ± 1.01 s) (Median ± median absolute deviation for all trials: 3.89 ± 2.90 s), while from trial initiation (Center In) to choice report (Side In), the median time taken by mice is around 600 ms (0.59 ± 0.19 s). Therefore, in order to test the inhibition effect after Side In, optical stimuli were delivered for a maximum period of 5000 ms (the time window was calculated based on rewarded trials). After Center In, light stimuli were delivered for up to 2000 ms or until Side In.

The LED was calibrated before each experiment so that light power measurements at the patchcord fibers tip matched the required light power to have 8mW at the tip of the implanted optic fibers. These measurements were verified using a power meter (PD1000-S130C, Thorlabs).

Table 1 – **Example of the distribution of the different optogenetic sessions throughout the 3 week-period of light manipulation experiments.**

Demonstration of the optogenetic session's arrangement throughout the period of light-manipulation experiments. Mice performed 5 consecutive 8 mW sessions, followed by two no-light sessions, for a period of 2 weeks. In the final week of experiments, 0 mW and 8mW_10stim sessions were intertwined. The example below displays one of the strategies used for the arrangement of sessions in the final week of experiments. Other often used strategies consisted of two consecutive 8 mW_10stim sessions in the final two days of experiments.

Optogenetic session	Day
8 mW	1
8 mW	2
8 mW	3
8 mW	4
8 mW	5
No-light	6
No-light	7
8 mW	8
8 mW	9
8 mW	10
8 mW	11
8 mW	12
No-light	13
No-light	14
0 mW	15
0 mW	16
8mW_10stim	17
0 mW	18
8mW_10stim	19
0 mW	20
8mW_10stim	21

2.5 Immunohistochemistry

After completion of the behavioral experiments, mice were sacrificed. Animals were first anesthetized with isoflurane, followed by intraperitoneal injection of a mixture of ketamine and xylazine and, finally, transcardially perfused with saline and 4% paraformaldehyde (PFA).

Brains were extracted for histological analysis, kept in 4% PFA overnight and washed in 1x Phosphate Buffer Saline (PBS) for at least 24 h. Before sectioning, brains were stored in 30% sucrose in 1x PBS solution for 1-2 days to provide cryoprotection. The brains were sectioned, coronally, in 50 µm slices using a sliding microtome (Leica, SM2000R). Slices were kept in 1x PBS solution before mounting or execution of immunostaining protocols.

Brain slices were stained with 4,6-diamidino-2-phenylindole (DAPI) (Sigma). The selected slices were first washed in fresh PBS 1x, then transferred to mixed solution of PBS 1x with DAPI (diluted 1:1000) where staining occurred for 15 minutes. Lastly, the slices were rinsed in PBS 1x prior to mounting.

Glass slides were coverslipped with Mowiol mounting medium, and the edges sealed with nail polish. Spread of opsin (stGtACR2) expression was confirmed, by imaging the FusionRed fluorescence (fluorophore fused to the opsin) on a Zeiss AxioImager M2 widefield fluorescence microscope, with sections being imaged with a 10x, or 20x, magnification objective.

2.6 Data analysis

To analyze the spread of opsin expression in M1 and DLS of mice used for opsin optimization in cortical and striatal conditions, measurement of the maximum horizontal extent of stGtACR2 expression around fiber tip was calculated using the FIJI/ImageJ software. A horizontal line was drawn between two points below the fiber tip (maximum 500 µm, vertically), where widest FusionRed fluorescence was observed.

Measurements were obtained by calculating the maximum distance between two points that presented 80% of the maximum fluorescence value within that horizontal line. Measurements were only performed on slices with the widest spread of expression, considering all the brain sections collected. Furthermore, for mice where no optic fibers were implanted, the points established for the drawing of the horizontal line were considered to be proximal to the injection site, while the measurement's criteria described above were also implemented.

Analysis of the behavioral data was performed on Python. Behavioral sessions included in the behavior analysis were composed of at least 100 trials and three choices per poke. This method was implemented to filter the data collected, allowing the analysis of sessions where good behavioral performance was attained. Furthermore, for mice taking a time period (in trials without light stimulation) similar to the one for the light stimulation from Side In to the initiation of the next trial (between 4 and 5 seconds), were removed from the analysis.

As previously explained, the median time that mice take to attempt the initiation of the next trial (Next Center In) depended on whether the previous trial resulted in a reward or not. After rewarded trials, the Next Center In had a higher probability of occurring outside the light manipulation period, when compared with non-rewarded ones, which may be related to the mice's behavior variability across individuals (e.g., the time spent on the consumption phase) (Figure 9).

Since we wanted to assess the effect of M1 and DLS inhibition on the performance of the action processes we studied, we decided that analysis on the event from Side In to Next Center In should avoid occurrences in which Next Center In was performed outside the time-window of light illumination. Additionally, the presumable variability in the mice's behavior after rewarded trials makes it difficult to evaluate if differences in the time spent to initiate the next trial is derived from impairment of DLS/M1 activity or related to the particular set of behaviors that each mouse displays after receiving a reward, even if Next Center In occurred within the 5 s light manipulation period. This observation must be taken into account when analyzing the involvement of DLS and M1 on the action initiation process. Therefore, if not stated otherwise, we only analyzed non-rewarded trials when assessing the M1 and DLS contribution to the action processes we studied, from Side In to Next Center In.

Plots were done using Matplotlib.

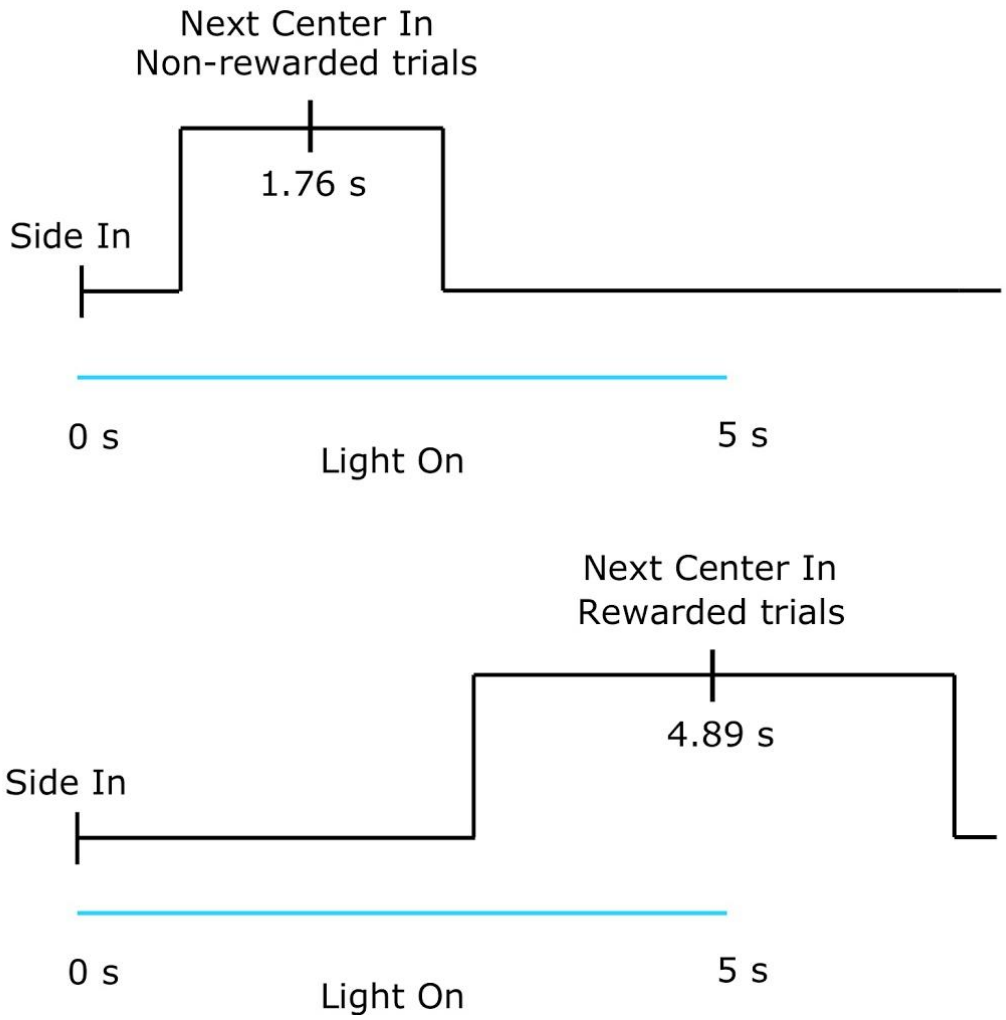

Figure 9 – **Median times to Next Center In after non-rewarded and rewarded trials.**

Median of times took by mice to Next Center In depend on the outcome of the previous trial. On top, medians of times for Next Center In after non-rewarded trials: 1.76 ± 1.01 s. Below, medians of times for Next Center In after rewarded trials: 4.89 ± 1.85 s. There is a higher probability of Next Center In events outside the light illumination period, after rewarded trials. From Side In to Next Center In, the light pulse is 5 seconds, maximum.

2.7 Statistical analysis

Statistical testing was performed using Python or GraphPad Prism 7 software.

For the statistical analysis, behavior data distribution was tested for normality by using the Shapiro-Wilk test. If not stated otherwise, unpaired t-tests were used for statistical comparisons between the groups in study. In bar plots, error bars represent the mean ± SEM. Statistical significance was considered for p-value < 0.05.

3. Results

3.1 Optimization of stGtACR2 expression in striatum and motor cortex

3.1.1 stGtACR2 expression in DLS and M1 is improved after virus delivery at diluted titers.

For usage of the stGtACR2 opsin on the optogenetic experiments, optimization of its expression in M1 and DLS was crucial. Besides being standard procedure to optimize all the variables taking place in an experiment, this step was especially crucial since stGtACR2 was only recently published [204]. Consequently, the literature using stGtACR2 is still scarce. Therefore, we decided to explore the virus expression' levels at different titers and volumes.

Our main priority was to achieve a sufficiently large volume of opsin expression in our regions of interest. Due to the inherently difficult feat of optogenetically inhibiting large neuronal populations[197], we optimized a series of parameters for the optogenetic inhibition experiments. First, based on the imaging experiments that used a 1 mm graded index lens for calcium imaging, we opted to use 400 µm-diameter fibers, instead of the usual use of 200 µm fibers in light-manipulation experiments [210–213]. To counter the effects of absorption and scattering resulting from light propagation in neuronal tissue [196,199,214], the use of larger optic fibers, with higher numerical apertures, improves the extent of light delivery throughout the targeted area. Therefore, the use of 400 µm-diameter fibers allowed us to illuminate a sufficiently large volume beneath the fiber tip. Next, we varied virus titer and injection volume to obtain dense and widespread opsin expression in M1 and DLS. For optimization purposes, we decided to test three different titers.

We first injected the virus AAV1-CKIIa-stGtACR2-FusionRed (virus used in all stGtACR2-related surgery procedures) at full titer [1.5*10^13 gc/ml] based on some of the stGtACR2-related literature that reported the usage of the virus at its original concentration[215–218]. This approach was implemented as neuronal expression of other opsins (such as ChR2, Jaws, ArchT) and calcium indicators (e.g., GCaMP6f for calcium imaging) is successfully achieved through virus delivery at high titers, in the range of 10^12 to 10^13 gc/ml [7,72,88,210,213,219–230].

We injected two mice with a small volume of 200 nl of virus at full titer: one mouse was injected in DLS (DV: 2.5 mm), while the other one was injected in M1 (DV: 0.6 mm). Figures 10A) and 10B) display the schematic traces of the injection locations in M1 and DLS, respectively. In Figures 10C) and 10D), we can observe images of the histological sections obtained from the brains of the injected mice. Brain' slices were stained for DAPI (a stain that strongly, and preferentially, binds to DNA) to assess if cell density was affected by expression of the opsin, since neurons tend to be weakly tolerant to over expression of exogenous proteins, as already reported for some opsins [231,232]. The results present heterogeneous DAPI marking in DLS, but not on M1. This pattern observed in DLS is also noticeable when analyzing the outline of stGtACR2 expression in both M1 and DLS, with lower expression beneath the fiber and with the higher fluorescence observed in areas further away from the injection coordinate. Nonetheless, the spread of the expression beneath the fiber tip revealed to be adequate for performance of inhibition experiments, since the length of horizontal expression is higher than the diameter of the optic fiber (400 µm), for both DLS (898 µm) and M1 (591 µm) (annex; Table S3). The heterogeneity of DAPI fluorescence in DLS suggests a possible neurotoxic event in the targeted regions.

Given that the use of the virus at full titer seems to affect the targeted regions at cell-level (mainly in DLS), and leads to unwanted patterns of opsin expression, we decided to analyze the expression patterns of diluted titers, an approach also observed in stGtACR2-related literature [233,234]. Therefore, we decided to inject a slightly larger volume of virus (300 nl) in a 1:10 dilution (final titer: 1.5*10^12 gc/ml), in both DLS and M1 (M1 was targeted on the left hemisphere, while the opposite hemisphere had the DLS as a target of viral injections).

In contrast with what we observed in Figure 10, we did not observe the apparent neurotoxic phenomena when injecting the virus at this diluted titer, since DAPI labeling looks homogeneous on the studied regions (Figures 11A) and 11B)). Furthermore, the distribution of opsin expression appears homogeneous around the injection site as it would be expected from the diffusion of the virus from the injection center. This suggests that titer, rather than volume, could be the cause not only for the detrimental effect on cell density, but also for the aberrant stGtACR2 expression observed in M1 and DLS after virus delivery at viral stock titer (Figures 11C) and 11D)).

However, despite the improved expression pattern, the width of opsin expression (M1 = 376 µm; DLS = 426 µm) appeared insufficient to a proper execution of our experiments, which constitutes a serious concern since the volume of expression was one of the main parameters we intended to optimize in this pilot experiment (annex; Table S4). Thus, a higher volume of 500 nl was used to achieve a bigger area of opsin

expression (n=6). Furthermore, we decided to deliver the virus at a more diluted concentration (1:30 dilution; final titer: 5*10^11 gc/ml), to assess stGtACR2 expression at higher diluted titers.

Three mice were injected in M1 (DV: 0.4 mm), while the remaining three mice were injected in DLS (DV: 2.1 mm). Mice had fibers implanted in bilateral M1 (Figure 12A)) and DLS (Figure 12B)), respectively. Across this cohort of six mice, we observed that the expression volume did not increase sufficiently. That is, as shown in Figure 12C) and 12D), the width of expression did not exceed 350 µm in M1 (271.05 µm ± 30.39; n= 6 injection sites, 3 mice), and for DLS, improvement was minimal (453.37 µm ± 80.72; n= 6 injection sites, 3 mice) (annex; Table S5).

The area of opsin expression beneath fiber tip is, as already mentioned, of considerable importance for proper execution of optogenetic experiments *in vivo*, especially when it involves large neuron populations. In light of these requirements, we decided to considerably increase the volume in DLS using multiple closeby injections (from 500 nl to 2x500 nl) and M1 (500 nl to 3x330 nl) for the injection procedures in a cohort of animals running behavioral experiments. Given the results we obtained from injecting at a dilution of 1:10 (no signs of heterogeneity in DAPI fluorescence, or abnormal stGtACR2 patterns), we decided to return to the medium titer (M1/DLS titer = 1.5*10^12 gc/ml) as an addition to the raise in viral volume.

By performing multiple, closeby injections per hemisphere (Figure 5, Methods section), we improved the spread of expression in M1 (Figures 13A) and C)) and DLS (Figures 13B) and D)). Indeed, measurement of the width of opsin expression in M1 was significantly higher when compared to the spread of expression in the first cohort of mice (M1: 623.31 µm ± 66.61; n= 10 injection sites, 5 mice; p-value = 0.0001), while an increase of opsin expression in DLS was also observed (DLS: 782.61 µm ± 154.56; n= 10 injection sites, 5 mice; p-value = 0.5924). Moreover, spread of eYFP expression in control mice was similar to the range of stGtACR2 expression in DLS (DLS: 722.78 µm ± 119.98; n= 6 injection sites, 3 mice), but shorter in M1 (M1: 448.994 µm ± 78.38; n= 10 injection sites, 5 mice), which may suggest a higher diffusion of the opsin virus in M1 (annex; Table S6).

Despite the heterogeneous pattern of stGtACR2 expression beneath fiber tip, DAPI fluorescence in both M1 (Figures 13C)) and DLS (Figure 13D)) was homogeneous, excluding the occurrence of neurotoxic effects derived from stGtACR2 expression. Consistent with the specific characteristics previously reported for this opsin, stGtACR2 expression in M1 and DLS neurons appears to be mainly localized in the somatic compartment and at membrane-level (Figure 14).

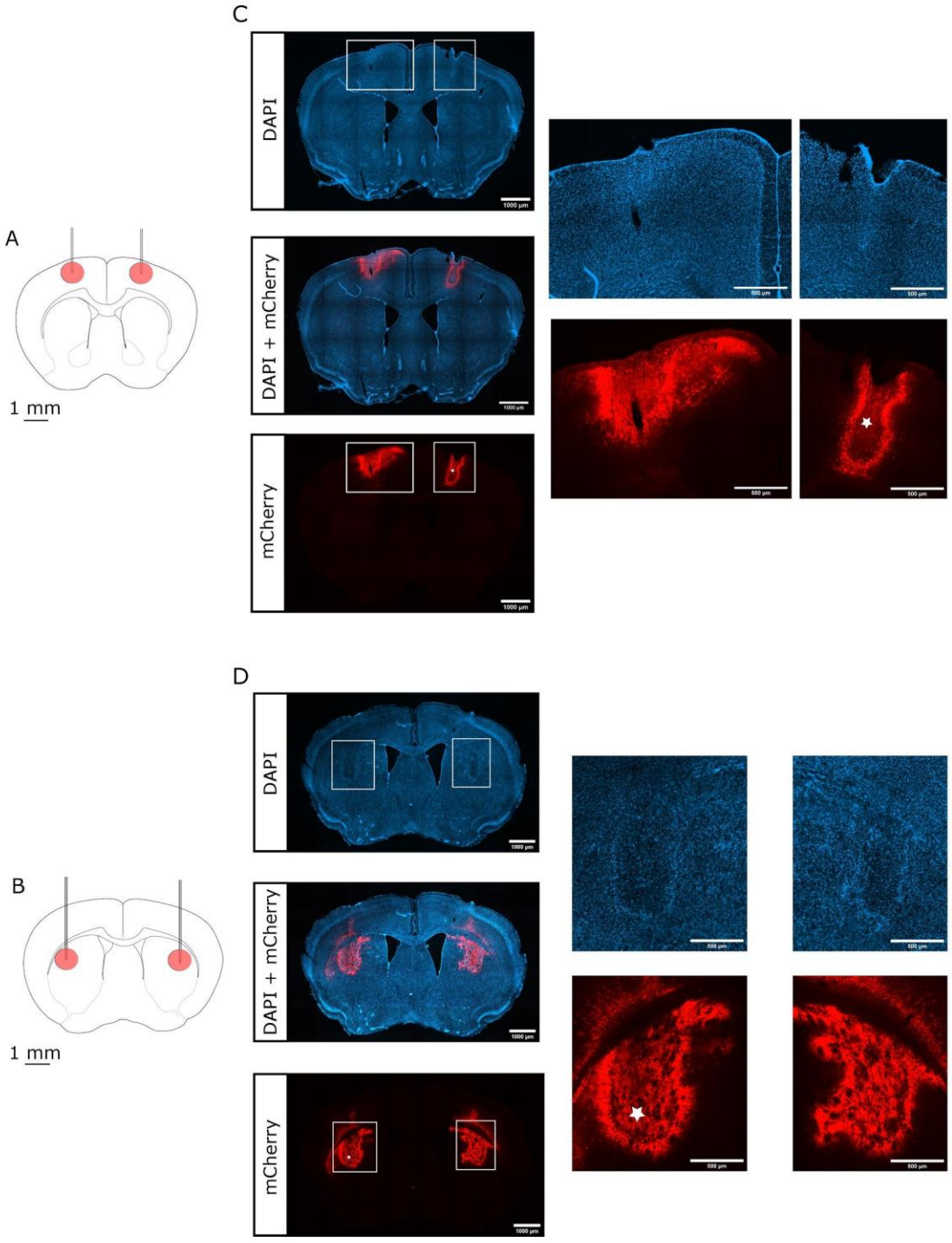

Figure 10 - **Virus delivery at maximum titer leads to reduced stGtACR2 expression at the injection center.**

(A) Schematic of the injection locations for the targeting of bilateral M1. Red circles represent the center of the expected area of opsin expression.

(B) Same as (A) for the DLS targeting.

(C) Example images of DAPI, DAPI and FusionRed fluorescence merged, and FusionRed fluorescence only, for a slice corresponding to the mouse bilaterally injected

in M1. White rectangles from DAPI image correspond to the detail images to the right, with DAPI marking only. White rectangles from FusionRed image correspond to the detail images to the right, with FusionRed marking only. The white star represents the injection site. Scale bar: 1000 µm in images from the whole brain section; 500 µm in detail images.

(D) Same as (C) for the DLS targeting. Reduced expression of FusionRed in the center close to the injection site (represented as a white star) and increased FusionRed fluorescence in the surroundings can be observed.

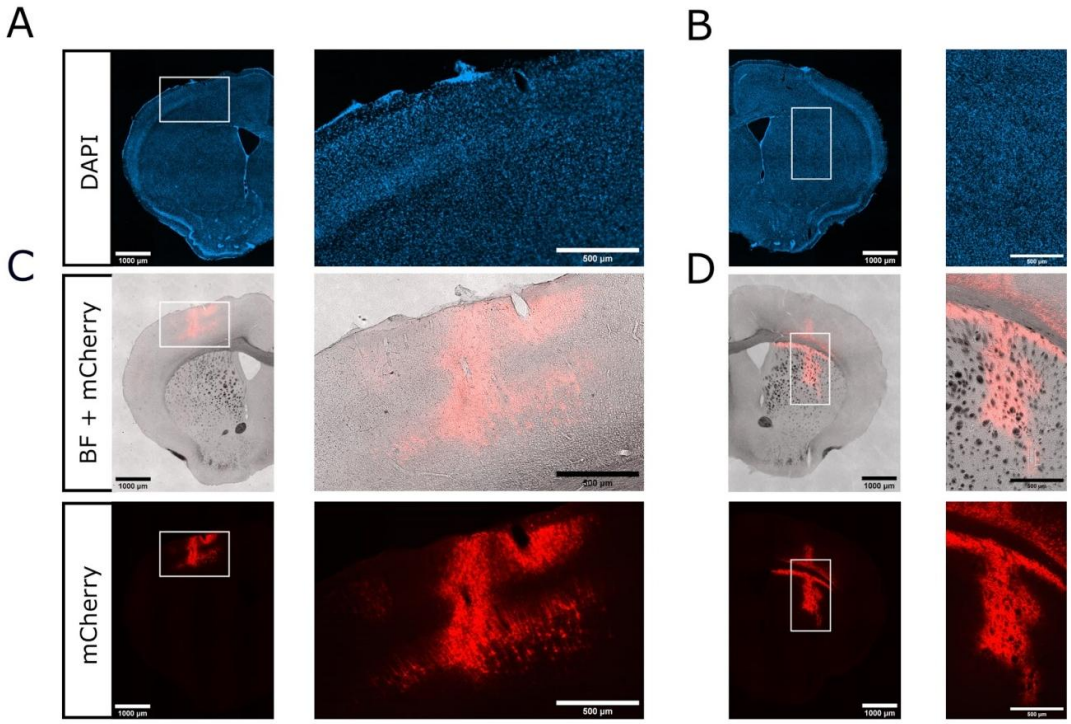

Figure 11 - **More homogeneous expression patterns of stGtACR2 in DLS and M1 after virus delivery at diluted titers.**

(A) Representative image of DAPI staining for a slice corresponding to the M1-injected hemisphere. White rectangle corresponds to the detail image to the right with DAPI labelling only. Scale bar: 1000 µm in image from the whole brain section; 500 µm in detail image.

(B) Same as (A) for a slice corresponding to the DLS-injected hemisphere.

(C) Representative images of brightfield (BF) and FusionRed fluorescence merged, and FusionRed fluorescence only, for a slice corresponding to the M1-injected hemisphere. White rectangle present in the image from FusionRed fluorescence corresponds to the detail image to the right with FusionRed fluorescence only. Scale bar: 1000 µm in image from the whole brain section; 500 µm in detail image.

(D) Same as (C) for a slice corresponding to the DLS-injected hemisphere.

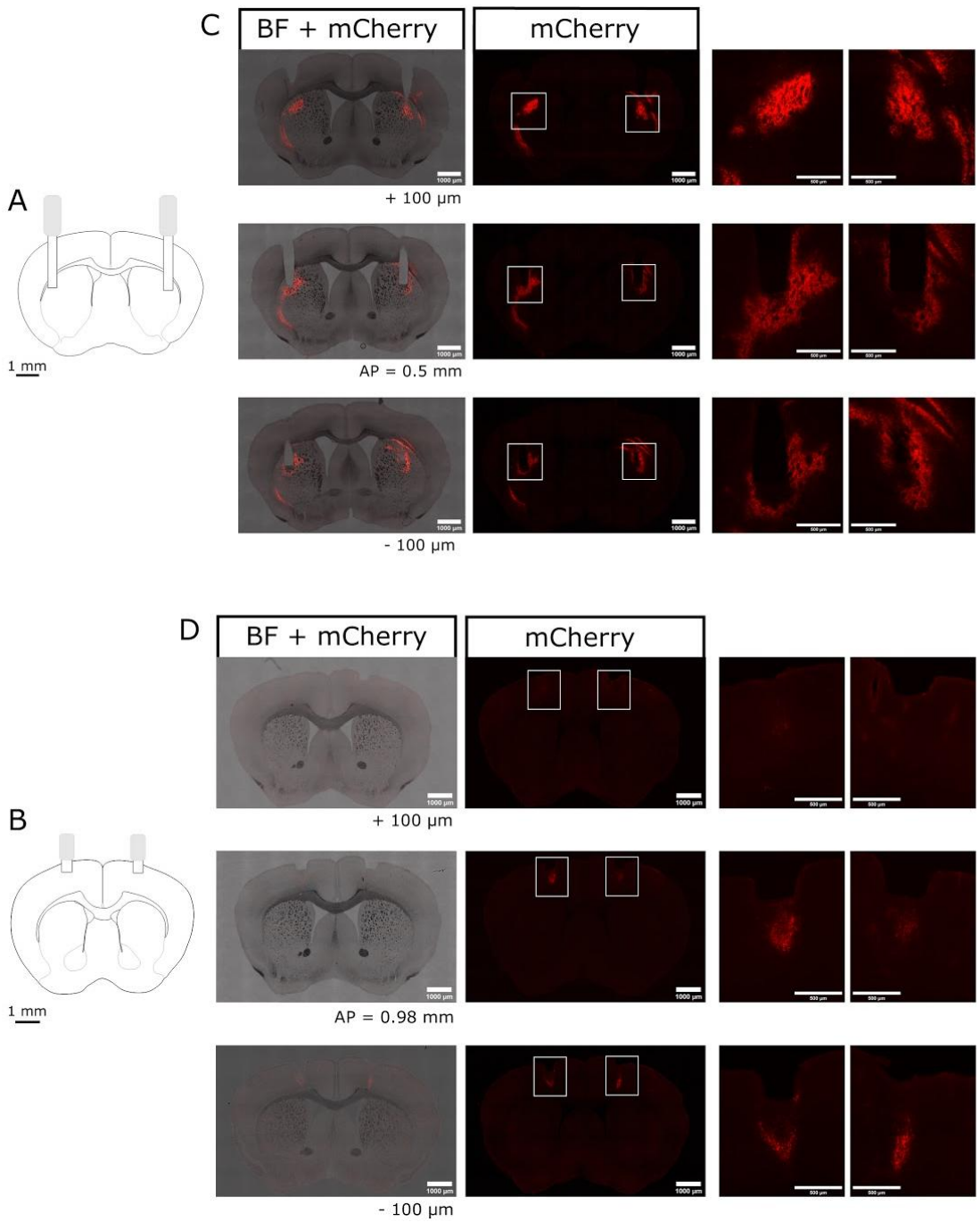

Figure 12 - **stGtACR2 injections at increased volume and diluted titer (5*10^11 gc/ml) led to low levels of expression in M1 and DLS.**

(A) and (B) show the representative traces of the fiber locations on DLS and M1, respectively.

(C) Representative images of BF and FusionRed fluorescence merged, and FusionRed fluorescence only, for slices corresponding to a mouse bilaterally injected in DLS. White rectangles in images from FusionRed fluorescence correspond to the detail images to their right. Top image: AP = 0.62 mm. Middle image: AP = 0.5 mm. Bottom

image: AP = 0.38 mm. Scale bar: 1000 µm in images from the whole brain section; 500 µm in detail images.

(D) Same as (C) for slices corresponding to a mouse bilaterally injected in M1. Top image: AP = 1.1 mm. Middle image: AP = 0.98 mm. Bottom image: AP = 0.86 mm. FusionRed fluorescence is reduced in M1, after virus delivery at higher diluted titers.

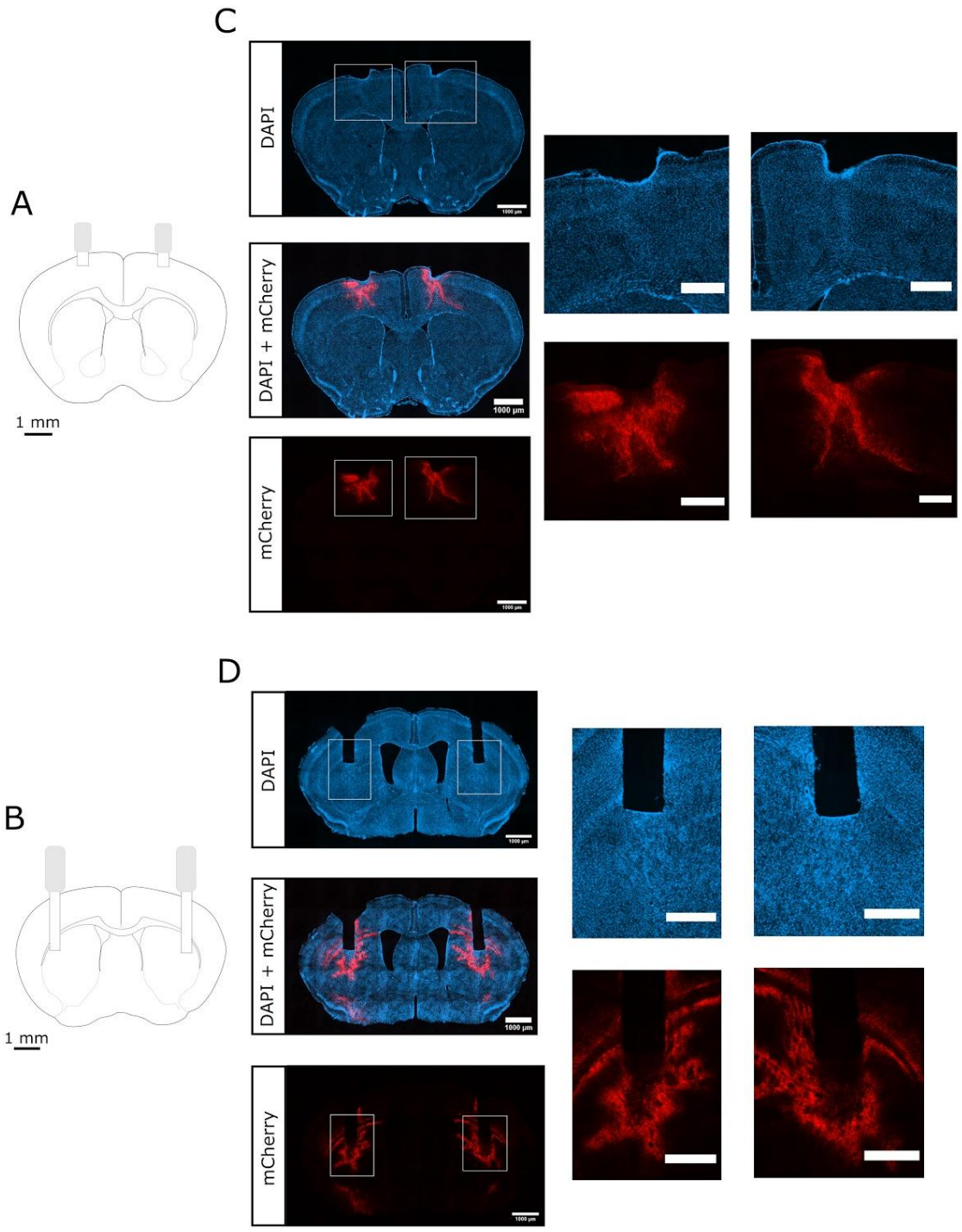

Figure 13 – **Attainment of proper spread of stGtACR2 expression in M1 and DLS after multiple injections, and the usage of higher volumes and medium titer (1.5*10^12 gc/ml).**

(A) and (B) show the representative traces of the fiber locations on DLS and M1, respectively.

(C) Example images of DAPI, DAPI and FusionRed fluorescence merged, and FusionRed fluorescence only, for a slice corresponding to a mouse bilaterally injected in M1. White rectangles from DAPI image correspond to the detail images to the right, with DAPI marking only. White rectangles from FusionRed image correspond to the detail images to the right, with FusionRed marking only. Scale bar: 1000 μm in images from the whole brain section; 500 μm in detail images.

(D) Same as (C) for the DLS targeting.

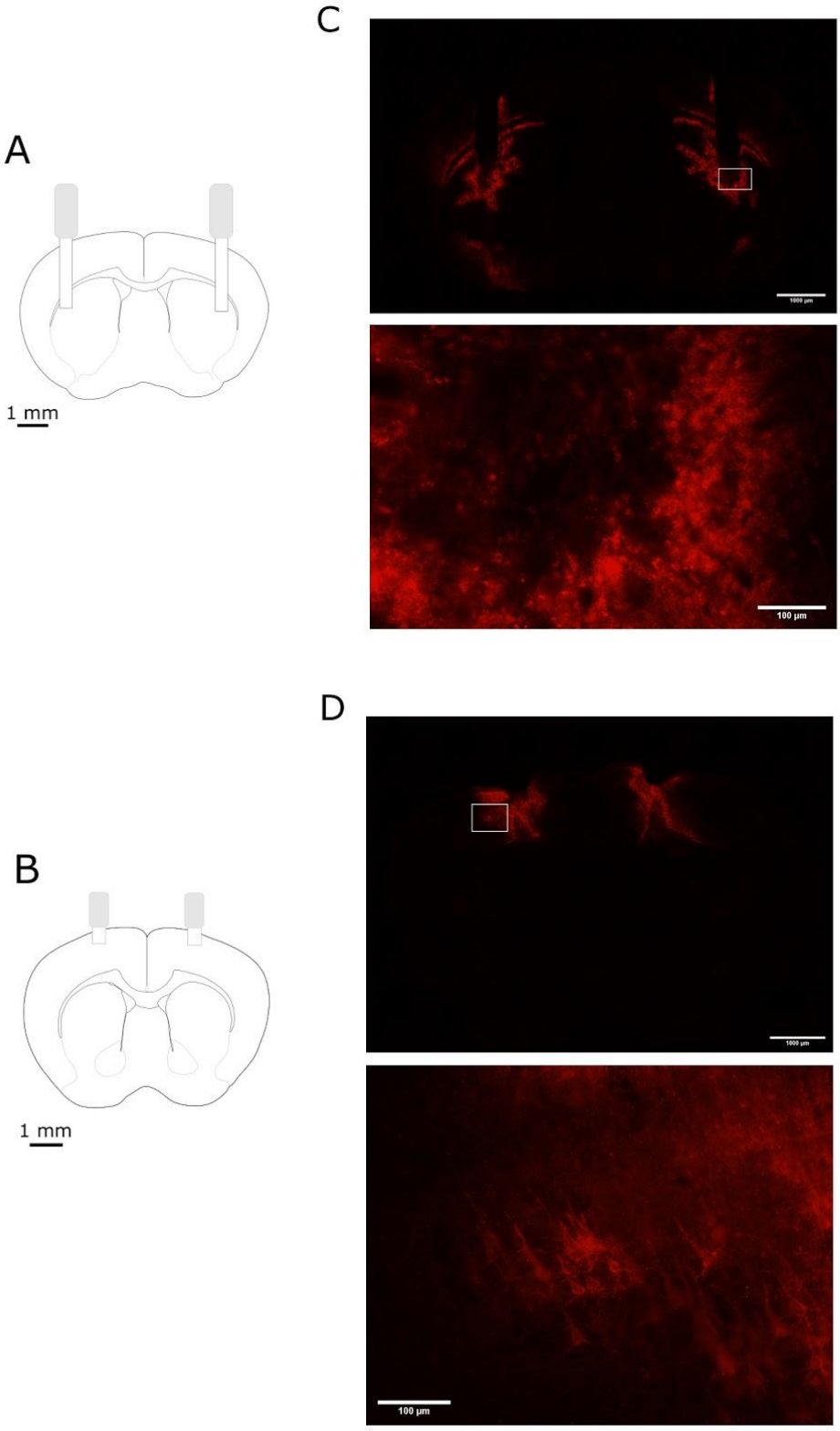
A
1 mm
B
1 mm
C
1000 µm
100 µm
D
1000 µm
100 µm

Figure 14 - **stGtACR2 expression profile in DLS and M1 neurons, after multiple injections and usage of higher volumes and medium titer (1.5*10^12 gc/ml).**

(A) and (B) show the representative traces of the fiber locations on DLS and M1, respectively.

(C) Example image of FusionRed fluorescence only, for a slice corresponding to a mouse bilaterally injected in DLS. White rectangle from FusionRed image corresponds to the detail image below, with FusionRed marking only. Scale bar: 1000 µm in image from the whole brain section; 100 µm in detail images.

(D) Same as (C) for the M1 targeting.

3.2 Behavioral analysis of the performance in the probabilistic three-alternative-choice task

3.2.1 Optogenetic inhibition of M1 and DLS show distinct effects on action initiation and choice execution

In order to study the role that M1 and DLS neuronal circuits exert in action initiation, execution and selection, we conducted inhibition experiments by optogenetically manipulating stGtACR2-expressing M1 and DLS neuronal populations on mice performing a probabilistic three-alternative-choice task already described in detail in the "Materials and Methods" section. In total, a cohort of 18 mice (Figure 15) was used for the opsin (stGtACR2) and control (eYFP) conditions (annex: Table S7).

A training period of approximately 3-4 weeks was implemented for the animals to learn the task structure. Mice adapted to the block structure and typically chose the option with higher reward probability (Figure 16A)). More specifically, mice reached steady performance within ~20 trials after a block switch (Figure 16B)).

The optogenetic sessions consisted of three trial types. First, ~84 % of all trials were normal trials without light illumination. Second, we manipulated ~8 % of trials with light stimulation from Center In to Side In (light delivered in a maximum time window of 2000 ms, 8 mW). Third, 8 % of trials were manipulated with light stimulation between Side In and Next Center In (maximum of 5 seconds of light delivery, 8 mW) (Figure 17). The time windows for each light pulse were determined based on the average time that mice take to perform the execution (Center In to Side In) and first attempt to initiation (Side In to Next Center In) phases of the task (see Materials and Methods).

Light manipulations from Center In to Side In were implemented in order to dissect the possible role of M1 and DLS in action execution. To investigate the possible role of the circuits for action initiation, we silenced neurons after mice reported their choice (i.e., Side In) until the Next Center In (maximum 5 s). As previously mentioned, it is important to note that, if mice try to initiate a trial within the ITI, the Next Center In does not result in next trial initiation (see Materials and Methods).

To probe for possible effects that light-induced trials could have in the mice's behavior, we quantified the distribution of time that mice took in each of the aforementioned phases of the task. Subsequently, to test for possible statistical differences between both experimental groups, the ratio of the medians for light on and off parameters was calculated for each group and compared. For mice expressing the opsin in DLS (n = 5), a difference was observed between Side In and Next Center In

(represented as “Side-to-center”) (light off/on trials: 2758/186), while the distribution is similar between light on and light off conditions, from Center In to Side In (represented as “Center-to-side”) (light off/on trials: 6206/474) (Figure 18A)). When comparing with DLS eYFP’ mice (n = 3), for which time distributions between light on and off conditions reveal a delay after light on trials, from both Center In to Side In (light off/on trials: 4812/395) and Side In to Next Center In events (light off/on trials: 2122/155) (Figure 18C)), we confirmed a significant difference between the ratios of DLS mice from Side In to Next Center In (mean of the ratios for eYFP/stGtACR2: 1.21/3.15; p-value = 0.011) (Figure 18E)).

In contrast, for mice expressing the opsin in M1 (n = 5), we observe differences in the performance from Center In to Side In (light off/on trials: 8752/674) and Side In to Next Center In (light off/on trials: 3822/274) (Figure 18B)). Interestingly, after comparison with M1 eYFP’ mice (n = 5) (Figure 18D)), for which time distributions (between light on and off conditions) also showcase a delay after light on trials, from both Center In to Side In (light off/on trials: 7082/594) and Side In to Next Center In events (Light off/on trials: 3259/272) (Figure 18C)), we observe a significant difference of the ratios in M1 mice from Center In to Side In (mean of the ratios for eYFP/stGtACR2: 1.21/1.47; p-value = 0.02) and from Side In to Next Center In (mean of the ratios for eYFP/stGtACR2: 1.44/2.34; p-value = 0.049) (Figure 18F)).

These results suggest that inhibition of DLS’s neuronal populations affects the timing of action initiation and not execution, whereas M1 inhibition affects both the timing of action initiation and execution.

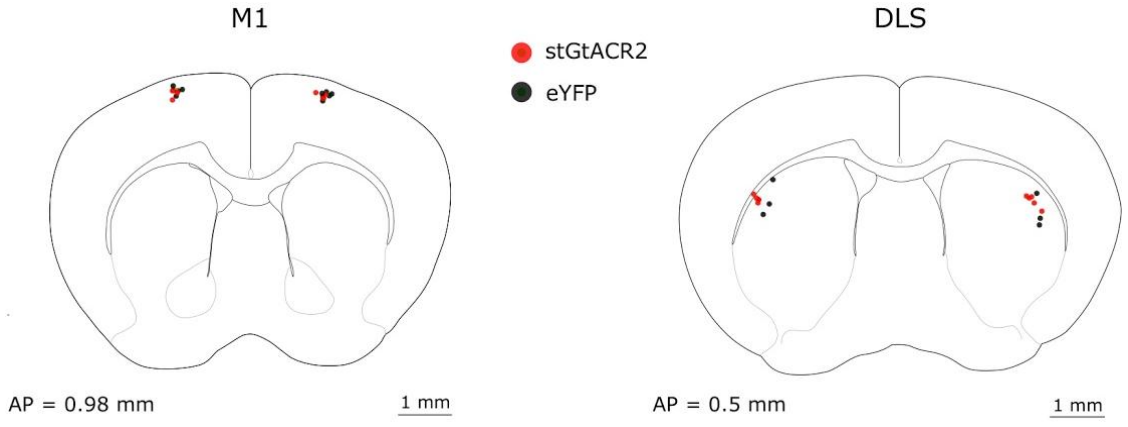

Figure 15 - **Fiber tip’s positions in M1 and DLS for both eYFP and stGtACR2 mice.**

Schematic image displaying the optic fibers position for all mice expressing eYFP and stGtACR2 in M1 (eYFP: n=5; stGtACR2: n=5) and DLS (eYFP: n=3; stGtACR2: n=5).

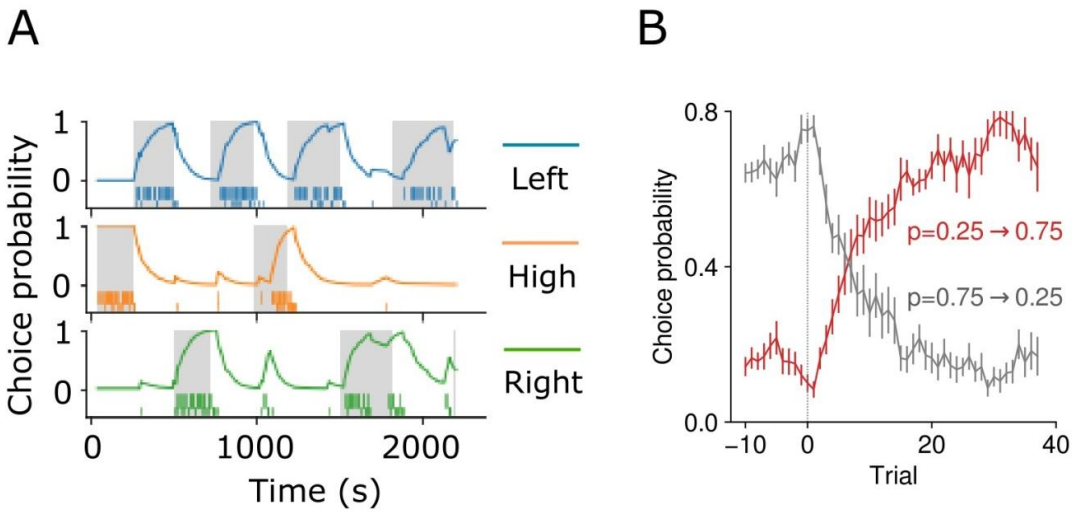

Figure 16 – **Mice learn the task and adjust their behavior to the block changes.**

(A) Example of a session with high behavioral performance. Number of trials: 270; Number of rewards: 164; Number of blocks: 9.

(B) Plot representing the ability of all mice to effectively switch between side holes after a block shift, demonstrated by the adjustment of the choice probability. Trial 0 (represented by the grey line in the graph) represents the block shift. n=20.

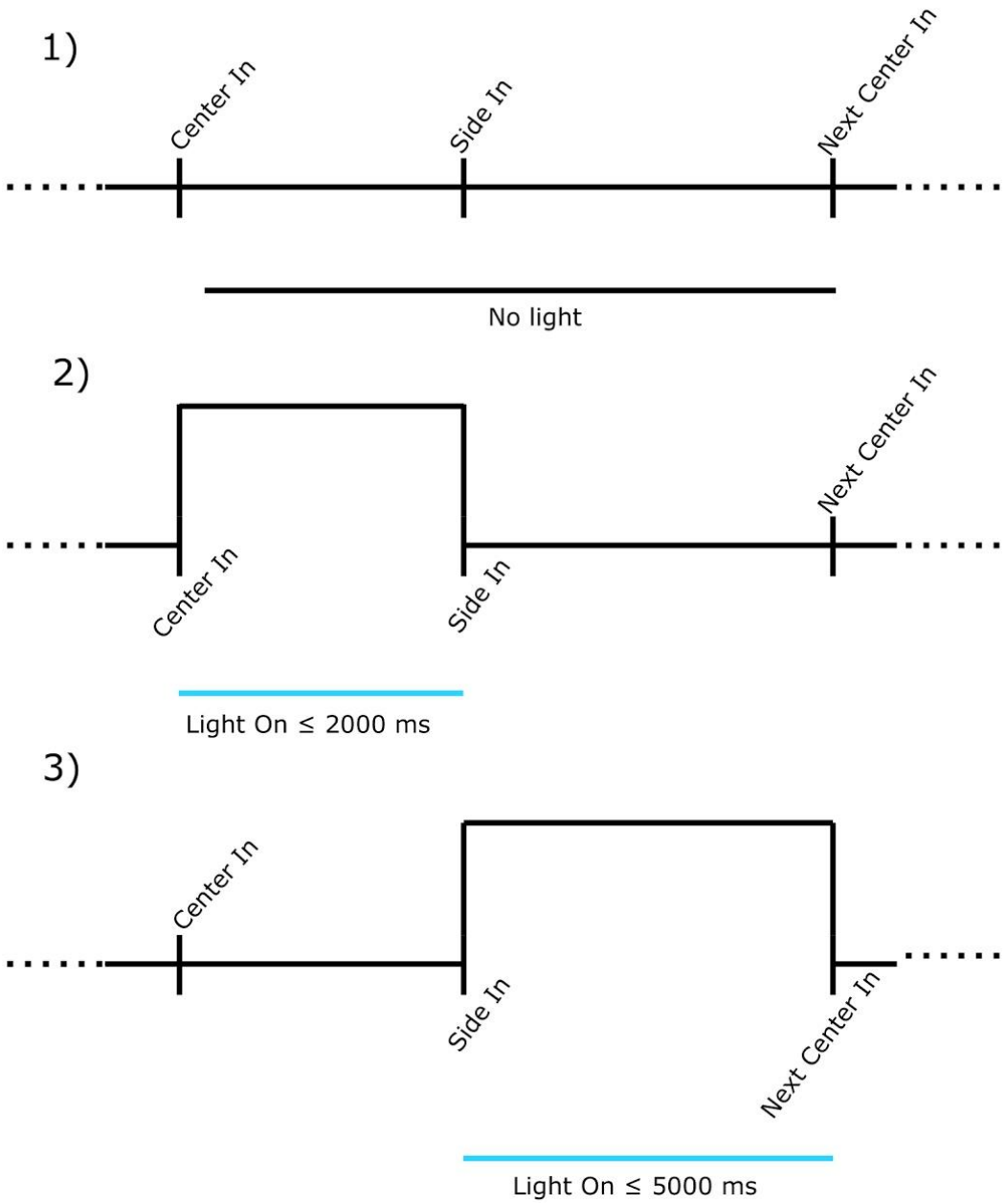

Figure 17 - **Optogenetic experimental design within the task structure.**

Schematic images of the different trial types within an optogenetic session. The image referent to “1)” represents trials without light illumination. In “2)”, trials with light illumination from Center In to Side In are depicted. Finally, in “3” is represented the situation in which light illumination occurs from Side In to Next Center In, if the attempt for the initiation of the next trial is executed outside the ITI.

.

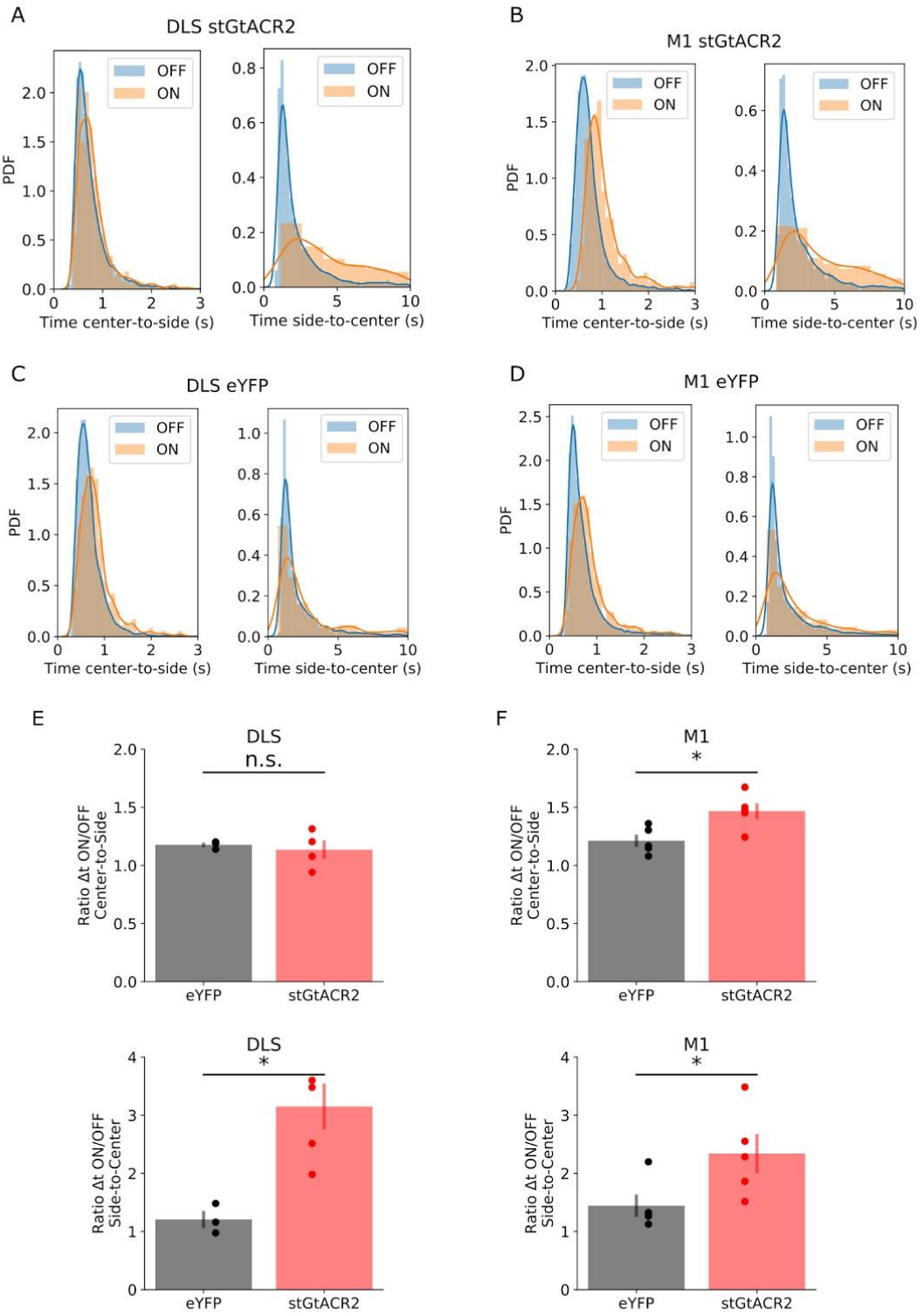

Figure 18 - **Inhibition of the DLS region delays action initiation (timing of Next Center In), while inhibition of M1 delays choice execution (timing of Side In).**

(A) Probability density function (PDF) of time intervals taken by DLS stGtACR2's mice from Center In to Side In ("Center-to-side") and from Side In to Next

Center In (“Side-to-center”). Data represent all time-intervals in a range from 0 to 3 seconds, for light-off trials (represented in blue) and light-on trials (represented in orange).

(B) Same as (A) for M1 stGtACR2’s mice.

(C) Same as (A) for DLS eYFP’s mice.

(D) Same as (A) for M1 eYFP’s mice.

(E) Comparison of the ratios of the time-intervals’ medians (Light on/light off), of all individual DLS mice (DLS eYFP bars represented in grey; DLS stGtACR2 bars represented in red), from Center-to-side (higher plot) and Side-to-center (lower plot) (paired t-test, n.s. > 0.05, * p-value < 0.05). Bars represent mean ± SEM.

(F) Same as (E) for all individual M1 mice (paired t-test,* p-value < 0.05).

3.2.2 Licking onset is not affected by optogenetic inhibition, while the licking pattern of activity is altered after M1 and DLS inhibition

To understand if the delays in initiating the action, when inhibiting the DLS, and reporting the choice, when targeting M1, are a consequence of the action we analyzed and not to a general delay in the initiation of a wide set of movements, we decided to investigate if licking execution was delayed after light stimulation. To do so, we first looked into the licking pattern of activity after M1 or DLS inhibition, focusing on the period of licking onset after Side In. For this analysis, we looked into both rewarded and non-rewarded trials, since licking activity occurs shortly after outcome evaluation (400 ms after Side In) and is more pronounced after a positive outcome, which suggests a very low probability of licking activity being performed outside the light illumination period.

In rewarded trials, we cannot discriminate any differences at onset of licking activity in control (DLS eYFP, n = 3: Light off/on licks: 45438/4550; M1 eYFP: n = 5: Light off/on licks: 56565/4771) (Figures 19A) and 19B)) and stGtACR2-expressing’ mice (DLS stGtACR2, n = 5: Light off/on licks: 48859/3568; M1 stGtACR2, n = 5: Light off/on licks: 68420/5090) (Figures 19C) and 19D)). Noteworthy, we observe a tenuous increase on licking activity, at around 1 second, after optogenetic manipulation on M1 and DLS mice expressing the opsin.

In non-rewarded trials, for both experimental groups of mice the trend, at onset, of licking activity is quite similar between light on and off trials (DLS eYFP, n = 3: Light off/on licks: 8926/703; M1 eYFP, n = 5: Light off/on licks: 4762/362; DLS stGtACR2, n

= 5: Light off/on licks: 2774/236; M1 stGtACR2, n = 5: Light off/on licks: 4562/478) (Figures 19E), F), G) and H)). Furthermore, for both light on and light off conditions, we observe a peak of licking activity before 1 second, followed by a second smaller peak arising at around 2 seconds, result of licking activity at the subsequent trial. Interestingly, in trials were M1 and DLS's neuronal circuits were inhibited, the trend of licking activity is quite different, with higher licking probability spreading throughout a larger time interval, along with a reduced second peak of activity.

Although these results suggest that the onset of licking activity is not affected after DLS and M1 inhibition, we decided to perform an additional analysis to assess if the inhibition of these regions may lead to a delay on licking activity. We first analyzed the time mice took to execute the first lick after Side In, in light on and light off trials. Only the rewarded trials were analyzed, given the large number of trials where mice didn't execute a first lick (higher than 80% of the trials for nearly half the mice, n=9) in non-rewarded trials.

In line with our expectations, timing for the first lick after Side In was not affected between light off and on trials, across all experimental groups (DLS stGtACR2, n = 5: Light on/off medians: 0.51/0.52 s; Light off/on trials: 3189/280; DLS eYFP, n = 3: Light on/off medians: 0.37/0.37 s; Light off/on trials: 2469/249; M1 stGtACR2, n = 5: Light on/off medians: 0.52/0.56 s; Light off/on trials: 4683/373; M1 eYFP, n = 5: Light on/off medians: 0.45/0.45 s; Light off/on trials: 3470/309) (Figures 20A), B), C) and D)). To quantify these results, we analyzed the ratio of the medians between light on and off conditions, to observe if there is any significant difference amid experimental groups, respective to the region in study (DLS eYFP vs DLS stGtACR2; M1 eYFP vs M1 stGtACR2). The results present no significant differences between the ratios, confirming our initial assessment (mean of the ratios in DLS eYFP/stGtACR2: 1.23/1.03; p-value = 0.16) (mean of the rations in M1 eYFP/stGtACR2: 1.06/1.16; p-value = 0.27) (Figure 20E) and F)).

Overall, this set of results shows that inhibition of DLS and M1 does not lead to a delay in the onset of licking and suggests that the observed effects on the timing of action initiation and execution (Figure 18) are not a result of a generalized delay in movement.

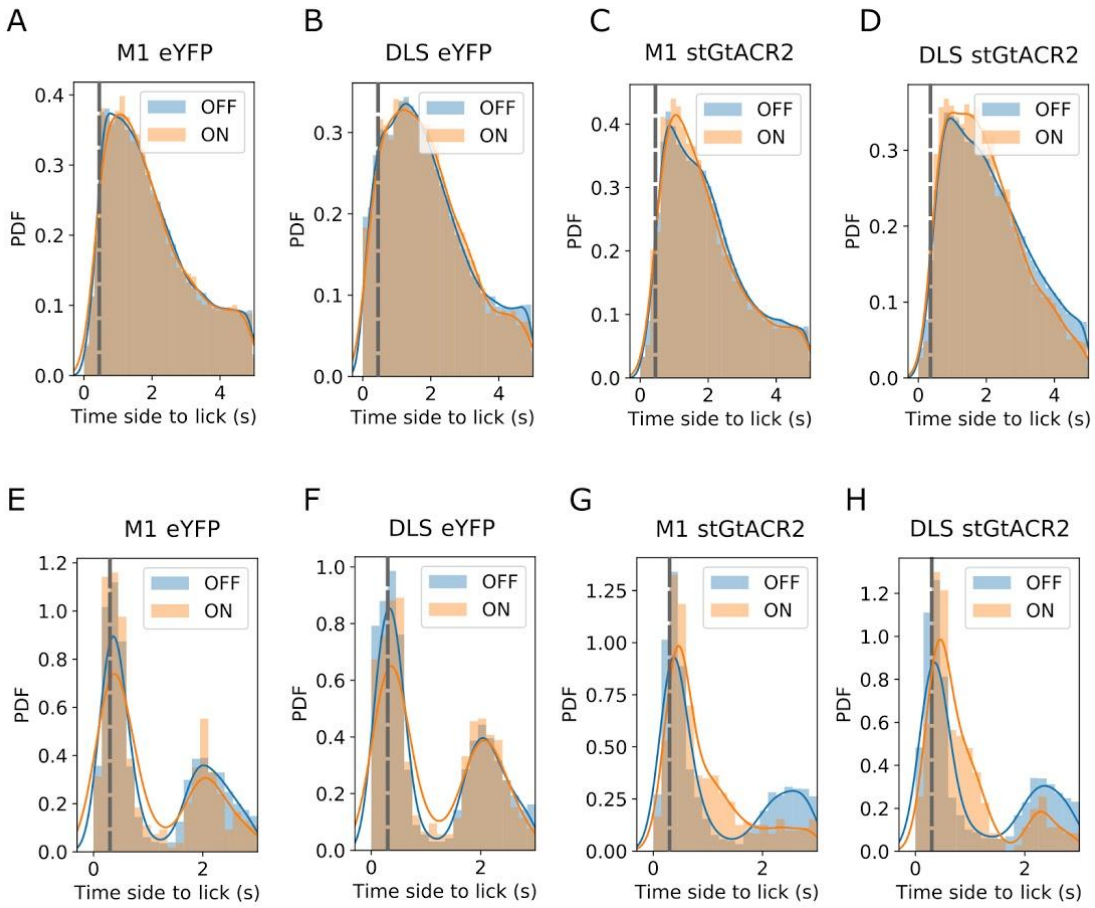

Figure 19 - **Time distribution of licking during light on and light off conditions.**

(A) Peri-event time histogram (PETH) of licks by M1 eYFP's mice, in reward trials. Data represents all time-intervals from onset of light stimulation to 5 seconds after, for light-off trials (represented in blue) and light-on trials (represented in orange). Grey dashed lines represent the event of outcome delivery (positive outcome in rewarded trials; 400 ms).

(B) Same as (A) for DLS eYFP's mice.

(C) Same as (A) for M1 stGtACR2's mice.

(D) Same as (A) for DLS stGtACR2's mice.

(E) PETH of licks by M1 eYFP's mice, in non-rewarded trials. Data represents all time-intervals from onset of light stimulation to 3 seconds after, for light-off trials (represented in blue) and light-on trials (represented in orange). Grey dashed lines represent the event of outcome delivery (negative outcome in non-rewarded trials; 400 ms).

(F) Same as (E) for DLS eYFP's mice.

(G) Same as (E) for M1 stGtACR2's mice.

(H) Same as (E) for DLS stGtACR2's mice.

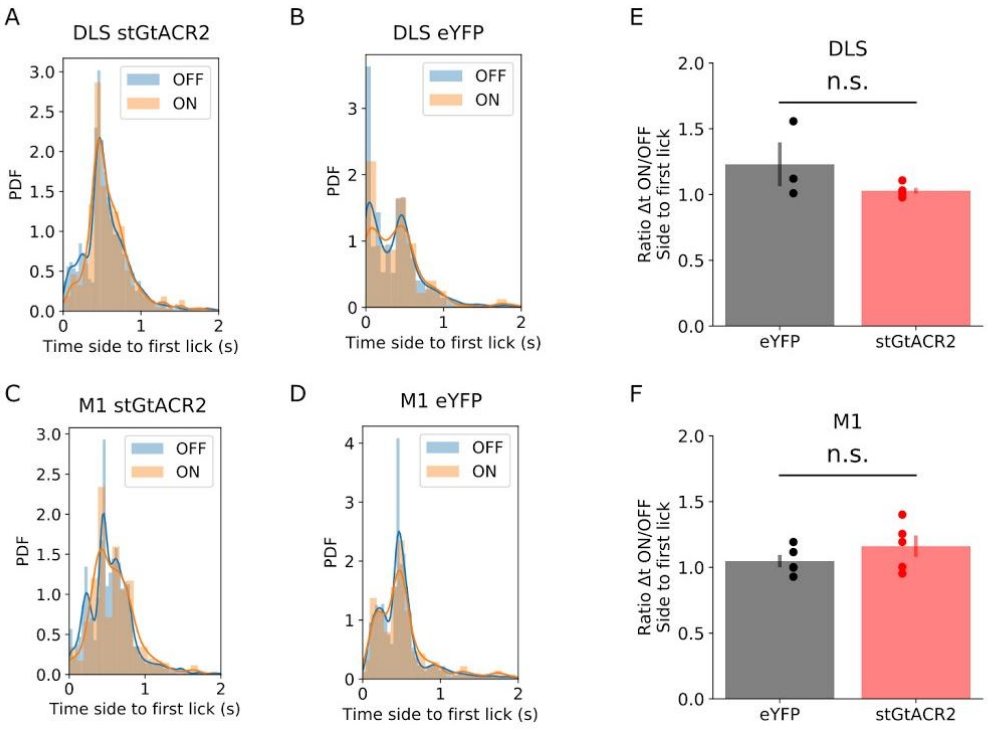

Figure 20 - **No delay in the initiation of licking activity after light-induced trials, in all experimental groups.**

(A) PDF of the time intervals taken by DLS stGtACR2's mice to execute the first lick after choice report. Data represent all time-intervals in a range from 0 to 2 seconds, for light-off trials (represented in blue) and light-on trials (represented in orange).

(B) Same as (A) for DLS eYFP's mice.

(C) Same as (A) for M1 stGtACR2's mice.

(D) Same as (A) for M1 eYFP's mice.

(E) Comparison of the ratios for the time-intervals' medians (light on/light off) of all individual DLS mice (DLS eYFP bars represented in grey; DLS stGtACR2 bars represented in red) (paired t-test, n.s. > 0.05). Bars represent mean ± SEM.

(F) Same as (E) for all individual M1 mice (paired t-test, n.s. > 0.05).

3.2.3 Optogenetic inhibition of DLS, but not M1, affects action choice.

The previous analysis highlighted an effect on the timing of the actions exerted by mice to complete the events comprising the behavioral task. In particular, we can propose that M1 activity is preponderant for proper performance between Center In and Side In, while activity in the DLS is important for the correct performance from Side In to the Next Center In.

However, the results presented in the sections above do not answer the question of whether inhibition of these regions' neuronal populations may affect the action in the subsequent trial, leading to a change in the choice selected. Therefore, to investigate whether these regions' neuronal circuits are required for action selection, we decided to perform an analysis on the mice's probability of switching the choice selected in the next trial, after DLS/M1 inhibition occurred during the initiation process (Side In to Next Center In) in the previous trial.

We considered trials that followed optogenetic inhibition in these events, since mice cognitively prepare the next action within the time interval of Side In to Next Center In. Although, as previously mentioned, there is a higher probability of events, after rewarded trials, where the first attempt to initiate the next trial takes place outside the time window of light stimulation (when compared with non-rewarded trials), both rewarded and non-rewarded trials were analyzed (separately) for this analysis. There are two different reasons for the implementation of this approach. First, even if, in rewarded trials, the Next Center In occurs when DLS and M1 neuronal activity is not disturbed (see Figure 9), the action selection process may have been performed during the stimulation time window (the selection process may be performed during outcome evaluation or in time periods distant from the initiation attempts). Secondly, it is important to separately analyze the effect of a positive or negative outcome on the choice selected in the subsequent trial, since the probability of mice changing the next choice is presumably different for both situations. If mice get a reward, there is a lower probability of switching to a different choice in the next trial, while the opposite is true in the case mice do not get a reward. This distinction may help us comprehend the involvement of DLS and M1 on action selection, as a significant difference on choice switching probability after rewarded trials may be a stronger indicator of the participation of these regions in this action process.

For all experimental groups, we obtained the probability of switching between the choice taken in the previous trial (Side In) and the choice taken after Next Center In after light on or light off conditions, for non-rewarded and rewarded trials.

Subsequently, we examined the difference of switching probability between both light-stimuli conditions (light on minus light off), either on non-rewarded or rewarded trials.

When comparing both M1 experimental groups, no significant differences were observed between the differences on the probability of switching the next choice after non-rewarded or rewarded trials (Figure 21A) and 21B); Non-rewarded trials: p-value = 0.26; Rewarded trials: p-value = 0.60). On the other hand, the same analysis on DLS experimental groups revealed a significant difference between the differences on the probability of choice switching after rewarded trials (Figure 21D); Rewarded trials: p-value = 0.02), while no significant differences were observed after non-rewarded trials for both situations (Figure 21C); Non-rewarded trials: p-value = 0.06). It should be noted that, as expected, the switch probability after non-rewarded trials is generally higher compared to rewarded trials. Thus, the lack of a statistical difference for the non-rewarded trials could therefore be a result of a ceiling effect.

The results obtained suggest that the DLS can influence action selection by modulating the probability to switch to another action in the next trial.

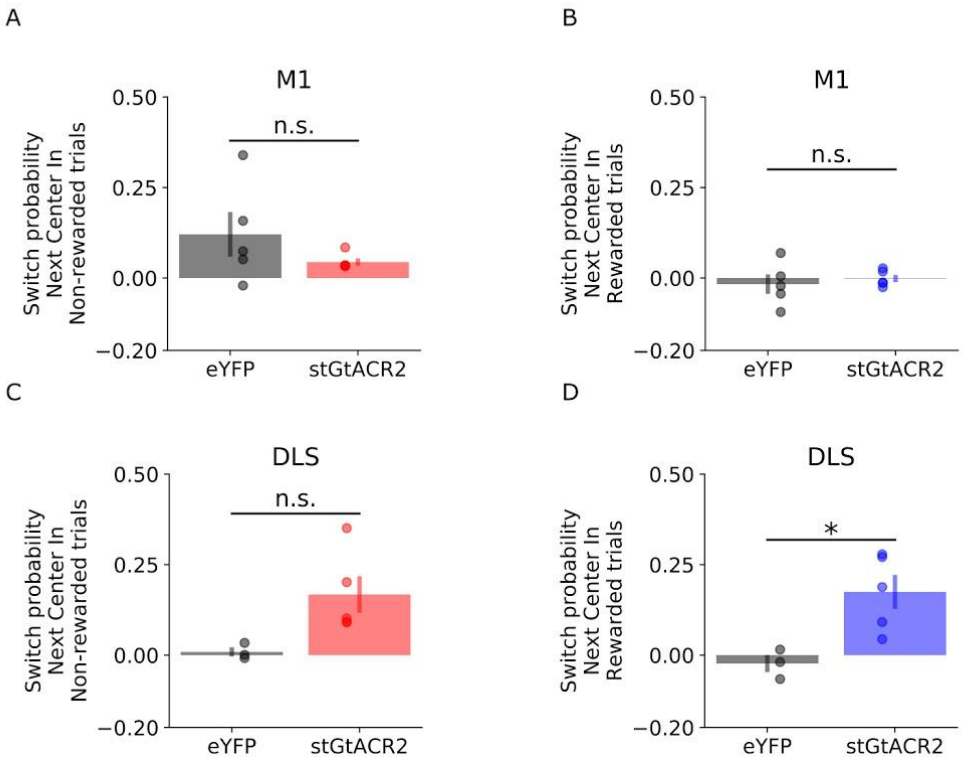

Figure 21 - **DLS inhibition, not M1, leads to an effect on choice selection in the subsequent trial and after attempting to initiate a trial.**

(A) Comparison of the switch probability between previous trial' choice and choice after Next Center In, for both M1 eYFP and M1 stGtACR2 mice, after non-

rewarded trials (M1 eYFP bars represented in grey; M1 stGtACR2 bars represented in red) (paired t-test, n.s. > 0.05). Bars represent mean ± SEM.

(B) Same as (A) for rewarded trials. (M1 eYFP bars represented in grey; M1 stGtACR2 bars represented in blue). n.s > 0.05.

(C) Comparison of the switch probability between previous trial' choice and choice after Next Center In, for both DLS eYFP and DLS stGtACR2 mice, after non-rewarded trials (M1 eYFP bars represented in grey; M1 stGtACR2 bars represented in red) (paired t-test, n.s. > 0.05). Bars represent mean ± SEM.

(D) Same as (C) for rewarded trials. (DLS eYFP bars represented in grey; DLS stGtACR2 bars represented in blue). * < 0.05.

Discussion

The project developed for my master thesis primarily aimed at exploring the role that the DLS and M1 exert on the action selection process by studying the effect of cell-type specific, optogenetic inhibition of these regions during the performance of a three-alternative-choice probabilistic task. I approached this topic by investigating the effects on action selection (quantified as changes in action choice, i.e., switching), action initiation and execution (quantified as changes in timing) that result from the transient inhibition of these regions' neuronal populations during specific task events

It is intuitive to understand our focus on studying these regions in order to gain insight on which neuronal areas are responsible for these processes. Not only is it known the involvement of both M1 and striatum on action execution and initiation [4,6,7,155,157], the striatum has been thoroughly linked to an action selection role, from a theoretical [8–10] to a practical perspective [191]. Nonetheless, despite this similarity concerning the functions that M1 and striatum perform, studies that explore the participation of both these regions in motor- and cognitive-related functions are extremely scarce [25,189]. This prevents the comprehension on whether these functions are indeed shared between both these regions, or is a result of experimentally different studies where assessment of the participation of M1 or striatum on action functions is based on distinct behavioral tasks and experimental methods.

In this project, by studying the effects of neuronal manipulation of either M1 or DLS, on animals performing the same behavioral task, we provide a more comprehensive analysis on the similarities and distinctions between these regions on action initiation, execution and selection. Furthermore, previous studies that demonstrate the importance of striatal circuits for the execution and selection of actions present experimental designs that need to be taken into account when considering the striatum participation on these functions. Although it has been demonstrated that disruption of striatal activity during action execution affects action performance[7], the execution phase of the task designed in that study concerns the execution of action sequences, which leads to reward delivery if performed accordingly with the requirements for correct trial performance (sequences of 8 lever presses leads to a reward). However, the implementation of such design leads to a prevalence of strategies based upon habits (habitual actions) by mice, which does not correspond to the execution strategy on our task (goal-directed actions). Regarding the participation of the striatum in action selection, the elegant study by Tai and colleagues [191] has its own limitations. Since it was used a two-alternative-choice task, and inhibition of D1- and D2-SPNs was

unilateral, one can question if the effects observed after striatal manipulation were the result of a cognitive function within the striatum (action selection), or a motor-related one. Although the study demonstrates the effect is not motor-related, it can't be discarded the possibility that unilateral striatal excitation may result in a motor effect, since a posterior study has shown that unilateral manipulation of striatal SPNs leads to contraversive movements [73].

In our study, a probabilistic three-alternative choice task was used so that mice had to choose the most appropriate action (i.e., choice of the left, high or right hole) at every single trial based on the current reward contingencies. This allowed me to measure not only the effects of inhibition on action timing but also on action selection. This is, in the three-alternative choice task, mice had a defined set of alternative choices, which is not the case for previously used sequence tasks [7]. As mentioned previously, this leads to the implementation of goal-directed action strategies by mice to complete the trials. Additionally, the use of a high poke, within the three alternative choices, restricts the assumption that changes in action choice may be related to the exertion of contraversive movements. This is further complemented by our strategy on inhibiting the mouse' striatum bilaterally, which is not observed in other studies that assign an action selection role to the striatum.

Since efficient inhibition experiments are far more difficult to accomplish than excitation strategies, we decided to use stGtACR2, a newly described opsin [204] that, presents itself as an inhibitory optogenetic tool capable of avoiding the majority of the problems presented when it comes to inhibiting neurons through optogenetics [197]. In particular, the high light-sensitivity by this opsin allows the use of lower light powers and shorter light-pulses, which consequently prevents the heating increase in the targeted tissue. This light-derived heating is a major caveat in optogenetic experiments, since it may lead to suppression of neuronal activity and influence animal's behavior [198], jeopardizing the integrity of the results obtained in optogenetic experiments. However, given its novelty, the extent of literature regarding the usage of the opsin is still scarce, which coupled with the lack of detailed information about its expression in M1, and mainly the striatum, led us to initiate the project by optimizing the expression of the opsin in the mentioned regions.

Various strategies were implemented in order to achieve optimal expression of the opsin in our targeted regions. In detail, viral delivery at the original stock titer (1.5*10^13 gc/ml) revealed inhomogeneous expression, since the heterogeneous DAPI fluorescence in DLS suggested the occurrence of a phenomenon of neurotoxic nature in this area. Further injections at lower concentrations (5*10^11 gc/ml and 1.5*10^12

gc/ml) provided better results concerning this effect, as DAPI fluorescence in M1 and DLS appeared to be unaffected.

Furthermore, volumes as high as 500 nl are not sufficient to achieve a spread of expression significantly wider than the width of the optic fibers, when injecting at diluted titers, while higher volumes injections (990/1000 nl) led to optimal results concerning the spread of opsin expression. Therefore, our experiments indicate that optimal expression of stGtACR2 in cortical and striatal conditions is achieved by virus injections of 990/1000 nl at diluted titers of 1.5*10^12 gc/ml.

After the optimization of stGtACR2 expression in our regions of interest we assessed the effects of this manipulation on the animal's behavior in the task. Since the regions we manipulated are involved in action initiation and execution, we decided to first analyze if inhibition of those circuits could lead to delays in the initiation and execution phases of the task. We report that DLS inhibition significantly delays the attempt to initiate the next trial, providing further evidence that striatal activity is crucial for proper action initiation. Given the calcium-imaging data (experiments performed prior to the start of my project) obtained for DLS activity in this phase of task, in which baseline activity is considerably low and slightly increases in time-periods very close to initiation of the trial (data not shown), future analysis should investigate the hypothesis that the small burst of DLS activity at the end of this phase is crucial for action initiation.

A significant delay in attempting the initiation of the next trial is also observed after M1 inhibition. These results are consistent with the calcium-imaging data obtained from M1 in mice performing this same task (high neuronal activity in M1 from Side In to Next Center In), as well as previous reports of M1 activity related to the onset of movement [4,155,157].

Regarding the inhibition of both regions during the action execution phase of the task, our results reveal once again a dichotomy between the importance of M1 and DLS for this action process. M1 inhibition led to a significant delay in executing the choice selection, consistent with the role that M1 has in motor command and motor control[151]. On the other hand, DLS inhibition did not affect motor execution. Although the importance of DLS activity for action execution has been described[7], the context in which the importance of DLS SPNs to this process was studied referred to the execution of action sequences, while in our experiments mice do not execute the action that leads to choice selection in a habitual manner, instead executing actions with goal-directed strategies, as described above. Furthermore, since we do not observe a significant effect of DLS inhibition on the timing to execute the chosen action, we may speculate that the high neuronal activity displayed in DLS within this phase of the task (obtained from calcium-imaging data) refers to either the encoding [184,185] or support [26]

of kinetic properties of the motor outputs. Analysis of the motion and video sensor data obtained in this project will provide additional insights and can be used to test this hypothesis.

Overall, our analysis on the time that mice expend to initiate and execute actions, suggests that M1 activity plays a role in action execution, while DLS activity is critical for action initiation.

To understand if these effects are the sole result of a delay respective to the movements necessary to perform the initiation and execution phases of the task, or are, instead, due to a general delay of various types of movement, we examined if DLS and M1 inhibition could lead to a delay on licking activity after Side In. We observe no significant differences between the times taken to execute the first lick across experimental groups. This observation confirms that the delays observed after DLS and M1 inhibition in action initiation and execution, respectively, are specific to the processes under evaluation, instead of a general effect on motor output.

Could the neuronal circuitries involved in licking activity been directly affected by the light manipulations of M1 and DLS? These regions are the anterior lateral motor cortex (ALM) [235–238] and the ventrolateral striatum (VLS) [239], respectively. To test whether inhibiting our targeted regions could also silence off-target neurons in some of these neighboring circuits, given the light spread throughout brain tissue, we analyzed licking activity in our task. It has been reported that this spread can reach over 1 mm of area [203]. The ALM, despite being located within the motor cortex, is far off the coordinates we used for our injections in M1 (in ALM, usually: AP = 2.5 mm; ML = 1.5 mm; in M1: AP = 1 mm; ML = 1.4 mm), which strongly suggests that ALM neuronal populations were not targeted during our inhibition experiments. On the contrary, the coordinates used to target the VLS are more similar to the ones we used for DLS targeting, when compared with those observed between ALM and M1 (in VLS: AP = 0.5 mm; ML = 2.25 mm; DV = 3 mm; in DLS: AP = 0.5 mm; ± 2.5 mm; DV: -2.1 to -2.5 mm). However, since we do not report a significant effect at the onset of licking after M1 or DLS inhibition, this suggests that neither ALM nor VLS neuronal populations were targeted in our optogenetic experiments.

Finally, we assessed the role that M1 and DLS have on action selection, which constituted the main goal of this project. Our results showed that M1 activity does not influence the selection of the next choice on neither of the conditions under analysis (rewarded vs non-rewarded trials; choice selected after next trial initiation' attempt). On the contrary, DLS inhibition resulted in a significant effect on the probability of switching the choice selected in rewarded trials, after the attempt to initiate a new trial. To observe this effect after rewarded trials is particularly striking, since it is less likely that

an animal opts for a different choice from the one selected previously if it resulted in a positive outcome [191].

These results assign a clear role on action selection to the DLS, a function which has been highly suggested to be performed at the striatal level. The operations underlying the striatum's ability to exert such a function have been long debated. In this study, we suggest a possible mechanism that enables the striatum to influence action selection. Given the results we collected from our experiments, I propose a simple model in which the striatum impacts the selection of upcoming actions by acting as a switch/repeat module for action choice [240].

The implementation of such a simplistic mechanism to determine the selection of actions to be exerted implies that the activity that arises from the striatum, and consequently the BG, results in an immediate effect upon action performance. Such an effect can be observed in our results, as DLS inhibition within the event of nose poking a side poke (report of choice) in a previous trial and the attempt to initiate the next trial significantly alters the choice of the next trial. Furthermore, we observe that in eYFP mice the difference in the probability of choice switching, after rewarded trials, is largely unaffected between trials with and without light manipulation, which suggests that, in normal conditions, the DLS supports the repetition of an action that previously led to a positive outcome. This is also a tendency in non-rewarded trials, which goes accordingly with the idea that a switch in action selection must be derived from a sequence of outcomes that do not match with the animal's expectations, instead of a lose-shift strategy [191]. However, we did not analyze the difference in the probability of switching to a different choice in upcoming trials after two or three negative outcomes, which would provide an additional insight about the relationship between DLS activity and the strategy implemented to exert the switch/repeat function that we propose.

This dichotomy in function suggest that the two SPNs neuronal populations represent, separately, the modules of repeating and switching, with the prevalence of D1- or D2-SPNs activity either increasing the frequency of repetitive actions, or promoting action switching. Various studies have attributed these properties to these different pathways, showcasing that D2-SPNs activity promotes behavioral switching [7,240] while D1-SPNS excitation contributes to maintaining the same action course (repetition) [240], depending on the previous outcome history of their choices.

This effect is probably the result of how these neuronal populations distinctively respond to the outcome of their actions. D1-SPNs mainly respond to positive outcomes, while D2-SPNs are not only more sensitive to negative outcomes, but also respond to this negative value more rapidly than D1-SPNs [240,241]. This suggests that D2-SPNs activity can quickly adjust following actions when previous ones did not

correspond to the animal's expectations, by eliciting a switch on the next action course, while D1-SPNs support the repetition of the same action previously exerted if it resulted in a positive outcome. Although we did not perform our inhibition experiments at SPN-specific level (see Conclusion and Future Directions), our results closely match the ones described in these studies. Interestingly, the aforementioned studies described these D1- and D2-SPNs properties on DMS's neuronal populations, while in our experiments we manipulated DLS's SPNs, prompting the revision on the theorized segregated functionality of DMS and DLS activity in respect to goal-directed and habitual actions, respectively.

Trying to fit this switch/repeat function in a model of activity that explains how both pathways work in concert to guide the selection of specific actions is difficult. Intuitively, if D1- and D2-SPNs activity encodes repeat and switch functions, then their activity should be exerted separately. However, a recent model that has been proposed to explain how the simultaneous activity of both SPNs populations may guide action selection, provides a comprehensive explanation on how the combinatory activity of switch and repeat signals results in the selection of an intended action. Named the "competitive model", it suggests that the resulting output of BG activity results from a competition between D1- and D2-SPNs populations that are tuned to the same action[242]. Depending on the value of the outcomes from previous actions, one of the SPNs populations will "win" in relation to the other, and decide whether to switch or repeat the action previously performed. This implies that different D1-and D2- SPNs populations have access to the same set of inputs/information, and that specific ensembles of activity between these populations are related to specific actions, which is true for both cases [72,76,77,160,162].

Moreover, the evidence linking imbalanced striatal activity with the emergence of neuropsychiatric diseases whose phenotype denounce inappropriate action initiation and selection functions, such as OCD, suits well with a switch/repeat mechanism underlying striatal activity. OCD patients display highly repetitive behaviors in the form of actions, and reveal an incapacity to counter the onset of these behaviors and to switch to an alternate action after the initiation of such actions [29,43]. It has been described that corticostriatal dysfunction is at the origin of this disorder at striatal level [49], and given the differential pattern of innervation by cortical areas on D1- and D2-SPNs [97] this may suggest that imbalance of the cortical inputs provided to these different populations may affect striatal activity, by strengthening/deficit of one SPNs' population in relation to the other.

Is important to mention that our results do not support the main models that attempt to explain how striatal activity relates to the functions performed by the striatum. In

detail, the rate model assumes that D1/ D2-SPNs activity supports/inhibits movement generation [23,27,70], but our results reveal that inhibition of the DLS does not lead to movement impairments (no delays in the timing for action execution). Regarding the rate model, which proposes that D1-SPNs activity supports the action to be exerted, while D2-SPNs activity suppresses all other competing actions [9,61], our results suggest that the activity that results from both SPNs support a repeat/switch module between these populations, for which D2-SPNs activity would contribute to switch the action previously exerted, therefore being action-specific.

Finally, our experiments further revealed that the selection process does not occur in time-periods that are close to the initiation of trials. As previously mentioned, analysis on the initiation of the next trial (Next Center In), after rewarded trials, leads to a higher probability of analyzed trials in which the light stimulation offset precedes this event (see Figure 5, Materials and Methods). However, we here report a significant effect of DLS inhibition on the probability of switching the choice selected after Next Center In, in rewarded trials. Therefore, even in trials where DLS was no longer inhibited in time-periods closer to the initiation of the next trial, previous inhibition of DLS was sufficient to affect the selection of the next choice, meaning that the selection process is not performed closer to the event of trial initiation in our task.

In summary, in this thesis, my results demonstrate distinct effects of M1 and DLS inhibition on the selection and initiation of actions, as well as their execution. These findings suggest that these two neuronal regions contribute, in different fashion, to proper action performance, providing a comprehensive study on where different action-related functions are performed in order to generate some of the first stages of motor activity.

Conclusion and Future Perspectives

Concluding, in this project, I used state-of-the art optogenetic and behavioral approaches to compare the role of M1 and DLS during action selection. My study provides new insights into the general functioning of DLS and M1 in action-related themes, particularly on the possible roles these regions have in the initiation, execution and selection of actions.

Our results indicate that DLS activity plays a role in action initiation, while also playing an effect on the selection of the upcoming action choice. M1 activity, on the other hand, seems crucial for both the initiation and execution phases of the task. The strength of my approach to studying these circuits was that I investigated both M1 and DLS within the same task. This approach therefore provides a common ground for the comparison of the inhibition effects on M1 and DLS.

To further dissect the role of DLS in action selection, it is important to understand how the two major neuronal cell-types of the striatum interact and contribute to the effects we observe. Since we suggest that D1- and D2-SPNs act as repeat and switch modules, respectively, selective inhibition of each of these pathways during the events of the task we analyzed to assess DLS activity's importance for action selection, would contribute to clarify this hypothesis and to allow a more detailed understanding on how both SPNs populations within the DLS contribute to this process.

To assess if the delays we observe during the execution and initiation phases of the task after M1 and DLS inhibition, respectively, are either the result of a delay of the onset to initiate the actions necessary to complete those events or the consequence of movement constraints related with the speed of the movements exerted, analysis on the accelerometer data we obtained from the motor outputs performed by the animals would provide interesting details on this matter.

Lastly, electrophysiological experiments *in vivo* will be performed to quantify the inhibition properties of stGtACR2 in M1 and DLS at the titers and volumes used in our surgeries, and under the light power chosen for our optogenetic experiments.

References

1. Arber, S. & Costa, R. M. Connecting neuronal circuits for movement. *Science (80-.).* **360**, 1403–1404 (2018).
2. Sanes, J. N. & Donoghue, J. P. Plasticity and Primary Motor Cortex. *Annu. Rev. Neurosci.* **23**, 393–415 (2000).
3. Shenoy, K. V, Sahani, M. & Churchland, M. M. Cortical Control of Arm Movements: A Dynamical Systems Perspective. *Annu. Rev. Neurosci.* **36**, 337–359 (2013).
4. Kaufman, M. T. *et al.* The Largest Response Component in the Motor Cortex Reflects Movement Timing but Not Movement Type. *eNeuro* **3**, (2016).
5. Thura, D. & Cisek, P. Deliberation and Commitment in the Premotor and Primary Motor Cortex during Dynamic Decision Making. *Neuron* **81**, 1401–1416 (2014).
6. Cui, G. *et al.* Concurrent activation of striatal direct and indirect pathways during action initiation. *Nature* **494**, 238–242 (2013).
7. Tecuapetla, F., Jin, X., Lima, S. Q. & Costa, R. M. Complementary Contributions of Striatal Projection Pathways to Action Initiation and Execution. *Cell* **166**, 703–715 (2016).
8. Kropotov, J. D. & Etlinger, S. C. Selection of actions in the basal ganglia–thalamocortical circuits: review and model. *Int. J. Psychophysiol.* **31**, 197–217 (1999).
9. Mink, J. W. THE BASAL GANGLIA: FOCUSED SELECTION AND INHIBITION OF COMPETING MOTOR PROGRAMS. *Prog. Neurobiol.* **50**, 381–425 (1996).
10. Redgrave, P., Prescott, T. J. & Gurney, K. The basal ganglia: a vertebrate solution to the selection problem? *Neuroscience* **89**, 1009–1023 (1999).
11. Büschges, A., Scholz, H. & El Manira, A. New Moves in Motor Control. *Curr. Biol.* **21**, R513–R524 (2011).
12. Kiehn, O. Development and functional organization of spinal locomotor circuits. *Curr. Opin. Neurobiol.* **21**, 100–109 (2011).
13. Arber, S. Motor Circuits in Action: Specification, Connectivity, and Function. *Neuron* **74**, 975–989 (2012).
14. Lemon, R. N. Descending Pathways in Motor Control. *Annu. Rev. Neurosci.* **31**, 195–218 (2008).
15. Ruder, L. & Arber, S. Brainstem Circuits Controlling Action Diversification. *Annu. Rev. Neurosci.* **42**, 485–504 (2019).
16. Grillner, S. & Robertson, B. The basal ganglia downstream control of brainstem motor centres—an evolutionarily conserved strategy. *Curr. Opin. Neurobiol.* **33**, 47–52 (2015).
17. Roseberry, T. K. *et al.* Cell-Type-Specific Control of Brainstem Locomotor Circuits by Basal Ganglia. *Cell* **164**, 526–537 (2016).
18. Takakusaki, K., Saitoh, K., Harada, H. & Kashiwayanagi, M. Role of basal ganglia–brainstem pathways in the control of motor behaviors. *Neurosci. Res.* **50**, 137–151 (2004).
19. Evarts, E. V. Relation of pyramidal tract activity to force exerted during voluntary movement. *J. Neurophysiol.* **31**, 14–27 (1968).
20. Svoboda, K. & Li, N. Neural mechanisms of movement planning: motor cortex and beyond. *Curr. Opin. Neurobiol.* **49**, 33–41 (2018).
21. Kakei, S. Muscle and Movement Representations in the Primary Motor Cortex. *Science (80-.).* **285**, 2136–2139 (1999).
22. Klaus, A., Alves da Silva, J. & Costa, R. M. What, If, and When to Move: Basal Ganglia Circuits and Self-Paced Action Initiation. *Annu. Rev. Neurosci.* **42**, 459–483 (2019).
23. Kravitz, A. V *et al.* Regulation of parkinsonian motor behaviours by optogenetic

control of basal ganglia circuitry. *Nature* **466**, 622–626 (2010).
24. Dudman, J. T. & Krakauer, J. W. The basal ganglia: from motor commands to the control of vigor. *Curr. Opin. Neurobiol.* **37**, 158–166 (2016).
25. Thura, D. & Cisek, P. The Basal Ganglia Do Not Select Reach Targets but Control the Urgency of Commitment. *Neuron* **95**, 1160-1170.e5 (2017).
26. Yttri, E. A. & Dudman, J. T. Opponent and bidirectional control of movement velocity in the basal ganglia. *Nature* **533**, 402–406 (2016).
27. Albin, R. L., Young, A. B. & Penney, J. B. The functional anatomy of basal ganglia disorders. *Trends Neurosci.* **12**, 366–375 (1989).
28. DeLong, M. R. & Wichmann, T. Circuits and Circuit Disorders of the Basal Ganglia. *Arch. Neurol.* **64**, 20–24 (2007).
29. Graybiel, A. M. & Rauch, S. L. Toward a Neurobiology of Obsessive-Compulsive Disorder. *Neuron* **28**, 343–347 (2000).
30. Berns, G. S. & Sejnowski, T. J. How the Basal Ganglia Make Decisions. in *Neurobiology of Decision-Making* (eds. Damasio, A. R., Damasio, H. & Christen, Y.) 101–113 (Springer Berlin Heidelberg, 1996).
31. Grillner, S., Hellgren, J., Ménard, A., Saitoh, K. & Wikström, M. A. Mechanisms for selection of basic motor programs – roles for the striatum and pallidum. *Trends Neurosci.* **28**, 364–370 (2005).
32. Aoki, S. *et al.* An open cortico-basal ganglia loop allows limbic control over motor output via the nigrothalamic pathway. *Elife* **8**, e49995 (2019).
33. Park, J., Coddington, L. T. & Dudman, J. T. Basal Ganglia Circuits for Action Specification. *Annu. Rev. Neurosci.* **43**, 485–507 (2020).
34. Bolam, J. P., Hanley, J. J., Booth, P. A. C. & Bevan, M. D. Synaptic organisation of the basal ganglia. *J. Anat.* **196**, 527–542 (2000).
35. Graybiel, A. M. The basal ganglia. *Curr. Biol.* **10**, R509–R511 (2000).
36. Utter, A. A. & Basso, M. A. The basal ganglia: An overview of circuits and function. *Neurosci. Biobehav. Rev.* **32**, 333–342 (2008).
37. Andre, V. M., Fisher, Y. E. & Levine, M. S. Altered Balance of Activity in the Striatal Direct and Indirect Pathways in Mouse Models of Huntington's Disease. *Front. Syst. Neurosci.* **5**, (2011).
38. Blumenstock, S. & Dudanova, I. Cortical and Striatal Circuits in Huntington's Disease. *Front. Neurosci.* **14**, (2020).
39. G. Vonsattel, J. P. & DiFiglia, M. Huntington Disease: *J. Neuropathol. Exp. Neurol.* **57**, 369–384 (1998).
40. Jankovic, J. Parkinson's disease: clinical features and diagnosis. *J. Neurol. Neurosurg. Psychiatry* **79**, 368–376 (2008).
41. Obeso, J. A. *et al.* Pathophysiology of the basal ganglia in Parkinson's disease. *Trends Neurosci.* **23**, S8–S19 (2000).
42. Poewe, W. *et al.* Parkinson disease. *Nat. Rev. Dis. Prim.* **3**, 1–21 (2017).
43. Burguière, E., Monteiro, P., Mallet, L., Feng, G. & Graybiel, A. M. Striatal circuits, habits, and implications for obsessive–compulsive disorder. *Curr. Opin. Neurobiol.* **30**, 59–65 (2015).
44. Durston, S. *et al.* Differential patterns of striatal activation in young children with and without ADHD. *Biol. Psychiatry* **53**, 871–878 (2003).
45. Hiebert, N. M. *et al.* Striatum-Mediated Deficits in Stimulus-Response Learning and Decision-Making in OCD. *Front. Psychiatry* **11**, (2020).
46. Lisboa, B. C. G. *et al.* Initial findings of striatum tripartite model in OCD brain samples based on transcriptome analysis. *Sci. Rep.* **9**, 3086 (2019).
47. Mills, K. L. *et al.* Altered Cortico-Striatal–Thalamic Connectivity in Relation to Spatial Working Memory Capacity in Children with ADHD. *Front. Psychiatry* **3**, (2012).
48. Petrovic, P. & Castellanos, F. X. Top-Down Dysregulation—From ADHD to Emotional Instability. *Front. Behav. Neurosci.* **10**, (2016).
49. Welch, J. M. *et al.* Cortico-striatal synaptic defects and OCD-like behaviours in

Sapap3 -mutant mice. *Nature* **448**, 894–900 (2007).
50. Tepper, J. M. & Koós, T. Chapter 8 - GABAergic Interneurons of the Striatum. in *Handbook of Behavioral Neuroscience* (eds. Steiner, H. & Tseng, K. Y.) vol. 24 157–178 (Elsevier, 2016).
51. Tepper, J. M., Tecuapetla, F., Koos, T. & Ibanez-Sandoval, O. Heterogeneity and Diversity of Striatal GABAergic Interneurons. *Front. Neuroanat.* **4**, (2010).
52. Tepper, J. M. *et al.* Heterogeneity and Diversity of Striatal GABAergic Interneurons: Update 2018. *Front. Neuroanat.* **12**, (2018).
53. Bishop, G. A., Chang, H. T. & Kitai, S. T. Morphological and physiological properties of neostriatal neurons: An intracellular horseradish peroxidase study in the rat. *Neuroscience* **7**, 179–191 (1982).
54. DiFiglia, M., Pasik, P. & Pasik, T. A Golgi study of neuronal types in the neostriatum of monkeys. *Brain Res.* **114**, 245–256 (1976).
55. Gerfen, C. R. & Wilson, C. J. Chapter II The basal ganglia. in *Handbook of chemical neuroanatomy* vol. 12 371–468 (Elsevier, 1996).
56. Wilson, C. J. & Groves, P. M. Fine structure and synaptic connections of the common spiny neuron of the rat neostriatum: A study employing intracellular injection of horseradish peroxidase. *J. Comp. Neurol.* **194**, 599–615 (1980).
57. Gerfen, C. R. *et al.* D1 and D2 dopamine receptor-regulated gene expression of striatonigral and striatopallidal neurons. *Science (80-.).* **250**, 1429–1432 (1990).
58. Parent, A., Bouchard, C. & Smith, Y. The striatopallidal and striatonigral projections: two distinct fiber systems in primate. *Brain Res.* **303**, 385–390 (1984).
59. Parent, A. & Hazrati, L.-N. Functional anatomy of the basal ganglia. I. The cortico-basal ganglia-thalamo-cortical loop. *Brain Res. Rev.* **20**, 91–127 (1995).
60. Hikosaka, O. GABAergic output of the basal ganglia. in *Progress in Brain Research* vol. 160 209–226 (Elsevier, 2007).
61. Hikosaka, O., Takikawa, Y. & Kawagoe, R. Role of the basal ganglia in the control of purposive saccadic eye movements. *Physiol. Rev.* **80**, 953–978 (2000).
62. Alexander, G. E. & Crutcher, M. D. Functional architecture of basal ganglia circuits: neural substrates of parallel processing. *Trends Neurosci.* **13**, 266–271 (1990).
63. Haber, S. & Mcfarland, N. R. The Place of the Thalamus in Frontal Cortical-Basal Ganglia Circuits. *Neurosci.* **7**, 315–324 (2001).
64. Takakusaki, K., Habaguchi, T., Ohtinata-Sugimoto, J., Saitoh, K. & Sakamoto, T. Basal ganglia efferents to the brainstem centers controlling postural muscle tone and locomotion: a new concept for understanding motor disorders in basal ganglia dysfunction. *Neuroscience* **119**, 293–308 (2003).
65. Mena-Segovia, J., Bolam, J. P. & Magill, P. J. Pedunculopontine nucleus and basal ganglia: distant relatives or part of the same family? *Trends Neurosci.* **27**, 585–588 (2004).
66. Bostan, A. C. & Strick, P. L. The basal ganglia and the cerebellum: nodes in an integrated network. *Nat. Rev. Neurosci.* **19**, 338–350 (2018).
67. Bostan, A. C., Dum, R. P. & Strick, P. L. The basal ganglia communicate with the cerebellum. *Proc. Natl. Acad. Sci.* **107**, 8452–8456 (2010).
68. Shires, J., Joshi, S. & Basso, M. A. Shedding new light on the role of the basal ganglia-superior colliculus pathway in eye movements. *Curr. Opin. Neurobiol.* **20**, 717–725 (2010).
69. Redgrave, P. *et al.* Interactions between the Midbrain Superior Colliculus and the Basal Ganglia. *Front. Neuroanat.* **4**, (2010).
70. DeLong, M. R. Primate models of movement disorders of basal ganglia origin. *Trends Neurosci.* **13**, 281–285 (1990).
71. Jin, X., Tecuapetla, F. & Costa, R. M. Basal ganglia subcircuits distinctively encode the parsing and concatenation of action sequences. *Nat. Neurosci.* **17**,

423–430 (2014).
72. Klaus, A. *et al.* The spatiotemporal organization of the striatum encodes action space. *Neuron* **95**, 1171–1180 (2017).
73. Tecuapetla, F., Matias, S., Dugue, G. P., Mainen, Z. F. & Costa, R. M. Balanced activity in basal ganglia projection pathways is critical for contraversive movements. *Nat. Commun.* **5**, 4315 (2014).
74. O'Hare, J. K. *et al.* Pathway-Specific Striatal Substrates for Habitual Behavior. *Neuron* **89**, 472–479 (2016).
75. Schmidt, R., Leventhal, D. K., Mallet, N., Chen, F. & Berke, J. D. Canceling actions involves a race between basal ganglia pathways. *Nat. Neurosci.* **16**, 1118–1124 (2013).
76. Markowitz, J. E. *et al.* The Striatum Organizes 3D Behavior via Moment-to-Moment Action Selection. *Cell* **174**, 44-58.e17 (2018).
77. Parker, J. G. *et al.* Diametric neural ensemble dynamics in parkinsonian and dyskinetic states. *Nature* **557**, 177–182 (2018).
78. Carlsson, A., Lindqvist, M., Magnusson, T. & Waldeck, B. On the Presence of 3-Hydroxytyramine in Brain. *Science (80-.).* **127**, 471 (1958).
79. Hornykiewicz, O. [The tropical localization and content of noradrenalin and dopamine (3-hydroxytyramine) in the substantia nigra of normal persons and patients with Parkinson's disease]. *Wien. Klin. Wochenschr.* **75**, 309–312 (1963).
80. Kim, K. M. *et al.* Optogenetic Mimicry of the Transient Activation of Dopamine Neurons by Natural Reward Is Sufficient for Operant Reinforcement. *PLoS One* **7**, e33612 (2012).
81. Montague, P. R., Dayan, P. & Sejnowski, T. J. A framework for mesencephalic dopamine systems based on predictive Hebbian learning. *J. Neurosci.* **16**, 1936–1947 (1996).
82. Schultz, W., Dayan, P. & Montague, P. R. A Neural Substrate of Prediction and Reward. *Science (80-.).* **275**, 1593–1599 (1997).
83. Stauffer, W. R. *et al.* Dopamine Neuron-Specific Optogenetic Stimulation in Rhesus Macaques. *Cell* **166**, 1564-1571.e6 (2016).
84. Watabe-Uchida, M., Eshel, N. & Uchida, N. Neural Circuitry of Reward Prediction Error. *Annu. Rev. Neurosci.* **40**, 373–394 (2017).
85. Howe, M. W. & Dombeck, D. A. Rapid signalling in distinct dopaminergic axons during locomotion and reward. *Nature* **535**, 505–510 (2016).
86. Jin, X. & Costa, R. M. Start/stop signals emerge in nigrostriatal circuits during sequence learning. *Nature* **466**, 457–462 (2010).
87. Mazzoni, P., Hristova, A. & Krakauer, J. W. Why Don't We Move Faster? Parkinson's Disease, Movement Vigor, and Implicit Motivation. *J. Neurosci.* **27**, 7105–7116 (2007).
88. da Silva, J. A., Tecuapetla, F., Paixão, V. & Costa, R. M. Dopamine neuron activity before action initiation gates and invigorates future movements. *Nature* **554**, 244–248 (2018).
89. Syed, E. C. J. *et al.* Action initiation shapes mesolimbic dopamine encoding of future rewards. *Nat. Neurosci.* **19**, 34–36 (2016).
90. Berke, J. D. What does dopamine mean? *Nat. Neurosci.* **21**, 787–793 (2018).
91. Doig, N. M., Moss, J. & Bolam, J. P. Cortical and Thalamic Innervation of Direct and Indirect Pathway Medium-Sized Spiny Neurons in Mouse Striatum. *J. Neurosci.* **30**, 14610–14618 (2010).
92. Guo, Q. *et al.* Whole-Brain Mapping of Inputs to Projection Neurons and Cholinergic Interneurons in the Dorsal Striatum. *PLoS One* **10**, e0123381 (2015).
93. Haber, S. N. & Calzavara, R. The cortico-basal ganglia integrative network: The role of the thalamus. *Brain Res. Bull.* **78**, 69–74 (2009).
94. Huerta-Ocampo, I., Mena-Segovia, J. & Bolam, J. P. Convergence of cortical and thalamic input to direct and indirect pathway medium spiny neurons in the

striatum. *Brain Struct. Funct.* **219**, 1787–1800 (2014).
95. Hunnicutt, B. J. *et al.* A comprehensive excitatory input map of the striatum reveals novel functional organization. *Elife* **5**, e19103 (2016).
96. Smith, Y. *et al.* The thalamostriatal system in normal and diseased states. *Front. Syst. Neurosci.* **8**, (2014).
97. Wall, N. R., De La Parra, M., Callaway, E. M. & Kreitzer, A. C. Differential Innervation of Direct- and Indirect-Pathway Striatal Projection Neurons. *Neuron* **79**, 347–360 (2013).
98. Kato, S. *et al.* Action Selection and Flexible Switching Controlled by the Intralaminar Thalamic Neurons. *Cell Rep.* **22**, 2370–2382 (2018).
99. Díaz-Hernández, E. *et al.* The Thalamostriatal Projections Contribute to the Initiation and Execution of a Sequence of Movements. *Neuron* **100**, 739-752.e5 (2018).
100. Guo, Z. V *et al.* Maintenance of persistent activity in a frontal thalamocortical loop. *Nature* **545**, 181–186 (2017).
101. Giber, K. *et al.* A subcortical inhibitory signal for behavioral arrest in the thalamus. *Nat. Neurosci.* **18**, 562–568 (2015).
102. Hoshi, E., Tremblay, L., Féger, J., Carras, P. L. & Strick, P. L. The cerebellum communicates with the basal ganglia. *Nat. Neurosci.* **8**, 1491–1493 (2005).
103. Xiao, L., Bornmann, C., Hatstatt-Burklé, L. & Scheiffele, P. Regulation of striatal cells and goal-directed behavior by cerebellar outputs. *Nat. Commun.* **9**, 3133 (2018).
104. Assous, M., Dautan, D., Tepper, J. M. & Mena-Segovia, J. Pedunculopontine Glutamatergic Neurons Provide a Novel Source of Feedforward Inhibition in the Striatum by Selectively Targeting Interneurons. *J. Neurosci.* **39**, 4727–4737 (2019).
105. Dautan, D. *et al.* A Major External Source of Cholinergic Innervation of the Striatum and Nucleus Accumbens Originates in the Brainstem. *J. Neurosci.* **34**, 4509–4518 (2014).
106. Watson, G. D. R., Smith, J. B. & Alloway, K. D. The Zona Incerta Regulates Communication between the Superior Colliculus and the Posteromedial Thalamus: Implications for Thalamic Interactions with the Dorsolateral Striatum. *J. Neurosci.* **35**, 9463–9476 (2015).
107. Choi, E. Y., Ding, S.-L. & Haber, S. N. Combinatorial Inputs to the Ventral Striatum from the Temporal Cortex, Frontal Cortex, and Amygdala: Implications for Segmenting the Striatum. *eNeuro* **4**, (2017).
108. Jiang, H. & Kim, H. F. Anatomical Inputs From the Sensory and Value Structures to the Tail of the Rat Striatum. *Front. Neuroanat.* **12**, (2018).
109. Pan, W. X., Mao, T. & Dudman, J. T. Inputs to the Dorsal Striatum of the Mouse Reflect the Parallel Circuit Architecture of the Forebrain. *Front. Neuroanat.* **4**, (2010).
110. Corbit, L. H., Leung, B. K. & Balleine, B. W. The Role of the Amygdala-Striatal Pathway in the Acquisition and Performance of Goal-Directed Instrumental Actions. *J. Neurosci.* **33**, 17682–17690 (2013).
111. Correia, S. S., McGrath, A. G., Lee, A., Graybiel, A. M. & Goosens, K. A. Amygdala-ventral striatum circuit activation decreases long-term fear. *Elife* **5**, e12669 (2016).
112. Klug, J. R. *et al.* Differential inputs to striatal cholinergic and parvalbumin interneurons imply functional distinctions. *Elife* **7**, e35657 (2018).
113. Mallet, N. *et al.* Dichotomous Organization of the External Globus Pallidus. *Neuron* **74**, 1075–1086 (2012).
114. Kondabolu, K. *et al. A selective projection from the subthalamic nucleus to parvalbumin-expressing interneurons of the striatum*. http://biorxiv.org/lookup/doi/10.1101/2020.11.26.400242 (2020).
115. Koshimizu, Y., Fujiyama, F., Nakamura, K. C., Furuta, T. & Kaneko, T.

Quantitative analysis of axon bouton distribution of subthalamic nucleus neurons in the rat by single neuron visualization with a viral vector. *J. Comp. Neurol.* **521**, 2125–2146 (2013).
116. Mallet, N. *et al.* Arkypallidal Cells Send a Stop Signal to Striatum. *Neuron* **89**, 308–316 (2016).
117. Hintiryan, H. *et al.* The mouse cortico-striatal projectome. *Nat. Neurosci.* **19**, 1100–1114 (2016).
118. Khibnik, L. A., Tritsch, N. X. & Sabatini, B. L. A Direct Projection from Mouse Primary Visual Cortex to Dorsomedial Striatum. *PLoS One* **9**, e104501 (2014).
119. Hooks, B. M. *et al.* Topographic precision in sensory and motor corticostriatal projections varies across cell type and cortical area. *Nat. Commun.* **9**, 3549 (2018).
120. Corbit, V. L., Manning, E. E., Gittis, A. H. & Ahmari, S. E. Strengthened Inputs from Secondary Motor Cortex to Striatum in a Mouse Model of Compulsive Behavior. *J. Neurosci.* **39**, 2965–2975 (2019).
121. Gremel, C. M. & Costa, R. M. Orbitofrontal and striatal circuits dynamically encode the shift between goal-directed and habitual actions. *Nat. Commun.* **4**, 2264 (2013).
122. Lee, C. R. *et al.* Opposing Influence of Sensory and Motor Cortical Input on Striatal Circuitry and Choice Behavior. *Curr. Biol.* **29**, 1313-1323.e5 (2019).
123. Pidoux, M., Mahon, S., Deniau, J.-M. & Charpier, S. Integration and propagation of somatosensory responses in the corticostriatal pathway: an intracellular study in vivo. *J. Physiol.* **589**, 263–281 (2011).
124. Terra, H. *et al.* Prefrontal Cortical Projection Neurons Targeting Dorsomedial Striatum Control Behavioral Inhibition. *Curr. Biol.* **30**, 4188-4200.e5 (2020).
125. Burton, A. C., Nakamura, K. & Roesch, M. R. From ventral-medial to dorsal-lateral striatum: Neural correlates of reward-guided decision-making. *Neurobiol. Learn. Mem.* **117**, 51–59 (2015).
126. Liljeholm, M. & O'Doherty, J. P. Contributions of the striatum to learning, motivation, and performance: an associative account. *Trends Cogn. Sci.* **16**, 467–475 (2012).
127. Groenewegen, H. J. & Trimble, M. The Ventral Striatum as an Interface Between the Limbic and Motor Systems. *CNS Spectr.* **12**, 887–892 (2007).
128. Groenewegen, H. J., Wright, C. I., Beijer, A. V. J. & Voorn, P. Convergence and Segregation of Ventral Striatal Inputs and Outputs. *Ann. N. Y. Acad. Sci.* **877**, 49–63 (1999).
129. Haber, S. N. Corticostriatal circuitry. *Dialogues Clin. Neurosci.* **18**, 7–21 (2016).
130. Humphries, M. D. & Prescott, T. J. The ventral basal ganglia, a selection mechanism at the crossroads of space, strategy, and reward. *Prog. Neurobiol.* **90**, 385–417 (2010).
131. McColgan, P., Joubert, J., Tabrizi, S. J. & Rees, G. The human motor cortex microcircuit: insights for neurodegenerative disease. *Nat. Rev. Neurosci.* **21**, 401–415 (2020).
132. Muñoz-Castañeda, R. *et al. Cellular Anatomy of the Mouse Primary Motor Cortex*. http://biorxiv.org/lookup/doi/10.1101/2020.10.02.323154 (2020).
133. Nambu, A., Takada, M., Inase, M. & Tokuno, H. Dual somatotopical representations in the primate subthalamic nucleus: evidence for ordered but reversed body-map transformations from the primary motor cortex and the supplementary motor area. *J. Neurosci.* **16**, 2671–2683 (1996).
134. Yamawaki, N. & Shepherd, G. M. G. Synaptic Circuit Organization of Motor Corticothalamic Neurons. *J. Neurosci.* **35**, 2293–2307 (2015).
135. Dum, R. P. & Strick, P. L. Frontal Lobe Inputs to the Digit Representations of the Motor Areas on the Lateral Surface of the Hemisphere. *J. Neurosci.* **25**, 1375–1386 (2005).
136. Hooks, B. M. *et al.* Organization of Cortical and Thalamic Input to Pyramidal

Neurons in Mouse Motor Cortex. *J. Neurosci.* **33**, 748–760 (2013).
137. Sano, N. *et al.* Cerebellar outputs contribute to spontaneous and movement-related activity in the motor cortex of monkeys. *Neurosci. Res.* (2020) doi:10.1016/j.neures.2020.03.010.
138. Lee, H. J. *et al.* Activation of Direct and Indirect Pathway Medium Spiny Neurons Drives Distinct Brain-wide Responses. *Neuron* **91**, 412–424 (2016).
139. Oldenburg, I. A. & Sabatini, B. L. Antagonistic but Not Symmetric Regulation of Primary Motor Cortex by Basal Ganglia Direct and Indirect Pathways. *Neuron* **86**, 1174–1181 (2015).
140. Huber, D. *et al.* Multiple dynamic representations in the motor cortex during sensorimotor learning. *Nature* **484**, 473–478 (2012).
141. Mao, T. *et al.* Long-Range Neuronal Circuits Underlying the Interaction between Sensory and Motor Cortex. *Neuron* **72**, 111–123 (2011).
142. Petrof, I., Viaene, A. N. & Sherman, S. M. Properties of the primary somatosensory cortex projection to the primary motor cortex in the mouse. *J. Neurophysiol.* **113**, 2400–2407 (2015).
143. Hosp, J. A., Pekanovic, A., Rioult-Pedotti, M. S. & Luft, A. R. Dopaminergic Projections from Midbrain to Primary Motor Cortex Mediate Motor Skill Learning. *J. Neurosci.* **31**, 2481–2487 (2011).
144. Molina-Luna, K. *et al.* Dopamine in Motor Cortex Is Necessary for Skill Learning and Synaptic Plasticity. *PLoS One* **4**, e7082 (2009).
145. Levy, S. *et al.* Cell-Type-Specific Outcome Representation in the Primary Motor Cortex. *Neuron* **107**, 954-971.e9 (2020).
146. Li, Q. *et al.* Refinement of learned skilled movement representation in motor cortex deep output layer. *Nat. Commun.* **8**, 15834 (2017).
147. Papale, A. E. & Hooks, B. M. Circuit Changes in Motor Cortex During Motor Skill Learning. *Neuroscience* **368**, 283–297 (2018).
148. Masamizu, Y. *et al.* Two distinct layer-specific dynamics of cortical ensembles during learning of a motor task. *Nat. Neurosci.* **17**, 987–994 (2014).
149. Guo, J.-Z. *et al.* Cortex commands the performance of skilled movement. *Elife* **4**, e10774 (2015).
150. Kawai, R. *et al.* Motor Cortex Is Required for Learning but Not for Executing a Motor Skill. *Neuron* **86**, 800–812 (2015).
151. Ebbesen, C. L. & Brecht, M. Motor cortex — to act or not to act? *Nat. Rev. Neurosci.* **18**, 694–705 (2017).
152. Georgopoulos, A. P. & Carpenter, A. F. Coding of movements in the motor cortex. *Curr. Opin. Neurobiol.* **33**, 34–39 (2015).
153. Watanabe, H. *et al.* Forelimb movements evoked by optogenetic stimulation of the macaque motor cortex. *Nat. Commun.* **11**, 3253 (2020).
154. Persichetti, A. S., Avery, J. A., Huber, L., Merriam, E. P. & Martin, A. Layer-Specific Contributions to Imagined and Executed Hand Movements in Human Primary Motor Cortex. *Curr. Biol.* **30**, 1721-1725.e3 (2020).
155. Sreenivasan, V. *et al.* Movement Initiation Signals in Mouse Whisker Motor Cortex. *Neuron* **92**, 1368–1382 (2016).
156. Griffin, D. M. & Strick, P. L. The motor cortex uses active suppression to sculpt movement. *Sci. Adv.* **6**, eabb8395 (2020).
157. Derosiere, G., Thura, D., Cisek, P. & Duque, J. Motor cortex disruption delays motor processes but not deliberation about action choices. *J. Neurophysiol.* **122**, 1566–1577 (2019).
158. Kaufman, M. T., Churchland, M. M., Ryu, S. I. & Shenoy, K. V. Cortical activity in the null space: permitting preparation without movement. *Nat. Neurosci.* **17**, 440–448 (2014).
159. Elsayed, G. F., Lara, A. H., Kaufman, M. T., Churchland, M. M. & Cunningham, J. P. Reorganization between preparatory and movement population responses in motor cortex. *Nat. Commun.* **7**, 13239 (2016).

160. Reig, R. & Silberberg, G. Multisensory Integration in the Mouse Striatum. *Neuron* **83**, 1200–1212 (2014).
161. Deng, Y. *et al.* Differential organization of cortical inputs to striatal projection neurons of the matrix compartment in rats. *Front. Syst. Neurosci.* **9**, (2015).
162. Kress, G. J. *et al.* Convergent cortical innervation of striatal projection neurons. *Nat. Neurosci.* **16**, 665–667 (2013).
163. Reiner, A., Hart, N. M., Lei, W. & Deng, Y. Corticostriatal Projection Neurons – Dichotomous Types and Dichotomous Functions. *Front. Neuroanat.* **4**, (2010).
164. Shepherd, G. M. G. Corticostriatal connectivity and its role in disease. *Nat. Rev. Neurosci.* **14**, 278–291 (2013).
165. Hart, G., Bradfield, L. A. & Balleine, B. W. Prefrontal Corticostriatal Disconnection Blocks the Acquisition of Goal-Directed Action. *J. Neurosci.* **38**, 1311–1322 (2018).
166. Hart, G., Bradfield, L. A., Fok, S. Y., Chieng, B. & Balleine, B. W. The Bilateral Prefronto-striatal Pathway Is Necessary for Learning New Goal-Directed Actions. *Curr. Biol.* **28**, 2218-2229.e7 (2018).
167. Friedman, A. *et al.* A Corticostriatal Path Targeting Striosomes Controls Decision-Making under Conflict. *Cell* **161**, 1320–1333 (2015).
168. Otis, J. M. *et al.* Prefrontal cortex output circuits guide reward seeking through divergent cue encoding. *Nature* **543**, 103–107 (2017).
169. Stalnaker, T. A., Berg, B., Aujla, N. & Schoenbaum, G. Cholinergic Interneurons Use Orbitofrontal Input to Track Beliefs about Current State. *J. Neurosci.* **36**, 6242–6257 (2016).
170. Sjöbom, J., Tamtè, M., Halje, P., Brys, I. & Petersson, P. Cortical and striatal circuits together encode transitions in natural behavior. *Sci. Adv.* **6**, eabc1173 (2020).
171. Turner, R. S. & DeLong, M. R. Corticostriatal Activity in Primary Motor Cortex of the Macaque. *J. Neurosci.* **20**, 7096–7108 (2000).
172. Durieux, P. F., Schiffmann, S. N. & de Kerchove d'Exaerde, A. Differential regulation of motor control and response to dopaminergic drugs by D1R and D2R neurons in distinct dorsal striatum subregions. *EMBO J.* **31**, 640–653 (2012).
173. Ito, M. & Doya, K. Distinct Neural Representation in the Dorsolateral, Dorsomedial, and Ventral Parts of the Striatum during Fixed- and Free-Choice Tasks. *J. Neurosci.* **35**, 3499–3514 (2015).
174. Sano, H., Chiken, S., Hikida, T., Kobayashi, K. & Nambu, A. Signals through the Striatopallidal Indirect Pathway Stop Movements by Phasic Excitation in the Substantia Nigra. *J. Neurosci.* **33**, 7583–7594 (2013).
175. Boyd, L. A. *et al.* Motor sequence chunking is impaired by basal ganglia stroke. *Neurobiol. Learn. Mem.* **92**, 35–44 (2009).
176. Graybiel, A. M. The Basal Ganglia and Chunking of Action Repertoires. *Neurobiol. Learn. Mem.* **70**, 119–136 (1998).
177. Jin, X. & Costa, R. M. Shaping action sequences in basal ganglia circuits. *Curr. Opin. Neurobiol.* **33**, 188–196 (2015).
178. Wymbs, N. F., Bassett, D. S., Mucha, P. J., Porter, M. A. & Grafton, S. T. Differential Recruitment of the Sensorimotor Putamen and Frontoparietal Cortex during Motor Chunking in Humans. *Neuron* **74**, 936–946 (2012).
179. Atallah, H. E., Lopez-Paniagua, D., Rudy, J. W. & O'Reilly, R. C. Separate neural substrates for skill learning and performance in the ventral and dorsal striatum. *Nat. Neurosci.* **10**, 126–131 (2007).
180. Costa, R. M., Cohen, D. & Nicolelis, M. A. L. Differential Corticostriatal Plasticity during Fast and Slow Motor Skill Learning in Mice. *Curr. Biol.* **14**, 1124–1134 (2004).
181. Featherstone, R. E. & McDonald, R. J. Dorsal striatum and stimulus-response learning: lesions of the dorsolateral, but not dorsomedial, striatum impair

acquisition of a stimulus-response-based instrumental discrimination task, while sparing conditioned place preference learning. *Neuroscience* **124**, 23–31 (2004).
182. Graybiel, A. M. & Grafton, S. T. The Striatum: Where Skills and Habits Meet. *Cold Spring Harb. Perspect. Biol.* **7**, a021691 (2015).
183. Yin, H. H. *et al.* Dynamic reorganization of striatal circuits during the acquisition and consolidation of a skill. *Nat. Neurosci.* **12**, 333–341 (2009).
184. Fobbs, W. C. *et al.* Continuous Representations of Speed by Striatal Medium Spiny Neurons. *J. Neurosci.* **40**, 1679–1688 (2020).
185. Rueda-Orozco, P. E. & Robbe, D. The striatum multiplexes contextual and kinematic information to constrain motor habits execution. *Nat. Neurosci.* **18**, 453–460 (2015).
186. Kim, H., Sul, J. H., Huh, N., Lee, D. & Jung, M. W. Role of Striatum in Updating Values of Chosen Actions. *J. Neurosci.* **29**, 14701–14712 (2009).
187. Lau, B. & Glimcher, P. W. Value Representations in the Primate Striatum during Matching Behavior. *Neuron* **58**, 451–463 (2008).
188. Samejima, K., Ueda, Y., Doya, K. & Kimura, M. Representation of Action-Specific Reward Values in the Striatum. *Science (80-.).* **310**, 1337–1340 (2005).
189. Seo, M., Lee, E. & Averbeck, B. B. Action Selection and Action Value in Frontal-Striatal Circuits. *Neuron* **74**, 947–960 (2012).
190. Yamada, H., Inokawa, H., Matsumoto, N., Ueda, Y. & Kimura, M. Neuronal basis for evaluating selected action in the primate striatum. *Eur. J. Neurosci.* **34**, 489–506 (2011).
191. Tai, L.-H., Lee, A. M., Benavidez, N., Bonci, A. & Wilbrecht, L. Transient stimulation of distinct subpopulations of striatal neurons mimics changes in action value. *Nat. Neurosci.* **15**, 1281–1289 (2012).
192. Crick, F. H. C. Thinking about the Brain. *Sci. Am.* **241**, 219–233 (1979).
193. Deisseroth, K. Optogenetics. *Nat. Methods* **8**, 26–29 (2011).
194. Sternson, S. M. & Roth, B. L. Chemogenetic Tools to Interrogate Brain Functions. *Annu. Rev. Neurosci.* **37**, 387–407 (2014).
195. Fenno, L., Yizhar, O. & Deisseroth, K. The Development and Application of Optogenetics. *Annu. Rev. Neurosci.* **34**, 389–412 (2011).
196. Yizhar, O., Fenno, L. E., Davidson, T. J., Mogri, M. & Deisseroth, K. Optogenetics in Neural Systems. *Neuron* **71**, 9–34 (2011).
197. Wiegert, J. S., Mahn, M., Prigge, M., Printz, Y. & Yizhar, O. Silencing Neurons: Tools, Applications, and Experimental Constraints. *Neuron* **95**, 504–529 (2017).
198. Owen, S. F., Liu, M. H. & Kreitzer, A. C. Thermal constraints on in vivo optogenetic manipulations. *Nat. Neurosci.* **22**, 1061–1065 (2019).
199. Stujenske, J. M., Spellman, T. & Gordon, J. A. Modeling the Spatiotemporal Dynamics of Light and Heat Propagation for In Vivo Optogenetics. *Cell Rep.* **12**, 525–534 (2015).
200. Cardin, J. A. *et al.* Targeted optogenetic stimulation and recording of neurons in vivo using cell-type-specific expression of Channelrhodopsin-2. *Nat. Protoc.* **5**, 247–254 (2010).
201. Mahn, M., Prigge, M., Ron, S., Levy, R. & Yizhar, O. Biophysical constraints of optogenetic inhibition at presynaptic terminals. *Nat. Neurosci.* **19**, 554–556 (2016).
202. Mattis, J. *et al.* Principles for applying optogenetic tools derived from direct comparative analysis of microbial opsins. *Nat. Methods* **9**, 159–172 (2012).
203. Li, N. *et al.* Spatiotemporal constraints on optogenetic inactivation in cortical circuits. *Elife* **8**, e48622 (2019).
204. Mahn, M. *et al.* High-efficiency optogenetic silencing with soma-targeted anion-conducting channelrhodopsins. *Nat. Commun.* **9**, 4125 (2018).
205. Govorunova, E. G., Sineshchekov, O. A., Janz, R., Liu, X. & Spudich, J. L. Natural light-gated anion channels: A family of microbial rhodopsins for advanced optogenetics. *Science (80-.).* **349**, 647–650 (2015).

206. Malyshev, A. Y. *et al.* Chloride conducting light activated channel GtACR2 can produce both cessation of firing and generation of action potentials in cortical neurons in response to light. *Neurosci. Lett.* **640**, 76–80 (2017).
207. Akam, T. *et al. Anterior cingulate cortex represents action-state predictions and causally mediates model-based reinforcement learning in a two-step decision task*. http://biorxiv.org/lookup/doi/10.1101/126292 (2017).
208. Guo, Z. V *et al.* Procedures for Behavioral Experiments in Head-Fixed Mice. *PLoS One* **9**, e88678 (2014).
209. Chuong, A. S. *et al.* Noninvasive optical inhibition with a red-shifted microbial rhodopsin. *Nat. Neurosci.* **17**, 1123–1129 (2014).
210. Botta, P. *et al.* An Amygdala Circuit Mediates Experience-Dependent Momentary Arrests during Exploration. *Cell* S0092867420311648 (2020) doi:10.1016/j.cell.2020.09.023.
211. Liu, X. *et al.* Optogenetic stimulation of a hippocampal engram activates fear memory recall. *Nature* **484**, 381–385 (2012).
212. Madisen, L. *et al.* A toolbox of Cre-dependent optogenetic transgenic mice for light-induced activation and silencing. *Nat. Neurosci.* **15**, 793–802 (2012).
213. Sakaguchi, M. *et al.* Inhibiting the Activity of CA1 Hippocampal Neurons Prevents the Recall of Contextual Fear Memory in Inducible ArchT Transgenic Mice. *PLoS One* **10**, e0130163 (2015).
214. Yona, G., Meitav, N., Kahn, I. & Shoham, S. Realistic Numerical and Analytical Modeling of Light Scattering in Brain Tissue for Optogenetic Applications. *eNeuro* **3**, (2016).
215. Kim, N. *et al.* A striatal interneuron circuit for continuous target pursuit. *Nat. Commun.* **10**, 2715 (2019).
216. Kirchberger, L. *et al. The Essential Role of Feedback Processing for Figure-Ground Perception in Mice*. https://papers.ssrn.com/abstract=3441074 (2019).
217. Lee, S. J. *et al.* Cell-type specific asynchronous modulation of PKA by dopamine during reward based learning. *bioRxiv* 839035 (2019) doi:10.1101/839035.
218. Murata, Y. & Colonnese, M. T. GABAergic interneurons excite neonatal hippocampus in vivo. *Sci. Adv.* **6**, eaba1430 (2020).
219. Fernandes, A. B. *et al.* Postingestive Modulation of Food Seeking Depends on Vagus-Mediated Dopamine Neuron Activity. *Neuron* **106**, 778-788.e6 (2020).
220. Jimenez, J. C. *et al.* Anxiety Cells in a Hippocampal-Hypothalamic Circuit. *Neuron* **97**, 670-683.e6 (2018).
221. Johansson, Y. & Silberberg, G. The Functional Organization of Cortical and Thalamic Inputs onto Five Types of Striatal Neurons Is Determined by Source and Target Cell Identities. *Cell Rep.* **30**, 1178-1194.e3 (2020).
222. Millan, E. Z., Kim, H. A. & Janak, P. H. Optogenetic activation of amygdala projections to nucleus accumbens can arrest conditioned and unconditioned alcohol consummatory behavior. *Neuroscience* **360**, 106–117 (2017).
223. Neely, R. M., Koralek, A. C., Athalye, V. R., Costa, R. M. & Carmena, J. M. Volitional Modulation of Primary Visual Cortex Activity Requires the Basal Ganglia. *Neuron* **97**, 1356-1368.e4 (2018).
224. Hughes, R. N. *et al.* Precise Coordination of Three-Dimensional Rotational Kinematics by Ventral Tegmental Area GABAergic Neurons. *Curr. Biol.* **29**, 3244-3255.e4 (2019).
225. Kim, J., Gulati, T. & Ganguly, K. Competing Roles of Slow Oscillations and Delta Waves in Memory Consolidation versus Forgetting. *Cell* **179**, 514-526.e13 (2019).
226. Asok, A. *et al.* Optogenetic silencing of a corticotropin-releasing factor pathway from the central amygdala to the bed nucleus of the stria terminalis disrupts sustained fear. *Mol. Psychiatry* **23**, 914–922 (2018).
227. Cummings, K. A. & Clem, R. L. Prefrontal somatostatin interneurons encode fear memory. *Nat. Neurosci.* **23**, 61–74 (2020).

228. Guo, B. *et al.* Anterior cingulate cortex dysfunction underlies social deficits in Shank3 mutant mice. *Nat. Neurosci.* **22**, 1223–1234 (2019).
229. Engelhard, B. *et al.* Specialized coding of sensory, motor and cognitive variables in VTA dopamine neurons. *Nature* **570**, 509–513 (2019).
230. Díaz-Hernández, E. *et al.* The Thalamostriatal Projections Contribute to the Initiation and Execution of a Sequence of Movements. *Neuron* **100**, 739-752.e5 (2018).
231. Gradinaru, V., Thompson, K. R. & Deisseroth, K. eNpHR: a Natronomonas halorhodopsin enhanced for optogenetic applications. *Brain Cell Biol.* **36**, 129–139 (2008).
232. Zhao, S. *et al.* Improved expression of halorhodopsin for light-induced silencing of neuronal activity. *Brain Cell Biol.* **36**, 141–154 (2008).
233. Hayat, H. *et al.* Locus-coeruleus norepinephrine activity gates sensory-evoked awakenings from sleep. *bioRxiv* 539502 (2019) doi:10.1101/539502.
234. Augustine, V. *et al.* Temporally and Spatially Distinct Thirst Satiation Signals. *Neuron* **103**, 242-249.e4 (2019).
235. Chen, T.-W., Li, N., Daie, K. & Svoboda, K. A Map of Anticipatory Activity in Mouse Motor Cortex. *Neuron* **94**, 866-879.e4 (2017).
236. Komiyama, T. *et al.* Learning-related fine-scale specificity imaged in motor cortex circuits of behaving mice. *Nature* **464**, 1182–1186 (2010).
237. Li, N., Chen, T.-W., Guo, Z. V, Gerfen, C. R. & Svoboda, K. A motor cortex circuit for motor planning and movement. *Nature* **519**, 51–56 (2015).
238. Guo, Z. V. *et al.* Flow of Cortical Activity Underlying a Tactile Decision in Mice. *Neuron* **81**, 179–194 (2014).
239. Lee, J., Wang, W. & Sabatini, B. L. Anatomically segregated basal ganglia pathways allow parallel behavioral modulation. *Nat. Neurosci.* 1–11 (2020) doi:10.1038/s41593-020-00712-5.
240. Nonomura, S. *et al.* Monitoring and Updating of Action Selection for Goal-Directed Behavior through the Striatal Direct and Indirect Pathways. *Neuron* **99**, 1302-1314.e5 (2018).
241. Shin, J. H., Kim, D. & Jung, M. W. Differential coding of reward and movement information in the dorsomedial striatal direct and indirect pathways. *Nat. Commun.* **9**, 404 (2018).
242. Bariselli, S., Fobbs, W. C., Creed, M. C. & Kravitz, A. V. A competitive model for striatal action selection. *Brain Res.* **1713**, 70–79 (2019).

Annex

Table S1 - **Mice utilized for the histological characterization of the stGtACR2 opsin in cortical and striatal conditions.**

Mouse ID	Region	Volume	Dilution and titer
m35991	M1	200 nl	Full titer; 1.5 x 10^13 gc/ml
m35994	DLS	200 nl	Full titer; 1.5 x 10^13 gc/ml
m35995	DLS/M1	300 nl	1:10 dilution; 1.5 x 10^12 gc/ml
m36224	M1	500 nl	1:30 dilution; 5 x 10^11 gc/ml
m36226	DLS	500 nl	1:30 dilution; 5 x 10^11 gc/ml
m36314	DLS	500 nl	1:30 dilution; 5 x 10^11 gc/ml
m36330	M1	500 nl	1:30 dilution; 5 x 10^11 gc/ml
m36315	M1	500 nl	1:30 dilution; 5 x 10^11 gc/ml
m36316	DLS	500 nl	1:30 dilution; 5 x 10^11 gc/ml

Table S2 - **Mice utilized for the behavioral experiments' section of the project. n.a. stands for Non applicable.**

Mouse ID	Region	Protein expressed	Volume	Dilution and titer	Notes (exclusions)
m37658	M1	eYFP	990 nl	1:12.5; 1.5*10^12 gc/ml	n.a.
m37659	M1	eYFP	990 nl	1:12.5; 1.5*10^12 gc/ml	n.a.
m37660	M1	eYFP	990 nl	1:12.5; 1.5*10^12 gc/ml	n.a.
m38009	M1	eYFP	990 nl	1:12.5; 1.5*10^12 gc/ml	Poor behavior
m38542	M1	eYFP	990 nl	1:12.5; 1.5*10^12 gc/ml	n.a.
m38572	M1	eYFP	990 nl	1:12.5; 1.5*10^12 gc/ml	n.a.
m37690	DLS	eYFP	1000 nl	1:12.5; 1.5*10^12 gc/ml	Poor behavior
m38017	DLS	eYFP	1000 nl	1:12.5; 1.5*10^12 gc/ml	n.a.
m38338	DLS	eYFP	1000 nl	1:12.5; 1.5*10^12 gc/ml	n.a.
m38339	DLS	eYFP	1000 nl	1:12.5; 1.5*10^12 gc/ml	Loss of fiber
m38316	DLS	eYFP	1000 nl	1:12.5; 1.5*10^12 gc/ml	n.a.
m38404	DLS	eYFP	1000 nl	1:12.5; 1.5*10^12 gc/ml	Loss of fiber
m38045	M1	stGtACR2	990 nl	1:10; 1.5*10^12 gc/ml	n.a.
m38073	M1	stGtACR2	990 nl	1:10; 1.5*10^12 gc/ml	n.a.
m38034	M1	stGtACR2	990 nl	1:10; 1.5*10^12 gc/ml	n.a.
m38036	M1	stGtACR2	990 nl	1:10; 1.5*10^12 gc/ml	Poor behavior
m38539	M1	stGtACR2	990 nl	1:10; 1.5*10^12 gc/ml	n.a.
m38541	M1	stGtACR2	990 nl	1:10; 1.5*10^12 gc/ml	n.a.
m38153	DLS	stGtACR2	1000 nl	1:10; 1.5*10^12 gc/ml	n.a.
m38402	DLS	stGtACR2	1000 nl	1:10; 1.5*10^12 gc/ml	n.a.
m38392	DLS	stGtACR2	1000 nl	1:10; 1.5*10^12 gc/ml	Fiber misplacement
m38393	DLS	stGtACR2	1000 nl	1:10; 1.5*10^12 gc/ml	n.a.
m38320	DLS	stGtACR2	1000 nl	1:10; 1.5*10^12 gc/ml	n.a.
m38739	DLS	stGtACR2	1000 nl	1:10; 1.5*10^12 gc/ml	n.a.

Table S3 - **Measurements for the length of stGtACR2 expression in mice injected with undiluted virus.**

Mouse ID	Region	Dilution and titer	Volume	Left hemisphere (µm)	Right hemisphere (µm)	Average (µm)
m35991	M1	No dilution/Full titer (1.5*10^13 gc/ml)	200 nl	616.798	566.929	591.8635
m35994	DLS	No dilution/Full titer (1.5*10^13 gc/ml)	200 nl	885.214	911.75	898.482

Table S4 - **Measurements for the length of stGtACR2 expression in a mouse after injection with 300 nl of the virus at a 1:10 dilution.**

Mouse ID	Region	Dilution and titer	Volume	Left hemisphere (µm)	Right hemisphere (µm)
m35995	M1/DLS	1:10; 1.5*10^12 gc/ml	300 nl	376.842 (M1)	426.528 (DLS)

Table S5 - **Measurements for the length of stGtACR2 expression in mice after injection with a 1:30 dilution of the virus.**

Mouse ID	Region	Dilution and titer	Volume	Left hemisphere (µm)	Right hemisphere (µm)	Average (µm)
m36224	M1	1:30; 5*10^11 gc/ml	500 nl	180.36	336.634	258.497
m36226	M1	1:30; 5*10^11 gc/ml	500 nl	266.623	359.229	312.926
m36314	M1	1:30; 5*10^11 gc/ml	500 nl	330.082	153.369	241.7255
m36330	DLS	1:30; 5*10^11 gc/ml	500 nl	297.222	762.162	529.692
m36315	DLS	1:30; 5*10^11 gc/ml	500 nl	306.911	376.471	341.691
m36316	DLS	1:30; 5*10^11 gc/ml	500 nl	607.895	369.534	488.7145

	M1	DLS
Average (µm)	271.0495	453.3658333

Table S6 - **Measurements for the width of stGtACR2 expression in mice after injection with 990/1000 nl of the virus, at a 1:10 dilution.**

Mouse ID	Region	Protein expressed	Dilution and titer	Volume	Left hemisphere (µm)	Right hemisphere (µm)	Average (µm)
m37658	M1	eYFP	1:12.5; 1.5*10^12 gc/ml	990 nl	415.137	404.301	409.719
m37659	M1	eYFP	1:12.5; 1.5*10^12 gc/ml	990 nl	436.297	269.231	352.764
m37660	M1	eYFP	1:12.5; 1.5*10^12 gc/ml	990 nl	381.836	424.837	403.3365
m38542	M1	eYFP	1:12.5; 1.5*10^12 gc/ml	990 nl	468.075	557.722	512.8985
m38572	M1	eYFP	1:12.5; 1.5*10^12 gc/ml	990 nl	531.271	601.231	566.251
m38017	DLS	eYFP	1:12.5; 1.5*10^12 gc/ml	1000 nl	405.229	718.954	562.0915
m38338	DLS	eYFP	1:12.5; 1.5*10^12 gc/ml	1000 nl	727.273	576.959	652.116
m38316	DLS	eYFP	1:12.5; 1.5*10^12 gc/ml	1000 nl	841.707	832.358	837.0325
m38045	M1	stGtACR2	1:10; 1.5*10^12 gc/ml	990 nl	664.122	636.364	650.243
m38073	M1	stGtACR2	1:10; 1.5*10^12 gc/ml	990 nl	562.242	507.576	534.909
m38034	M1	stGtACR2	1:10; 1.5*10^12 gc/ml	990 nl	668.264	735.738	702.001
m38539	M1	stGtACR2	1:10; 1.5*10^12 gc/ml	990 nl	555.556	503.268	529.412
m38541	M1	stGtACR2	1:10; 1.5*10^12 gc/ml	990 nl	642.855	664.122	653.4885
m38153	DLS	stGtACR2	1:10; 1.5*10^12 gc/ml	1000 nl	871.46	542.523	706.9915
m38402	DLS	stGtACR2	1:10; 1.5*10^12 gc/ml	1000 nl	1031.653	812.929	922.291
m38393	DLS	stGtACR2	1:10; 1.5*10^12 gc/ml	1000 nl	522.876	1045.752	784.314
m38320	DLS	stGtACR2	1:10; 1.5*10^12 gc/ml	1000 nl	882.74	1045.772	964.256
m38739	DLS	stGtACR2	1:10; 1.5*10^12 gc/ml	1000 nl	635.241	435.115	535.178

	M1 eYFP	DLS eYFP	M1 stGtACR2	DLS stGtACR2
Average (µm)	448.9938	722.77725	623.3115833	782.6061
Standard deviation	78.38409915	119.9767296	66.61178707	154.5637129

Table S7 - **Mice whose behavior performance was analyzed. The coordinates represented correspond to the fiber tip position, which denote a close approximation between its position after histological observation and the intended coordinates prior to the surgery procedures.**

Mouse ID	Region	Protein expressed	Coordinates (from surgery)			Coordinates (from reference image)		
			AP (mm)	ML (mm)	DV (mm)	AP (mm) (L/R)	ML (mm) (L/R)	DV (mm) (L/R)
m37658	M1	eYFP	1	1.4	0.3	0.98	1.328 / 1.318	0..336 / 0.398
m37659	M1	eYFP	1	1.4	0.3	0.98 - 1.1	1.375 / 1.391	0.344 / 0.234
m37660	M1	eYFP	1	1.4	0.3	0.98 - 1.1	1.258 / 1.438	0.250 / 0.281
m38542	M1	eYFP	1	1.4	0.3	0.62 - 0.74	1.422 / 1.305	0.156 / 0.273
m38572	M1	eYFP	1	1.4	0.3	0.98 - 1.1	0/ 1.484	0 / 0.234
m38017	DLS	eYFP	0.5	2.5	2	0.5	2.375 / 2.547	2.008 / 2.101
m38338	DLS	eYFP	0.5	2.5	2	0.02 - 0.14	2.305 / 2.484	1.594 / 1.672
m38316	DLS	eYFP	0.5	2.5	2	0.5	2.484 / 2.531	2.156 / 2.227
m38045	M1	stGtACR2	1	1.4	0.3	0.98 - 1.1	1.422 / 1.188	0.227 / 0.273
m38073	M1	stGtACR2	1	1.4	0.3	0.98	1.352 / 1.320	0.266 / 0.359
m38034	M1	stGtACR2	1	1.4	0.3	0.5 - 0.62	1.352 / 1.375	0.289 / 0.273
m38539	M1	stGtACR2	1	1.4	0.3	0.62	1.438 / 1.320	0.219 / 0.320
m38541	M1	stGtACR2	1	1.4	0.3	1.1	1.438 / 1.336	0.398 / 0.328
m38153	DLS	stGtACR2	0.5	2.5	2	0.5 - 0.62	2.570 / 2.578	1.859 / 1.961
m38402	DLS	stGtACR2	0.5	2.5	2	0.02 - 0.14	2.578 / 2.391	1.898 / 1.773
m38393	DLS	stGtACR2	0.5	2.5	2	0.5	2.570 / 2.344	1.859 / 1.812
m38320	DLS	stGtACR2	0.5	2.5	2	0.02 - 0.14	2.609 / 2.297	1.805 / 1.797
m38739	DLS	stGtACR2	0.5	2.5	2	0.26	2.656 / 2.438	1.711 / 1.875